5-2013

Development of Miniature Full Flow and Model Pipeline Probes for Testing of Box Core Samples of Surficial Seabed Sediments

Adriane G. Boscardin
University of Massachusetts Amherst, agb25@cornell.edu

DEVELOPMENT OF MINIATURE FULL FLOW AND MODEL PIPELINE PROBES FOR TESTING OF BOX CORE SAMPLES OF SURFICIAL SEABED SEDIMENTS

A Dissertation Presented

by

ADRIANE G. BOSCARDIN

Submitted to the Graduate School of the

University of Massachusetts Amherst in partial fulfillment

of the requirements for the degree of

DOCTOR OF PHILOSOPHY

May 2013

Civil and Environmental Engineering

DEVELOPMENT OF MINIATURE FULL FLOW AND MODEL PIPELINE PROBES FOR TESTING OF BOX CORE SAMPLES OF SURFICIAL SEABED SEDIMENTS

A Dissertation Presented

by

ADRIANE G. BOSCARDIN

Approved as to style and content by:

_____

Don J. DeGroot, Chair

_____

Ching S. Chang, Member

_____

Jonathan D. Woodruff, Member

_____

Richard N. Palmer, Department Head

Civil and Environmental Engineering

DEDICATION

To my family and friends for all their love and support.

ACKNOWLEDGMENTS

This thesis is based upon work supported in part by the US National Science Foundation under Grants No. OISE-0530151. Any opinions, findings, conclusions, and recommendations expresses in this thesis are those of the author and do not necessarily reflect the views of the National Science Foundation.

I would also like to thank the following institutions and people for helping make this research possible and enjoyable: the Norwegian Geotechnical Institute for their collaboration and support in the development of full flow penetrometer testing equipment for the box corer, especially Tom Lunne and Morten Sjursen for coordinating offshore site investigations with the box corer; the Center for Offshore Foundation Systems, including Mark Randolph, for suggesting toroid testing in the box corer; Melissa Landon Maynard and the University of Maine for facilitating box core testing off the coast of Maine; Dr. Don J. DeGroot, academic advisor and committee chair, for his guidance and support; Dr. Ching S. Chang and Dr. Jonathan D. Woodruff, committee members, for serving as committee members for this research; Rick Miastkowski, Dave Glazier, and the UMass Amherst College of Engineering Machine Shop for all their help, effort, and guidance in developing testing equipment for this research; past and present graduate students for all their support; my family and friends for all their encouragement.

ABSTRACT

DEVELOPMENT OF MINIATURE FULL FLOW AND MODEL PIPELINE PROBES FOR TESTING OF BOX CORE SAMPLES OF SURFICIAL SEABED SEDIMENTS

MAY 2013

ADRIANE BOSCARDIN, B.S., CORNELL UNIVERSITY

M.S., UNIVERSITY OF MASSACHUSETTS AMHERST

Ph.D., UNIVERSITY OF MASSACHUSETTS AMHERST

Directed by: Professor Don J. DeGroot

The box corer is a relatively new tool used in the geotechnical community for collection of soft seabed sediments. Miniature full flow and model pipeline probes were developed as tools to characterize and obtain soil parameters of soft seabed sediments collected in the box core for design of offshore pipelines and analysis of shallow debris flows. Probes specifically developed for this study include the miniature t-bar, ball, motorized vane (MV), and toroid. The t-bar, ball, and MV were developed to measure intact and remolded undrained shear strengths (s_u and s_{ur}). The t-bar and ball can obtain continuous strength profiles and measure s_{ur} at discrete depths in the box corer while the MV measures s_u and s_{ur} at discrete depths. The toroid is a form of model pipeline testing which was developed to investigate pipe-soil interaction during axial pipeline movement. Vertical loading and displacement rates can be selected for the toroid to mimic axial pipeline displacement for a variety of pipe weights. A load frame for both miniature penetrometer and toroid testing was developed for testing directly on box core samples offshore. This research presents results from offshore and laboratory testing of the box core and recommended testing procedures for full flow and toroid probes on box core samples.

TABLE OF CONTENTS

Page

LIST OF TABLES

Table Page

LIST OF FIGURES

Figure Page

CHAPTER 1

INTRODUCTION

Oil and gas field development is moving further offshore and into deeper waters and with increasing water depth, the cost and difficulty of pipeline construction increases. Deep water pipelines operate at high temperatures and pressures. Additionally, between startup and shutdown cycles, the pipeline contracts and expands resulting in axial and lateral movement of the pipeline along the seabed.

Controlled lateral buckling has become an increasingly common method of deep water pipeline construction. This construction method engages soil resistance in the first half meter of the seabed which influences pipeline movement. Soft fine-grained sediments are commonly found in this zone with undrained shear strengths often less than 10 kPa (Dingle et al. 2008; Hill et al. 2008). Collecting undisturbed samples and *in situ* strength testing of these soft soils is very difficult with conventional methods. Due to these difficulties, soil resistances in the first 20 cm of the seabed are often ignored in pipeline design (Bruton et al. 2008). Box core sampling is a new method of sample collection used to collect intact samples of the first half meter of the seabed. The box core collects a 50 cm x 50 cm x 50 cm (0.125 m^3) soil sample.

This research focuses on profiling soil strength and obtaining soil parameters for offshore pipeline design through development of equipment and a comprehensive testing protocol for testing of box core samples of soft offshore sediments. The research focused on developing test procedures for miniature full flow penetrometers, motorized vane (MV), and a toroid penetrometer (a model pipeline test). Full flow penetrometers were specifically developed to provide profiles of intact and remolded undrained shear strength in box core samples. Intact and remolded shear strengths are also useful for modeling of shallow debris flow

events. The toroid is a model pipeline test device used to simulate pipe-soil interaction during axial displacement events of pipelines. These research objectives for this dissertation were accomplished through the following tasks:

1. Develop and evaluate miniature full flow penetrometers for laboratory testing of very soft remolded soils.
2. Design and fabricate a computer controlled load frame for testing of box care samples using miniature full flow penetrometers and MV for direct testing of box core samples offshore to obtain intact and remolded undrained shear strength profiles of very soft sediments.
3. Develop a recommended testing protocols for full flow penetrometer and MV testing of offshore box core samples.
4. Develop a toroid penetrometer for testing of box core samples to model axial movement of pipelines along the seabed.
5. Develop recommended test protocols for toroid testing offshore box core testing.

The research methods, results, and interpretation of results are presented in the form of three manuscripts that have been prepared for submission to peer reviewed journals. These manuscripts are presented in chapters 2, 3, and 4. Chapter 5 presents a summary and conclusions of the research.

Chapter 2 presents results of cyclic miniature penetrometer and push cone testing of soft clays in the laboratory for measurement of remolded undrained shear strengths. The author is the lead author, responsible for writing and organizing the paper, development of testing equipment, testing and evaluating experimental results. This paper will be submitted to

ASCE Journal of Geotechnical and Geoenvironmental Engineering. Coauthor on this paper is expected to be DeGroot, D.J.

Chapter 3 presents results and recommended testing protocol for site characterization using miniature full flow penetrometer and MV testing of offshore box core samples. The author is the lead author, responsible for writing and organizing the paper, development of testing equipment, testing and evaluating experimental results. This paper will be submitted to *ASCE Journal of Geotechnical and Geoenvironmental Engineering*. Coauthors on this paper are expected to be DeGroot, D.J. and Lunne, T.

Chapter 4 presents results and recommended test protocol of the toroid based on laboratory testing as a form of model pipeline testing in box core samples. The toroid is a model pipeline test which mimics axial movement of pipelines along the seabed. The author is the lead author, responsible for writing and organizing the paper, development of testing equipment, testing and evaluating experimental results. This paper will be submitted to *ASTM Geotechnical Testing Journal*. Coauthor on this paper is expected to be DeGroot, D.J.

CHAPTER 2

EVALUATION OF LABORATORY TESTING OF REMOLDED UNDRAINED SHEAR STRENGTH OF SOFT CLAYS USING CYCLIC MINIATURE PENETROMETERS AND PUSH CONE

2.1 Abstract

Remolded undrained shear strength, s_{ur}, is an important parameter in debris flow modeling. In general, many offshore soils, especially in the upper meter of the seabed, are soft, sensitive, structured clays, lose strength upon disturbance and difficult to reliably measure strength. This research focused on development of new methods to more accurately measure s_{ur}.

Two types of miniature full flow penetrometers (ball and t-bar) and push cone were developed to evaluate the remolded shear strength, s_{ur}, of soft clays. Remolded undrained shear strength values from the miniature penetrometers were compared to fall cone, torvane, and miniature laboratory vane measurements on soft clays collected from both onshore and offshore test sites.

Remolded undrained shear strengths were measured by cycling the miniature penetrometers over a 50 mm stroke at 1 mm/s in the laboratory and at 2 mm/s in the field until resistance stabilized on a minimum value, typically within 10 cycles. A resistance factor of N = 13 was typically used to evaluate s_{ur} for the ball and t-bar based on theoretical and empirical recommendations presented in the literature. Resistance factors were also back calculated in reference to the fall cone, torvane, laboratory vane and motorized vane. The range of N_{Ball} = 5.4-29.4 and $N_{T\text{-}bar}$ = 4.5-20.6 in the laboratory. In the box corer, N_{Ball} = 1.4-29.6 and $N_{T\text{-}bar}$ = 0.4-62.2.

The push cone proved to be a simple method for assessing and providing a unique solution for s_{ur} of a given soil. A cone with a 60^{o} apex was pushed into test specimens at a rate of

1 mm/s to a depth of approximately 5 cm. Based on theoretical analysis of a conical footing, s_{ur} was calculated based on test geometry and resistance curves.

The miniature ball and t-bar is well suited for very soft to soft clays, especially in box core samples, and the push cone shows potential for stiffer soils.

2.2 Introduction

Remolded undrained shear strength, s_{ur}, is a parameter important for design of offshore structures and pipelines, to assess slope stability, and for debris flow modeling (both on and offshore). In general, many offshore soils are soft, sensitive, structured clays and lose strength upon shearing. The first full flow penetrometers, the ball and t-bar, were developed in the laboratory and adopted for *in situ* testing in the early 1990's to address some disadvantages with peizocone (CPTU) testing in deep offshore waters. Full flow penetrometers in comparison to the CPTU require a smaller overburden pressure correction to the measured soil resistance. Additionally, the large surface area of the full flow penetrometers allows theses probes to detect small changes in soil strength. To eliminate special equipment for *in situ*, these penetrometers were designed to fit on CPTU push rod.

The objective of this study was to further assess the use of these full flow probes to measure s_{ur} in the laboratory. The full flow probes studied include the miniature ball and t-bar penetrometers. Additionally, the push cone was investigated as potential tools for measuring s_{ur}. Differences in surface finishes (smooth verses rough) were also studied for the miniature ball and t-bar.

This paper presents s_{ur} measurement methods and typical results for the miniature ball and t-bar in the laboratory and in the box corer. The push cone was only tested in the laboratory. These results were compared with s_{ur} measurements from the laboratory vane,

motorized vane, fall cone, and torvane tests on the same set of test soils. Back calculated resistance factors for the miniature ball and t-bar (N_{Ball} and $N_{T\text{-}bar}$) are also presented.

2.3 Test soils

Miniature penetrometer and push cone testing were performed on six natural fine grained soils in the laboratory:

1. Processed EPK Kaolin (mixed to 60% water content)
2. Boston Blue Clay (Newbury, Massachusetts)
3. Burswood (Perth, Western Australia)
4. Dalia (coast of Angola, West Africa)
5. Gulf of Mexico (Gulf of Mexico)
6. Onsøy (Norway)

Table 2.1 presents the as tested water content and Atterberg Limits for these soils. Dalia and the Gulf of Mexico (GOM) clays were collected from offshore locations, Boston Blue Clay (Landon et al. 2007) and Onsøy (Lunne et al. 2003) are terrestrial marine clays, and Burswood is terrestrial estuary clay.

Miniature penetrometer and motorized vane testing was performed in the field in box core samples offshore Egypt (3 sites), Norway (2 sites), Maine, and Australia. Box core samples tested at all test sites except Australia consisted of very soft clay. A summary of soil properties is presented in Table 2.2.

2.4 Miniature Full Flow Penetrometers and Push Cone Equipment

2.4.1 Miniature Penetrometers

Two types of miniature penetrometers were developed for this study at the University of Massachusetts Amherst to measure s_{ur}, the ball and t-bar. Stainless steel ball and t-bar with a smooth and a sandblasted rough surface finish were used in laboratory testing (Figure 2.1). The projected area of laboratory miniature ball and t-bar penetrometers are approximately $1/10^{th}$ the size of those used for *in situ* testing (e.g., Randolph 2004). The diameter of the ball is 11.1 mm with a rod diameter of 3.2 mm. The ratio of projected area of the ball to rod is 12:1, which is slightly larger than the 10:1 ratio for the *in situ* ball. The t-bar has a length of 25.4 mm and diameter of 4.0 mm; giving a length to diameter (L/D) ratio of 6.25:1 (same L/D ratio of the *in situ* testing probe). The rod diameter of the t-bar is the same as the ball of 3.2 mm.

Only smooth stainless steel penetrometers were developed for box core testing. Based on laboratory testing, smooth penetrometers tended to converge on a minimum resistance in fewer strokes than rough penetrometers. The ball used for box core testing has a diameter of 22.2 mm, the t-bar has a length 49.3 mm and diameter of 7.9 mm, and a rod diameter of 6.35 mm.

2.4.2 Push Cone

The push cone, developed at the University of Massachusetts Amherst, was investigated as a potential tool for measuring s_{ur} of soft soils. The push cone is a stainless steel polished cone with a 60^{o} apex and height of 50.8 mm shown in Figure 2.1.

2.5 Test Program

2.5.1 Laboratory Specimen Preparation

Remolded soil samples were prepared using “low energy” hand remolding by kneading soil samples in plastic bags until soil consistency became uniform. The remolded soil was then transferred to the test specimen container for miniature penetrometer, lab vane, and index testing (index tests included fall cone and torvane) by building a specimen in the test specimen container.

The specimen was built in four lifts using a container divided into four sections to prevent entrapping air during the specimen preparation process (Figure 2.2). After building a lift, the top of the lift was roughened before adding the next lift. Torvane and fall cone tests were performed after the completion of the second lift. The final specimen was 12.8 cm in height and 10 cm in diameter and typically tested within 5 to 10 minutes after completion of specimen preparation to minimize potential thixotropic effects.

2.5.2 Miniature Penetrometer Cyclic Testing in the Laboratory

Figure 2.3 shows the laboratory test setup, which consisted of a GeoJac load frame, Pittman servo motor, Interface low capacity (50 N) load cell, and data acquisition. The prepared specimen was secured to the base of the load frame prior to testing.

The ball and t-bar followed the same cyclic testing procedure: (1) zero load cell outside the specimen, (2) lower the penetrometer to the starting depth of 5 cm, (3) cycle the penetrometer between 5 cm and 10 cm depth at a rate of 1 mm/s for 10 cycles (a cycle consists of a down- and an up-stroke), and (4) after the completion of cyclic testing, remove the penetrometer from the specimen and a take posttest zero reading of the load cell.

Separate specimens were prepared for ball and t-bar. These tests were performed in the center of the specimen to minimize potential edge effects from the container. Cyclic testing with a rod of the same diameter as the t-bar and ball rod was performed last to determine the rod resistance correction for the ball and t-bar.

2.5.3 Push Cone Testing

Push cone testing used the same load frame and data acquisition as the miniature penetrometers. Figure 2.1 shows the push cone which has a 60^{o} apex, a height of 50.8 mm, and a smooth polished surface. The push cone testing procedure was as follows: (1) zero the load cell with the probe attached, (2) lower the cone tip to the top of the specimen, and (3) push the probe into the specimen at a constant rate of 1 mm/s to a maximum depth of 5 cm or load cell capacity was reached.

2.5.4 Box Core Miniature Penetrometer and Testing

A similar test procedure was followed for miniature t-bar and ball testing in the box corer. A profile was first obtained using the t-bar to full sample depth which was then followed by cyclic testing centered around 150 mm depth. A cyclic test consisted of 10 down- and up-strokes over a 50 mm length at a rate of 2 mm/s. A faster rate was used for box core testing to reduce test time while maintaining a penetration of less than half a penetrometer diameter per second. Depending on sample recovery, between one and three cyclic test were performed in each sample with at least 50 mm between cyclic tests to mitigate disturbance.

Rod testing down the same hole as the t-bar followed to correct for rod resistance during t-bar testing. Ball testing followed the same procedures as the t-bar in an undisturbed portion of the sample. Though when there were time constrains cyclic ball testing was omitted

because as seen from laboratory testing more there was more confidence of the full flow mechanism being engaged around the t-bar than the ball.

2.6 Remolded Undrained Shear Strength Measurement Results

2.6.1 Evaluation of Remolded Undrained Shear Strength

2.6.1.1 Miniature Ball and T-bar Penetrometers

Remolded undrained shear strength was evaluated using both the total measured resistance and the total resistance corrected for rod resistance. The ball and t-bar was corrected for rod resistance because the load cell is located at the top of the penetrometer rod verses behind the probe as shown in Figure 2.3. Based on the total measured resistance, s_{ur} was evaluated using:

$$s_{ur} = q/N \quad (2.1)$$

where:

q = penetration resistance = F/A_p (kPa)

F = measured force (kN)

A_p = projected area (m^2)

N = resistance factor

The resistance measured at mid-depth of the 10^{th} stroke up-stroke was taken as q. The remolded undrained shear strength corrected for rod resistance was calculated by:

$$s_{ur} = q_{adj}/N \quad (2.2)$$

where:

q_{adj} = corrected resistance $(F - F_{rod})/A_p$ (kPa)

F_{rod} = force measured by rod (N)

The force used to correct for F_{rod} in the laboratory was determined using linear regression on the 10^{th} cycle of the up-stroke of the rod, and F_{rod} was taken the resistance at mid-cycle. Since a cavity of approximately 2 cm depth formed during all ball and t-bar tests, the correction, F_{rod}, reduced to account for no contact in the cavity.

A rod correction was applied to the ball and t-bar in a similar manner in the box corer. After the completion of a t-bar or ball test, a profile with only the rod was run in the same hole as the ball/t-bar.

2.6.1.2 Push Cone

The push cone resistance was converted to s_{ur} using analytical analysis of conical footing by Houlsby & Martin's (2003). The penetration stress, q, is expressed in terms of s_{ur} and a dimensionless factor, N_{c0}, as:

$$q = N_{c0}s_{ur} \tag{2.3}$$

The dimensionless factor, N_{c0}, is a function of the cone geometry (including angle and radius), cone roughness, depth of embedment, and the rate of strength increase with depth of the clay. Assuming cone roughness is zero, for a push not exceeding the push cone height N_{c0} = 4.608.

Expressing q in terms of force (F) and cone diameter (d), and assuming $s_u = s_{ur}$, Equation2.3 can be rewritten as:

$$F_{Cone} = 4.8255s_{ur}d^2 \tag{2.4}$$

After fitting a power function in the form of $y = mx^b$ forcing b equal to 2 to the push cone force-depth penetration curves, s_{ur} is simply calculated by:

$$s_{ur} = m/4.8255 \tag{2.5}$$

2.6.2 Summary of Full Flow Penetrometer Results

2.6.2.1 Rough verses Smooth Penetrometer Testing in the Laboratory

Remolded shear strength was evaluated using the up-stroke of the 10^{th} cycle, but to ensure that the soil was remolded during cyclic testing, the resistance measurements of at least the last two cycles needed to overlap. Figure 2.4 presents stress curves for BBC using the smooth and rough t-bar.

The rough and smooth penetrometer cyclic curves are of similar shape. The smooth t-bar cyclic curves stabilized on steady state strength in fewer cycles than the rough t-bar. The rough t-bar initially measured higher resistances than the smooth t-bar because the rough surface mobilizes soil flow quicker than probes with a smooth surface.

Strength degradation of the ball was similar in behavior to the rough and smooth t-bar. On average, the rough ball resistance was generally 11% higher than the smooth ball, and the resistance of the rough t-bar was 4% higher than the smooth.

Since both the rough and smooth penetrometers converged to similar minimum resistances during cyclic testing and because the smooth t-bar curves stabilized faster than the rough t-bar curves, only smooth penetrometers were used on the other six test soils.

2.6.2.2 Smooth Miniature Laboratory Cyclic Ball and T-bar Plots

2.6.2.2.1 Force Curve Behavior

Figure 2.5 presents typical force and degradation curves for the miniature ball and t-bar penetrometers in the laboratory. A half cycle number corresponds to a down-stroke and a whole cycle number to an up-stroke on the force degradation curves.

In general, the ball resistance slightly increased with depth during the down-stroke and fairly uniform on the up-stroke. Though only in the Gulf of Mexico specimen did the up-stroke force mimic the down-stroke by decreasing with decreasing depth. This increase in resistance with depth is more pronounced in the cyclic t-bar curves. Like the ball, the t-bar resistance decreases with decreasing depth during the up-stroke in the Gulf of Mexico specimen. Probe resistance also tended to spike right before a change in stroke direction. The spike occurred in a travel distance of less than half a probe diameter of the ball and t-bar. After a change in stoke direction, the resistance stabilized within one probe diameter of the ball and within two t-bar diameters.

For the first 1 to 3 cycles of the ball and ½ to 1 cycles of the t-bar, a "low" resistance was measured. After these initial cycles, the resistance increased then gradually stabilized on a minimum resistance. The down-stroke resistance was always higher than the up-stroke for a given cycle. In general, the t-bar took more cycles than the ball to stabilize to a constant resistance.

The "low" resistance initially measured is believed to result from the formation of a cavity during the initial probe penetration. White et al. (2010) defines flow of soil in the cavity as shallow flow mechanism. Gradual closure of the void occurred throughout cyclic testing. Though in most specimens, the void remained open to a depth of approximately 2 cm at the end of cyclic testing. The full flow mechanism is believed to have not initiated upon first penetration, but developed after one to two cycles. Soil needs to fully flow around the probe to evaluate shear strength using theoretical analysis by Randolph et al. (2000). The increase in resistance after the first couple of cycles is evidence of gradual development of the full flow mechanism.

Since the up-strokes of the force curves were more uniform and stabilized in fewer cycles, s_{ur} was evaluated from the force measured during the up-stroke of the 10^{th} cycle at mid-stroke (7.5 cm depth). These forces ranged between 2.31 N (BBC) and 5.45 N (Burswood) for the ball penetrometer and between 2.20 N (BBC) and 5.10 (GOM) for the t-bar.

The relationship of the up- and down-stroke was investigated by plotting the average F_{down}/F_{up} over three depths of 6 cm, 7.5 cm, and 9 cm for cycles in which the soil was believed to be remolded. These results are presented in Figure 2.6 for both the t-bar and ball. In generally, the average F_{down}/F_{up} increases with depth, except for the GOM and Burswood (t-bar only) for which F_{down}/F_{up} remained fairly constant. The range of average F_{down}/F_{up} was 1.0 to 1.3 for the ball and 1.1 to 1.2 for the t-bar. The difference between the up- and down-stroke was also measured. The up-stroke resistance was generally higher than the down-stroke and remained fairly constant after the first few cycles (0.3 - 0.7 N). The difference tended to be greater for the t-bar than the ball.

2.6.2.2.2 Stress Curve Behavior

The force plots were converted to stress by dividing force by projected probe area (Figure 2.7). The remolded undrained shear strength is a function of the stress at mid-stoke of the 10^{th} up-stroke and the bearing factor, N. The mid-depth stress ranged from 23.8 kPa (BBC) to 56.2 kPa (Burswood) for the ball and between 21.3 kPa (BBC) and 55.0 kPa (GOM) for the t-bar.

2.6.2.3 Remolded Undrained Shear Strength Laboratory Results

Equation 2.1 converts the measured resistance, q, to s_{ur} using a resistance factor N. Randolph et al. (2000) developed this analytical solution for N assuming an elastic perfectly-

plastic soil response and Tresca failure criterion. Subsequent analytical work (e.g., Randolph & Andersen 2006) and empirical results from field and lab testing (e.g., Lunne et al. 2005) show that N varies with soil type, stress history, and the reference s_u or s_{ur} (e.g., fall cone, field vane, etc.). Thus far, published work suggests N_{ball} is 11-15.5 and $N_{T\text{-}bar}$ is 8-14 (Stewart & Randolph 1994; Lu et al. 2001; Einav & Randolph 2005; Lunne et al. 2005; Low & Randolph 2010; DeJong 2011; Lunne et al. 2011). Yafrate & DeJong (2006) found the lower bound of N to be as low as 5.8 (ball) and 5.9 (t-bar) and the range of N to expand to 7 - 40 for remolded soils.

Considering these findings and N-values derived in this study, a nominal N of 13 was selected to interpret s_{ur} from the miniature ball and t-bar and presented in Table 2.3. The remolded shear strength were 1.8 kPa (BBC) - 4.3 kPa (Burswood) for $s_{ur,ball}$ and 1.6 kPa (BBC) to 3.8 kPa (Burswood) after correcting for rod resistance. For the t-bar, s_{ur} was 1.6 kPa (BBC) - 3.8 kPa (GOM) and 1.4 kPa (BBC) – 3.1 kPa (BBC at $0.8w_L$) after rod resistance correction.

2.6.2.4 Evaluation of $N_{T\text{-}bar}$ and N_{Ball}

Empirical studies show N is a function of soil type, stress history, and upon remolding. Yafrate & DeJong (2005; 2006) observed an increase in N with decreasing soil strength and an increase in N with soil remolding. Randolph and Andresen (2006) found N to depend on anisotropy, strain softening, and degree of remolding based on analytical analysis. This study evaluated N for the t-bar and ball in reference to: (1) the fall cone (NGI and SGI methods); (2) the laboratory vane for LV-HR and LV-HR-VR samples; and (3) the torvane. Table 2.4 and Figure 2.8 present N-factors for both the ball and t-bar based on these reference values. Figure 2.10 present N_{ball} verse $N_{t\text{-}bar}$ for each test soil.

In reference to the laboratory vane, N was generally higher than those in reference to the fall cone. For all test soils, $N_{Ball(FC\text{-}NGI)}$ is 5.4 - 9.9 and $N_{Ball(LV\text{-}HR\text{-}VR)}$ is 12.8 - 23.4. The range of N

in reference to the fall cone and laboratory vane is similar for the ball and t-bar of $N_{T\text{-}bar(FC\text{-}NGI)}$ = 4.5 - 8.8 and $N_{T\text{-}bar(LV\text{-}HR\text{-}VR)}$ = 10.6 - 20.6. Generally, $N_{LV\text{-}HR} < N_{LV\text{-}HR\text{-}VR}$ which suggests that hand remolding samples did not break down soil to its weakest state. The N-factors for the ball and t-bar in reference to the torvane were the lowest, averaging $N_{Ball,TV}$ = 6.0 and $N_{T\text{-}bar,TV}$ = 5.3. These N values are in reference to s_{ur} not corrected for rod resistance. Table 2.5 and Figure 2.8 present N corrected for rod resistance.

This study found N_{FC} to be less than those presented by Yafrate & DeJong (2006) for remolded Burswood and Onsøy. On average, for a given test soil and reference s_{ur}, $N_{Ball}/N_{T\text{-}bar}$ is approximately 1.1 which agrees with Lu et al. (2001) and Yafrate & DeJong (2005) where $N_{Ball} > N_{T\text{-}bar}$ by 10% to 20%.

Randolph & Andersen (2006) found $N_{T\text{-}bar}$ to increases with surface roughness and, hence, $s_{ur(smooth)} > s_{ur(rough)}$. This study observed a slight decrease in strength with surface roughness, as shown in Figure 2.4. This difference is less than 10%.

2.6.2.5 Miniature Ball and T-bar Rod Resistance Correction

This study evaluates s_{ur} using theoretical analysis by Stewart & Randolph (1991). The resistance, q, is the stress measured by the probe. The test set-up in this study measures resistance of the rod and probe because the load cell is located at the top of the rod. The advantage of the load cell in this location is zero shifts due to temperature change are eliminated. The disadvantage is a rod resistance correction needs to be applied to q to accurately assess s_{ur}.

Rod resistance, in general, accounted for over 10% of the total measured resistance. Table 2.7 and Table 2.8 show, on average, the resistance of the smooth rod at accounted for

12% to 26% of the total ball resistance and 11% to 25% of the total t-bar resistance. Therefore, a rod correction is recommended with this test set-up and was corrected for in this study.

The rod correction was additionally adjusted for cavity formation in the upper 2 cm providing a lower bound estimate. Table 2.7 and Table 2.8 present estimates of rod resistance with a 2 cm deep cavity (rod resistance at 5.5 cm depth). Rod resistance reduced to less than 10% of the total t-bar resistance in EPK Kaolin and Onsøy. For all other test specimens, the rod resistance accounted for 11% to 20% of the total resistance.

2.6.2.6 Adjusting $N_{T\text{-}bar}$ for Shallow Embedment

During this study, it was observed that in general the upper 2 cm of soil did not fill in behind the probe. Therefore, full flow of soil around the penetrometers was not steady. White et al. (2010) divided soil flow around the t-bar into shallow flow and full flow. Based on White et al. (2010), N tends to increase with depth and flow mechanism. Meaning N is smaller during shallow flow than deep flow.

During shallow flow, the cavity behind the probe remains open and surface heave continues during penetration until the full flow mechanism develops. The depth at which the flow mechanism changes from shallow to deep is called the transition depth, $\hat{w}_{deep}$, and defined as:

$$\hat{w}_{deep} = 2.58(s_{ur}/\gamma' D)^{0.46} + 0.24(s_{ur}/\gamma' D)^{-0.63} \quad (2.6)$$

where :

$\hat{w}_{deep} = w_{deep}/D$

w_{deep} = transition depth (m)

γ' = submerged unit weight (kN/m^3)

D = probe diameter (m)

Large deformation finite element (LDFE) analysis shows that $N_{T\text{-}shallow}$ is a function of $N_{T\text{-}deep}$, $\hat{w}$, $\hat{w}_{deep}$, and $s_{ur}/\gamma'D$ and is defined as:

$$N_{T\text{-}shallow} = 2 + (N_{T\text{-}deep} - 2)(\hat{w}/\hat{w}_{deep})^{p} \quad (2.7)$$

where:

$p = 0.61(s_{ur}/\gamma'D)^{-0.31}$

$N_{T\text{-}deep}$ = full flow bearing factor

$\hat{w} = w/D$

w = penetrometer depth (m)

White et al. (2010) observed that as $s_{ur}/\gamma'D$ decreases, the transition depth from shallow to full flow increases. The transition depth fell between 7 and 11 cm among all test soils as presented in Table 2.9. Therefore, the depth at which the s_{ur} was measures typically fell in the zone of shallow flow. Table 2.9 shows that the adjustment of N from deep to shallow flow was less than 3%.

2.6.3 Box Core Full Flow Penetrometer Results

Cyclic testing in the box core produced similar stress depth curves and force degradation plots to laboratory testing, except during the initial strokes the resistance of the previous stroke was always greater than the current until the soil broke down to its weakest state (s_{ur}). Figure 2.9 presents typical cyclic and force degradations curves.

Across all offshore test sites, N ranged from 0.4 to 62.2 in remolded soils (Table 2.10). The average remolded $N_{t\text{-}bar}$ across all test sites was 6.8-15.5 and 5.7-14.9 for N_{ball} which match laboratory N-values on similar strength soils. Average t-bar and ball N-values tended to be on the lower end of what was reported by Yafrate & DeJong (2006). Note that Yafrate & DeJong (2006) used the fall cone as the reference strength verses the motorized vane in this study. This

study also observed that the average N_{ball} and $N_{t\text{-}bar}$ were within a similar range. Though only at Norway test sites was cyclic ball testing performed in addition to the cyclic t-bar.

Critical depth, the transition between shallow and deep flow, was assesses in each box for the ball and t-bar following theory developed by White et al. (2010). The average critical depth for the t-bar was 12.4 cm and 20.2 cm for the ball. Based on these observations, the location of the first cyclic test with the ball should be performed at 22.5 cm depth. Cyclic testing of the t-bar around 15 cm is unaffected by changing flow conditions. Therefore, it is recommended to perform cyclic tests with the t-bar when time is limited because cyclic testing can be performed over a wider range of depths.

Average t-bar s_{ur} fell between 0.35-1.6 kPa and the ball was 0.6-1.4 kPa. Remolded shear strengths were also measured by the motorized vane and ranged from approximately 0.5-2.0 kPa.

Fall cone and laboratory vane tests were performed in subsamples collected from the box corers. In general, s_{ur} was within the same range in the box and sub-samples. Remolded strength testing with the t-bar was on average higher than the fall cone at all Egypt sites, lower at both Norway test sites. T-bar s_{ur} was lower than the laboratory vane at all Egypt sites. The average s_{ur} of the ball was higher than the fall cone at Norway-L, but lower at Norway-O. All box core strength testing results are presented in Table 2.11.

2.6.4 Summary of Push Cone Penetrometer Results

Push cone remolded shear strength was evaluated by fitting a power equation to the force-depth curve. Figure 2.11 presents a typical curve. Table 2.12 presents the s_{ur} for all test soils. The remolded undrained shear strength of Burswood was the highest of 7 kPa, and Onsøy and BBC had the lowest s_{ur} of 3.5 kPa. The power function fit the data very well for all test soils

with the coefficient of correlation (r^2) varying between 0.97 (BBC) and 0.96 (Onsøy). Curve fitting was also performed on the first 3 cm of the push to eliminate potential edge effects from the specimen container. At 3 cm depth, at least one probe diameter was between the soil tested and the container edge. Table 2.12 presents s_{ur} of the push cone to 3 cm depth. The remolded shear strength reduced and r^2 increased, showing edge effects were present in s_{ur} calculated from a full push.

2.7 Recommendations and Conclusions

Remolded undrained shear strength measurements using miniature penetrometers and push cone in the laboratory are simple and repeatable tests. Rough and smooth ball and t-bar penetrometers were compared in BBC and found to reduce to similar strengths during cyclic testing. Only smooth penetrometers were tested on the remaining test soils to reduce the rod resistance correction.

Accurately assessing rod resistance during miniature ball and t-bar testing was very difficult. In this study, rod resistance was measured in a fresh area of the specimen and used as the rod correction. A more accurate measure of rod resistance was obtained in the box corer by pushing the rod down the same hole as the ball and t-bar after the completion of cyclic testing.

The miniature ball and t-bar measured highest resistances during down-stroke. The difference of the down- to up-stroke was 0.2 - 1.0 N for the ball and t-bar. In general, the ratio of up-stroke resistance to down-stroke increased with depth. Since the curves were more uniform during the up-stroke, s_{ur} was evaluated based on the steady state resistance measured during the up-stroke. This resistance was typically taken from mid-stroke (z = 7.5 cm).

The push cone is a quick and simple test which produces a unique s_{ur} based on analysis developed by Houlsby and Martin (2003) for embedment of a shallow conical footing. The push

cone resistance with depth was fit with a power function to evaluate a unique s_{ur} for a given test specimen. The remolded undrained shear strength measured by the push cone most closely matched fall cone-NGI and torvane results. These three tests measured the highest s_{ur} values. To prevent edge effects on push cone s_{ur} measurements, it is recommended to use data only collected from the first 3 cm of the push. The push cone was favored over other test methods because the test is simple and gives a unique s_{ur}.

The miniature t-bar and push cone can measure s_{ur} for a range of soil strengths, although an upper limit has not yet been determined. The miniature ball should be limited to testing on soft soils for unconsolidated specimens to ensure the full flow mechanism is engaged during testing.

In this study, N derived for the ball and t-bar spanned the low and high end of previously published N-values. In reference to the fall cone, N_{ball} = 5.4 - 15.8 and $N_{t\text{-}bar}$ = 4.5 - 14.2. Based on the laboratory vane, N_{ball} = 12.5 - 23.4 and $N_{t\text{-}bar}$ = 11.2 - 20.6. Adjusting N for shallow flow as suggested by White et al. (2010) resulted in a 3% reduction in N. From these findings, it is recommended to select N based on probe type (although the range of vales are very similar), probe roughness, soil properties, the reference test to obtain N, and the need of the design problem (i.e., upper verses lower bound solution).

Miniature cyclic t-bar and ball testing can be successfully performed in the box corer. Due to larger sample and probe dimensions a faster push rate of 2 mm/s was used to reduce testing time. Cyclic testing with the t-bar is recommended in all boxes with the first cyclic test depth centered around 15 cm. Cyclic testing with the ball is recommended, but may be excluded if time is limited, starting at a test depth centered around 22.5 cm.

Acknowledgements
This work was supported in part by the National Science Foundation under grant OISE-0530151.

2.8 References

DeJong, J.T., Yafrate, N.J. and DeGroot, D.J. (2011). “Evaluation of undrained shear strength using full-flow penetrometers.” *Journal of Geotechnical and Geoenvironmental Engineering*, 137(1), 14-26.

Einav, I., and Randolph, M. F. (2005). "Combining upper bound and stain path methods for evaluating penetration resistance." *International Journal for Numerical Methods in Engineering*, 63, 1991-2016.

Houlsby, G.T., and Martin, C.M. (2003). “Undrained bearing capacity factors for conical footings on clay.” *Géotechnique*, 53(5), 513-520.

Landon, M.M., DeGroot, D.J., and Sheahan, T.C. (2007). "Non-Destructive sample quality assessment using shear wave velocity." *Journal of Geotechnical and Geoenvironmental Engineering*. 133(4), 424-432.

Low, H.E., and Randolph, M.F. (2010). “Strength measurement for near-seabed surface soft soil using manually operated miniature full-flow penetrometer.” *Journal of Geotechnical and Geoenvironmental Engineering*, 136(11), 1565-1573.

Lu, Q., Hu, Y., and Randolph, M. F. (2001). “Deep penetration in soft clays with strength increasing with depth.” *Proceedings of the Eleventh (2001) International Offshore and Polar Engineering Conference*, 453-458.

Lunne, T., Long, M., and Forsberg, C.F. (2003). "Characterisation and engineering properties of Onsøy clay." *Characterisation and Engineering Properties of Natural Clay*, 1, 395-427.

Lunne, T., Randolph, M. F., Chung, S. F., Andersen, K. H., and Sjursen, M. (2005) “Comparison of cone and T-bar factors in two onshore and one offshore clay sediments.” *Frontiers in Offshore Geotechnics*, 981-989.

Lunne, T., Andersen, K.H., Low, H.E., Randolph, M.F., and Sjursen, M. (2011). “Guidelines for offshore in situ testing and interpretation of deepwater soft clays.” *Canadian Geotechnical Journal*, 48(4), 543-556.

Randolph, M. F. (2004). "Characterization of soft sediments for offshore applications." *Proceedings ISC-2 on Geotechnical and Geophysical Site Characterization*, 209-232.

Randolph, M.F., and Andersen, K.H. (2006). “Numerical analysis of t-bar penetration in soft clay.” *International Journal of Geomechanics*, 6(6), 411-420.

Randolph, M. F., Martin, C. M., and Hu, Y. (2000). "Limiting resistance of a spherical penetrometer in cohesive material." *Geotechnique*, 50(5), 573-582.

Stewart, D.P., and Randolph, M.F. (1991). "A new site investigation tool for the centrifuge." *Proc. Centrifuge 91*, Boulder, CO, 531-538.

Stewart, D.P., and Randolph, M.F. (1994). "T-bar penetration testing in soft clay." *Journal of Geotechnical Engineering*, 120(12), 2230-2235.

White, D.J., Gaudin, G., Boylan, N., and Zhou, H. (2010). "Interpretation of t-bar penetrometer tests at shallow embedment and in very soft soils." *Canadian Geotechnical Journal*, 47, 218-229.

Yafrate, N.J., and DeJong, J.T. (2005). "Considerations in evaluating the remoulded undrained shear strength from full flow penetrometer cycling." *ISFOG-05: International Symposium on Offshore Geotechnics*, Perth Western Australia, 991-997.

Yafrate, N.J., and DeJong, J.T. (2006). "Interpretation of sensitivity and remolded undrained shear strength with full flow penetrometer." *ISOPE*-06: *International Society for Offshore and Polar Engineering*, San Franciso, CA.

Table 2.1. Summary of index and classification results for laboratory test soils.

Soil	Water Content[†] (%)	w_n (%)	$LL_{(FC)}$ (%)	PL (%)	PI (%)	LI[#] (--)	G_s (Mg/m^3)	% sand (%)	% silt (%)	% clay (%)	Activity (-)	Sensitivity (s_u/s_{ur})	USCS (-)
EPK Kaolin	59.6	--	62.6	35.0	27.6	0.9	2.73	0.0	43.0	57.0	0.48	--	MH
BBC	53.2	54.9	48.2	23.9	24.3	1.2	2.74	0.4	39.6	60.0	0.41	2-30[a]	CL
BBC ($0.8w_L$)	39.6	--	48.2	23.9	24.3	0.6	--	--	--	--	--	--	--
Burswood	64.9	62.7	72.8	39.1	33.7	0.8	2.72	12.6	40.6	46.8	0.72	2-9[b,c]	MH
Dalia	127.8	127.2	136	46.3	89.7	0.9	2.78	2.5	6.2	91.2	0.98	6[a]	CH
Gulf of Mexico	63.7	63.7	78.0	35.0	43.0	0.7	2.73	0.0	36.4	63.6	0.68	--	CH
Onsøy	65.7	66.1	73.1	32.5	40.6	0.8	2.62	1.9	19.5	78.6	0.52	6-8[b,d]	CH

[†] Water content at time of s_{ur} testing

[#] LI based on water content at time of s_{ur} testing

From a) Fall Cone tests (Dunaj 2006); b) Field Vane Tests (Dunaj 2006); c) Levy et al. (2002); d) Lunne et al. (2003)

Note:

LL, PL and hydrometer data from Dunaj (2006) except Gulf of Mexico.

Table 2.2. Summary of average offshore test site soil properties.

Site	w_c	γ_T	PL	LL	PI	LI	Grain Size Distribution			$s_{u,fc}$ [+]		$s_{u,t\text{-}bar}$	
							clay	clay+silt	clay+silt +sand				
							< 2 μm	< 0.063 mm	< 2 mm	ave.	max.	ave.	max.
	%	kN/m^3	%	%	%	%	%	%	%	kPa	kPa	kPa	kPa
Egypt-G	100.2 (35.7-157)	15.36 (13.61-17.80)	38.7 (34.6-41.6)	79.6 (67.1-87.1)	41.0 (32.5-47.9)	1.52 (0.60-2.78)	46.0 (29.9-60.7)	94.4 (76.0-99.5)	99.0 (92.0-100)	3.2	12.0	2.1	5.5
Egypt-R	118.8 (76.5-181.3)	14.36 (13.52-16.3)	39.4 (33.6-42.1)	83.4 (74.3-91.4)	44.0 (36.5-49.3)	1.71 (1.22-2.34)	48.6 (37.9-60.7)	96.1 (76.0-100)	99.3 (92.0-100)	2.0	5.2	1.9	5.4
Egypt-T	100.3 (64.2-192.4)	14.14 (11.81-16.30)	40.3 (34.6-43.9)	86.3 (67.1-109.2)	46.1 (32.5-66.2)	1.57 (0.60-3.81)	15.2 (3.9-52.8)	51.2 (29.9-67.0)	96.7 (76.0-100)	4.3	17.0	3	41.3
Norway-L	84.5 (35.2-116.7)	15.30 (13.89-18.55)	25.9 (16.0-31.3)	66.2 (37.0-88.4)	40.3 (21.0-49.1)	1.45 (0.91-1.99)	46.3 (32.2-60.8)	85.6 (64.3-97.1)	98.1 (82.9-100)	5.4	9.6	4.4	7.6
Norway-O	166.6 (151.9-176.0)	12.88 (12.70-13.13)	43.2 (38.6-47.7)	95.5 (87.8-103.0)	52.2 (40.1-63.8)	2.47 (2.11-2.79)	48 (46-50)	97 (96-98)	100	4.0	6.4	2.7	3.8
Australia*	-	-	-	-	-	-	-	-	-	9.8	10	9.2	13.8
Maine	-	-	-	-	-	-	-	-	-	2.5	5.3	2.4	4.6

(min.-max.)

*sandy

[+]onshore lab

Table 2.3. Summary of s_{ur} values for the miniature ball and t-bar test in the laboratory using N=13 based on results presented by Randolph and Andersen (2006) and Yafrate and DeJong (2006).

				s_{ur} (kPa) for N=13			
	Force (N)			Ball		T-bar	
Soil	Ball	T-bar	Shaft*	uncorrected	corrected	uncorrected	corrected
EPK Kaolin	2.86	2.77	0.24	2.3	2.1	2.1	1.9
BBC	2.31	2.20	0.24	1.8	1.6	1.6	1.5
Burswood	5.45	4.42	0.68	4.3	3.8	3.3	2.8
Dalia	3.40	3.47	0.57	2.7	2.2	2.6	2.2
Gulf of Mexico	5.10	5.10	0.88	4.0	3.3	3.8	3.1
Onsøy	2.85	2.51	0.25	2.3	2.1	1.9	1.7

Table 2.4. Summary of laboratory N_{Ball} and $N_{T\text{-}bar}$ uncorrected for shaft resistance.

Soil	N_{Ball}					$N_{T\text{-}bar}$					$q_{Ball}/q_{T\text{-}bar}$
	FC-NGI	FC-SGI	TV	LV-HR	LV-HR-VR	FC-NGI	FC-SGI	TV	LV-HR	LV-HR-VR	
EPK Kaolin	8.5	13.5	6.3	14.7	21.1	7.7	12.3	5.7	13.4	19.2	1.10
BBC	9.9	15.8	6.6	12.5	13.2	8.8	14.2	5.9	11.2	11.8	1.12
Burswood	5.9	9.4	5.6	17.0	23.4	4.5	7.2	4.3	13.0	17.8	1.31
Dalia	7.4	11.8	5.8	13.0	15.9	7.1	11.3	5.5	12.5	15.3	1.04
Gulf of Mexico	6.8	10.8	5.9	17.0	21.9	6.4	10.2	5.6	15.9	20.6	1.06
Onsøy	5.4	8.6	5.5	12.8	12.8	4.5	7.1	4.6	10.6	10.6	1.21
Average =	7.3	11.7	5.5	14.6	17.7	6.5	10.4	5.5	16.0	18.6	1.04

Table 2.5. Summary of laboratory N_{Ball} and $N_{T\text{-}bar}$ corrected for shaft resistance.

Soil	N_{Ball}					$N_{T\text{-}bar}$					$q_{Ball}/q_{T\text{-}bar}$
	FC-NGI	FC-SGI	TV	LV-HR	LV-HR-VR	FC-NGI	FC-SGI	TV	LV-HR	LV-HR-VR	
EPK Kaolin	7.4	11.9	5.5	12.9	18.5	6.7	10.7	5.0	11.7	16.7	1.10
BBC	8.5	13.6	5.7	10.8	11.4	7.6	12.1	5.1	9.6	10.1	1.13
Burswood	5.0	8.0	4.8	14.4	19.8	3.6	5.8	3.5	10.5	14.5	1.37
Dalia	5.6	9.0	4.4	9.9	12.2	5.4	8.7	4.2	9.6	11.7	1.04
Gulf of Mexico	5.1	8.2	4.5	12.8	16.5	4.8	7.7	4.2	12.0	15.5	1.06
Onsøy	4.8	7.6	4.9	11.3	11.3	3.9	6.2	4.0	9.2	9.2	1.23
Average =	6.1	9.7	4.6	11.9	14.4	5.3	8.5	4.6	13.4	15.6	1.04

Table 2.6. Summary of laboratory s_{ur} results.

	Remolded Undrained Shear Strength, s_{ur} (kPa)									
	FC			LV		Miniature Penetrometers		Rod (down)	Push Cone	
Soil	NGI	SGI	TV	HR	HR-VR	Ball	T-bar	Rod (up)	5 cm	3 cm
EPK Kaolin	3.5	2.2	4.7	2.0	1.4	2.0	2.2	1.1	4.7	4.0
BBC	2.4	1.5	3.6	1.9	1.8	1.5	1.7	1.1	3.5	3.0
Burswood	9.6	6.0	10.0	3.3	2.4	3.6	3.3	0.9	7.0	6.7
Dalia	4.8	3.0	6.1	2.7	2.2	2.0	2.5	1.1	4.9	4.6
Gulf of Mexico	7.8	4.9	8.9	3.1	2.4	3.0	3.5	1.1	7.1	6.8
Onsøy	5.4	3.4	5.3	2.3	2.3	2.0	2.0	1.5	3.5	2.7

Table 2.7. Estimate of rod resistance during miniature ball penetrometer laboratory testing.

	Load (N)			Rod/Ball	
	Ball	Rod**		(%)	
Soil	7.5 cm	5.5 cm	7.5 cm	5.5 cm	7.5 cm
EPK Kaolin	2.86	0.24	0.35	9	12
BBC	2.31	0.24	0.32	10	14
Burswood	5.45	0.68	0.84	13	15
Dalia	3.40	0.57	0.81	17	24
Gulf of Mexico	5.10	0.88	1.26	17	25
Onsøy	2.85	0.25	0.33	9	12

**Based on linear regression in the form of y=mx+b.

Note: Reduced rod resistance corresponds to z = 5.5 cm

Table 2.8. Estimate of rod resistance during miniature t-bar penetrometer laboratory testing.

	Load (N)			Rod/T-bar	
	T-bar	Rod**		(%)	
Soil	7.5 cm	5.5 cm	7.5 cm	5.5 cm	7.5 cm
EPK Kaolin	2.77	0.24	0.35	9	13
BBC	2.20	0.24	0.32	11	15
Burswood	4.42	0.68	0.84	15	19
Dalia	3.47	0.57	0.81	17	23
Gulf of Mexico	5.10	0.88	1.26	17	25
Onsøy	2.51	0.25	0.33	10	13

**Based on linear regression in the form of y=mx+b.

Note: Reduced rod resistance corresponds to z = 5.5 cm

Table 2.9. Summary of critical depth and $N_{T\text{-}shallow}$ for N_T=13 for laboratory testing.

Soil	s_{ur}	$s_u/(\gamma' D)$	$\hat{w}_{deep}$	$w_{deep\text{-}crit}$	$N_{T\text{-}shallow}$	Change
	kPa	-	-	cm	-	%
EPK Kaolin	2.2	83.1	18.3	8.08	12.9	-0.57
BBC	1.7	59.7	16.9	6.95	13.1	-2.7
Burswood	3.3	131.9	24.4	10.0	12.6	1.7
Dalia	2.5	159.0	26.6	10.9	12.5	2.4
Gulf of Mexico	3.5	137.8	24.9	10.2	12.6	1.9
Onsoy	2	83.5	19.8	8.11	12.9	-0.5

Table 2.10. Summary of offshore N.

Site		N_{rem}						Count
		T-bar			Ball			
		min-max	ave	st dev	min-max	ave	st dev	rem
Egypt	R	4.4 - 26.1	11.3	6.7	na	na	na	12
	G	0.4 - 15.5	7.3	4.2	na	na	na	10
	T	4.8 - 62.2	15.5	13.8	na	na	na	29
Australia		-	7.2	-	-	-	-	-
Norway	O	1.7 - 16.5	6.8	5.3	1.4 - 17.0	5.7	5.5	7
	L	6.2 - 27.6	13.5	6.2	7.6 - 29.6	14.9	6.6	15
Maine		3.0 - 13.1	7.2	-	na	na	na	2

Table 2.11. Summary of offshore remolded shear strength measurements.

	Remolded Shear Strength					
	Box Core				Subsamples	
	Motorized Vane	T-bar	Ball		Fall Cone	Lab Vane
Site	kPa	kPa	kPa	Version	kPa	kPa
Egypt-G	0.64 (0.28-1.24)	0.36 (0.03-0.60)	NA	alpha	0.96 (0.50-2.30)	0.62 (0.28-1.24)
Egypt-R	0.61 (0.14-1.35)	0.41 (0.18-0.99)	NA	alpha	0.76 (0.40-1.30)	0.63 (0.14-1.35)
Egypt-T	0.55 (0.25-1.21)	0.64 (0.09-2.52)	NA	alpha	1.68 (0.40-7.30)	0.68 (0.25-3.84)
Norway-L	1.35 (0.79-2.95)	1.18 (0.64-2.40)	1.41 (0.82-2.58)	alpha	1.14 (0.50-2.10)	NA
Norway-O	2.07 (0.37-4.43)	0.77 (0.47-1.13)	0.62 (0.38-0.82)	beta	0.7 (0.4-0.8)	NA
Australia*	1.85 (1.60-2.10)	1.60	NA	alpha	NA	NA
Maine	1.09 (0.53-1.79)	1.18 (0.30-2.55)	NA	beta	NA	NA

(min.-max.)

*One box tested

Table 2.12. Push Cone analysis at full and reduced penetration depths.

Soil	s_{ur}		$s_{ur(3\ cm)}$	
	(kPa)	r^2	(kPa)	$r^2_{(3\ cm)}$
EPK Kaolin	4.7	0.984	4.0	0.9954
BBC	3.5	0.9756	3.0	0.9961
Burswood	7.0	0.9963	6.7	0.9977
Dalia	4.9	0.9959	4.6	0.998
Gulf of Mexico	7.1	0.9969	6.8	0.9985
Onsøy	3.5	0.9611	2.7	0.9933

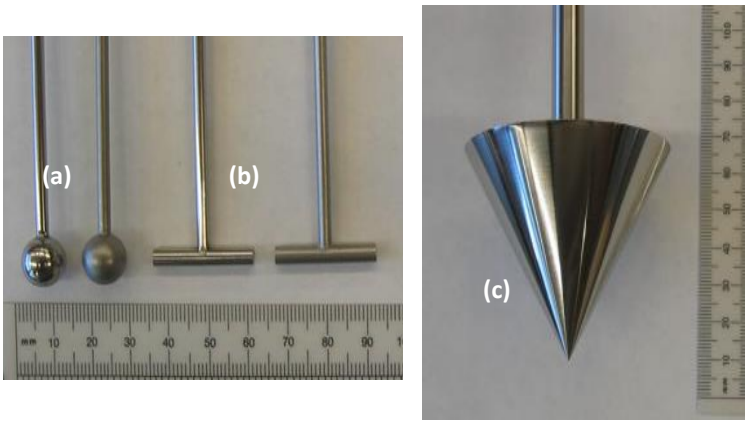

Figure 2.1. Smooth (left) and rough (right) miniature (a) ball and (b) t-bar penetrometers and (c) push cone with smooth surface finish.

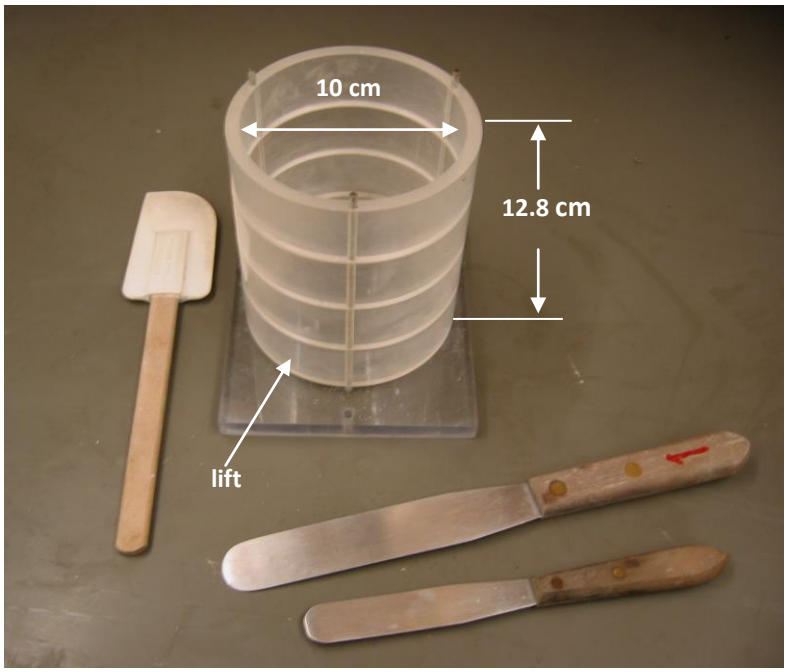

Figure 2.2. Specimen container with spatulas used for specimen preparation.

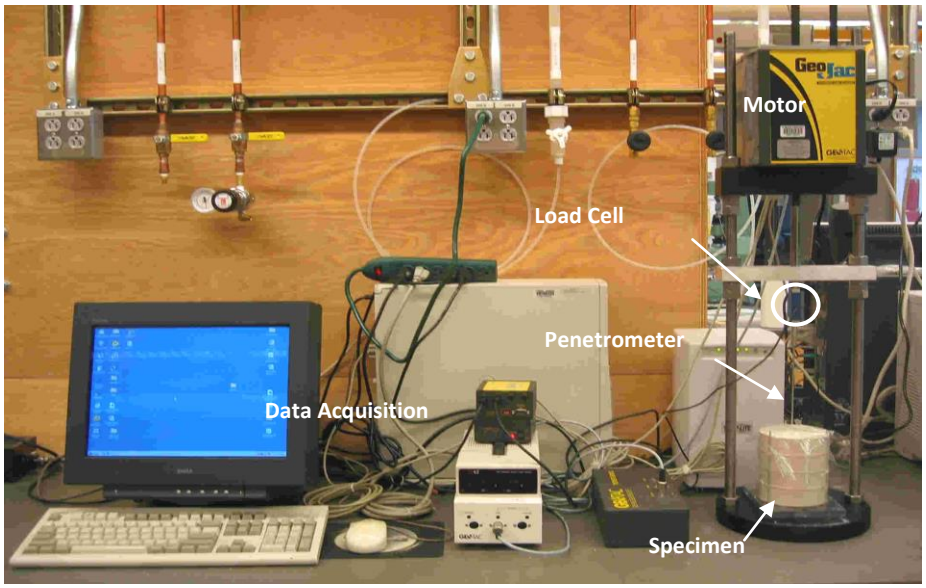

Figure 2.3. Data acquisition and load frame for miniature penetrometer and Cone testing.

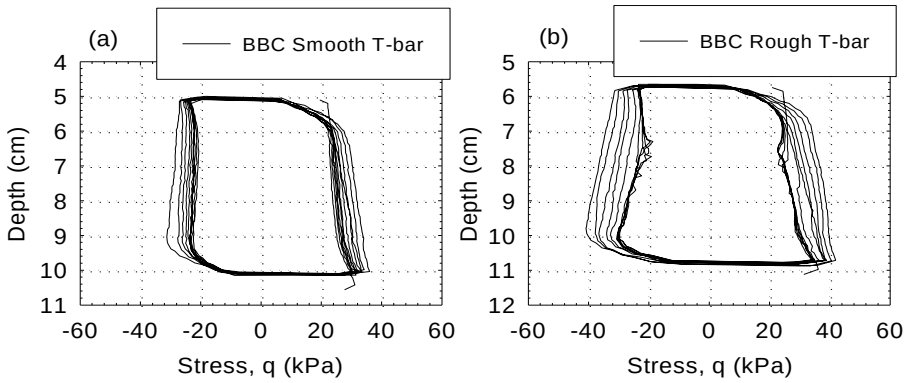

Figure 2.4. Cyclic stress curves using a (a) smooth and (b) rough t-bar penetrometer in BBC.

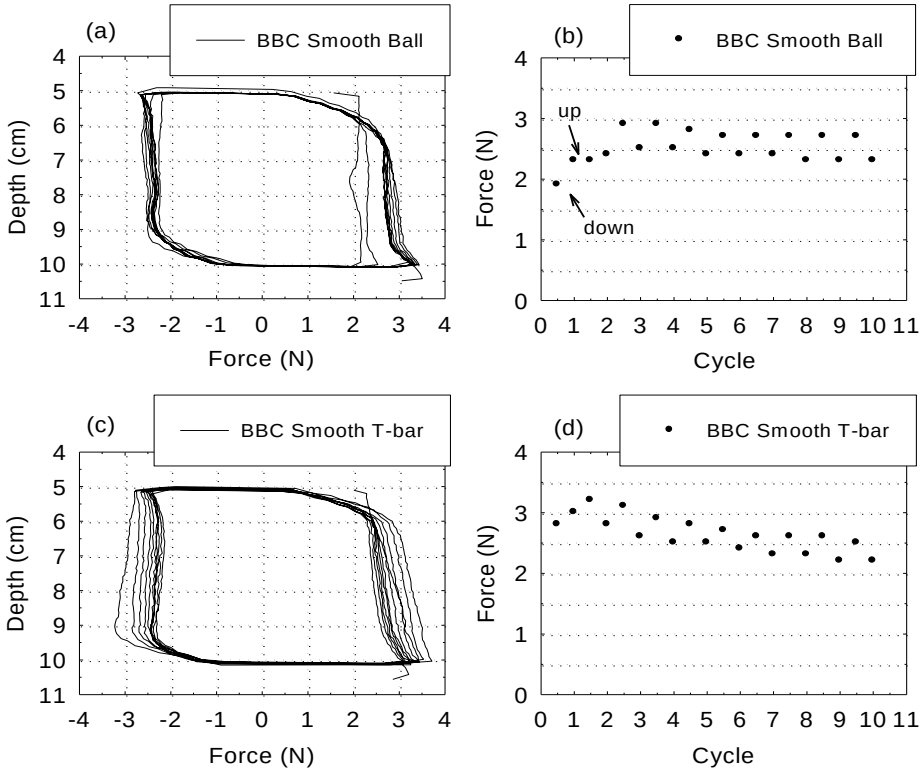

Figure 2.5. Smooth ball penetrometer (a) cyclic force-depth curve, and (b) force-cycle data for z = 7.5 cm, and smooth t-bar (c) cyclic force-depth curve, and (c) force-cycle data for z = 7.5 cm in BBC.

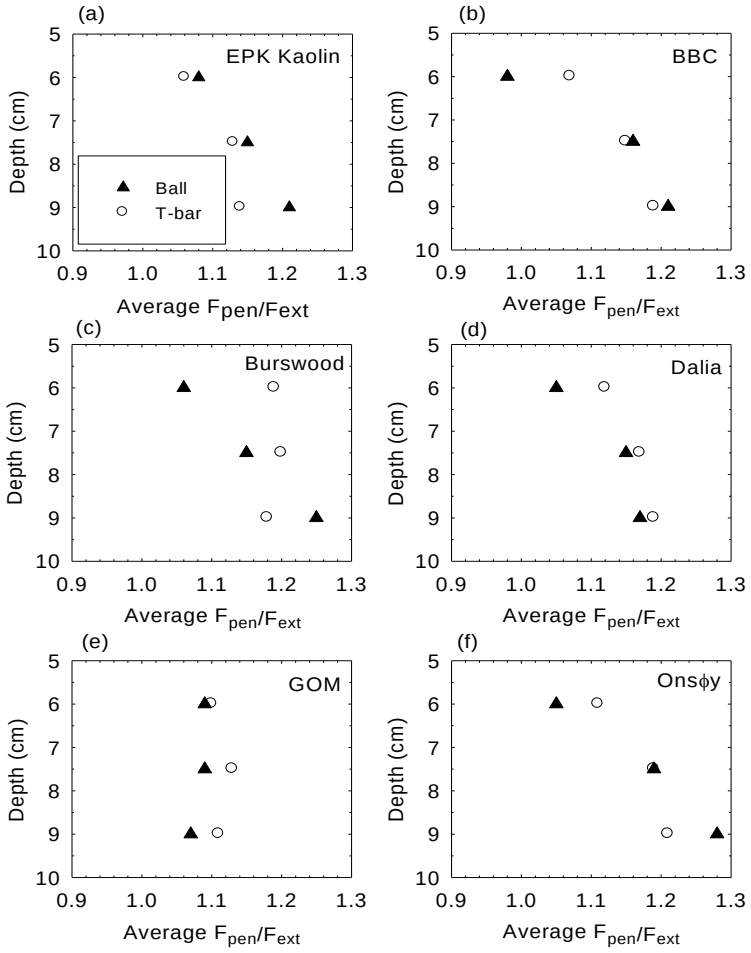

Figure 2.6. Depth verse average F_{pen}/F_{ext} for (a) EPK Kaolin, (b) BBC, (c) Burswood, (d) Dalia, (e) Gulf of Mexico, and (f) Onsøy.

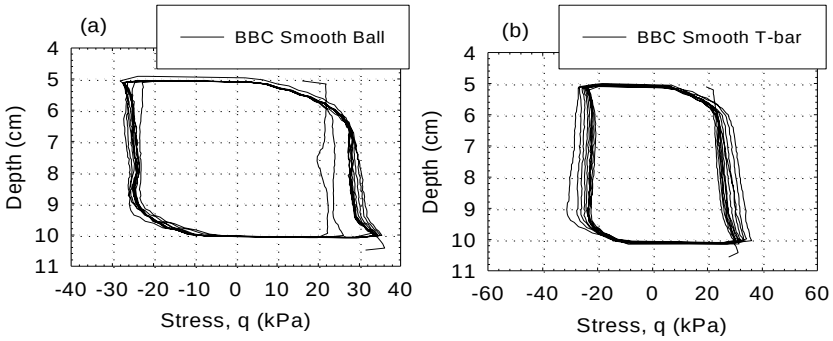

Figure 2.7. Cyclic stress curve using the smooth (a) ball and (b)t-bar penetrometer on BBC.

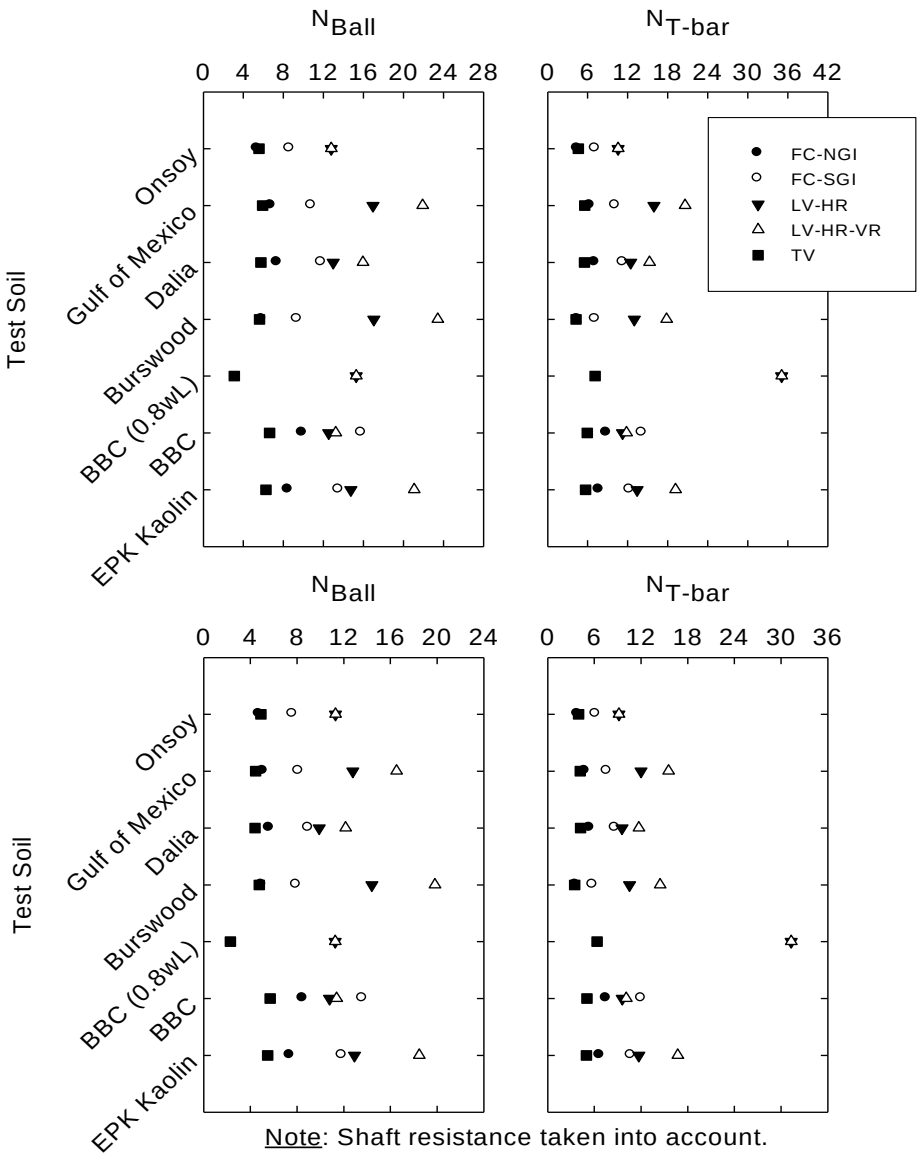

Figure 2.8. Summary of range of N-factors calculated for all test soils uncorrected (above) and corrected (below) for rod resistance.

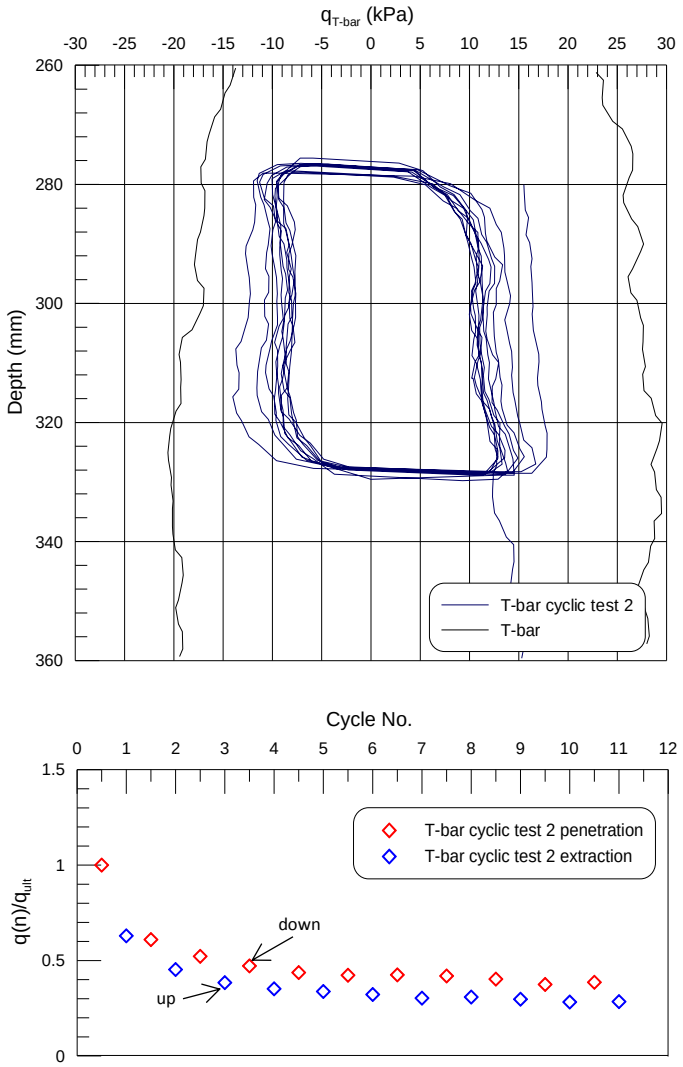

Figure 2.9. Example results from a cyclic test and force degradation curve taken from Egypt-G (BC59).

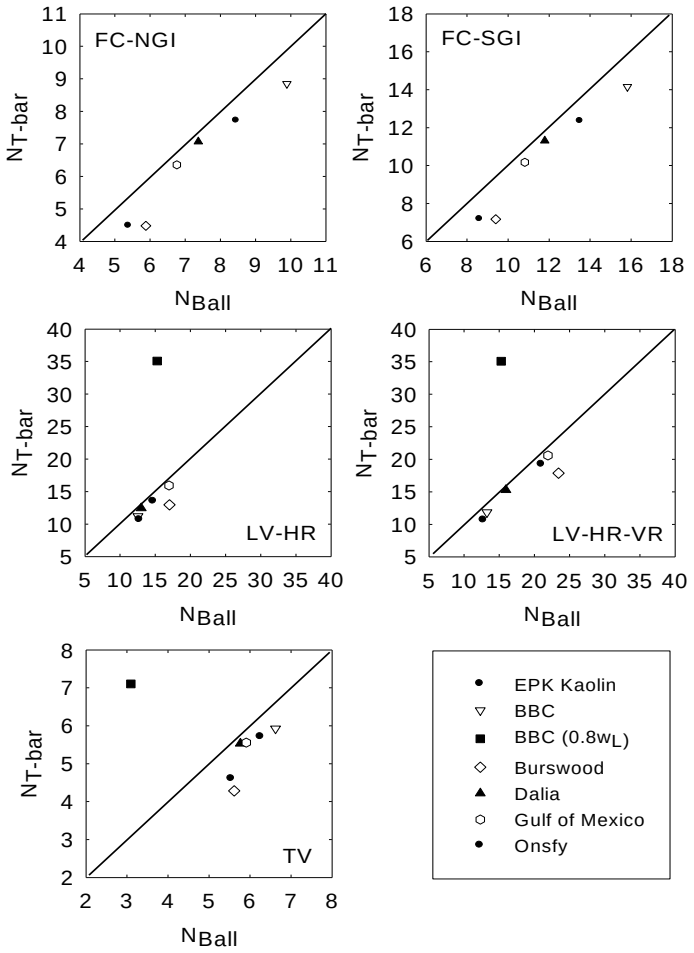

Figure 2.10. Correlations between N_{Ball} and $N_{T\text{-}bar}$ for a given reference test.

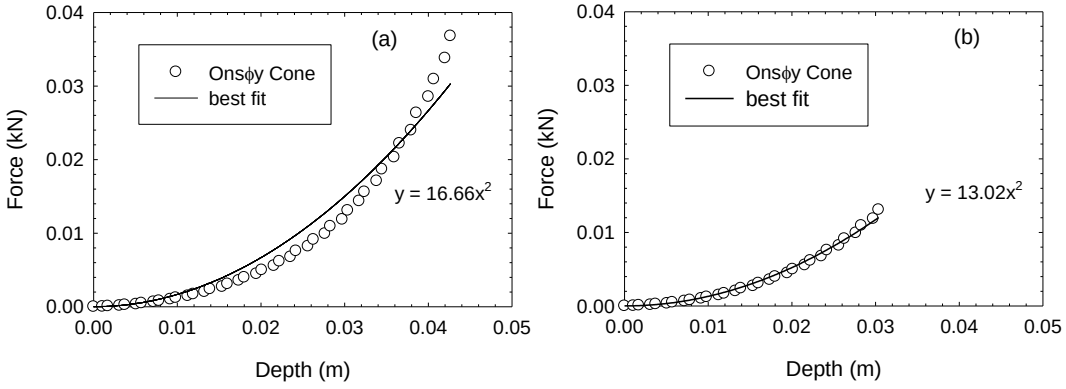

Figure 2.11. Force curves for (a) full penetration and (b) to a depth of 3 cm using the smooth push cone penetrometer in Onsøy.

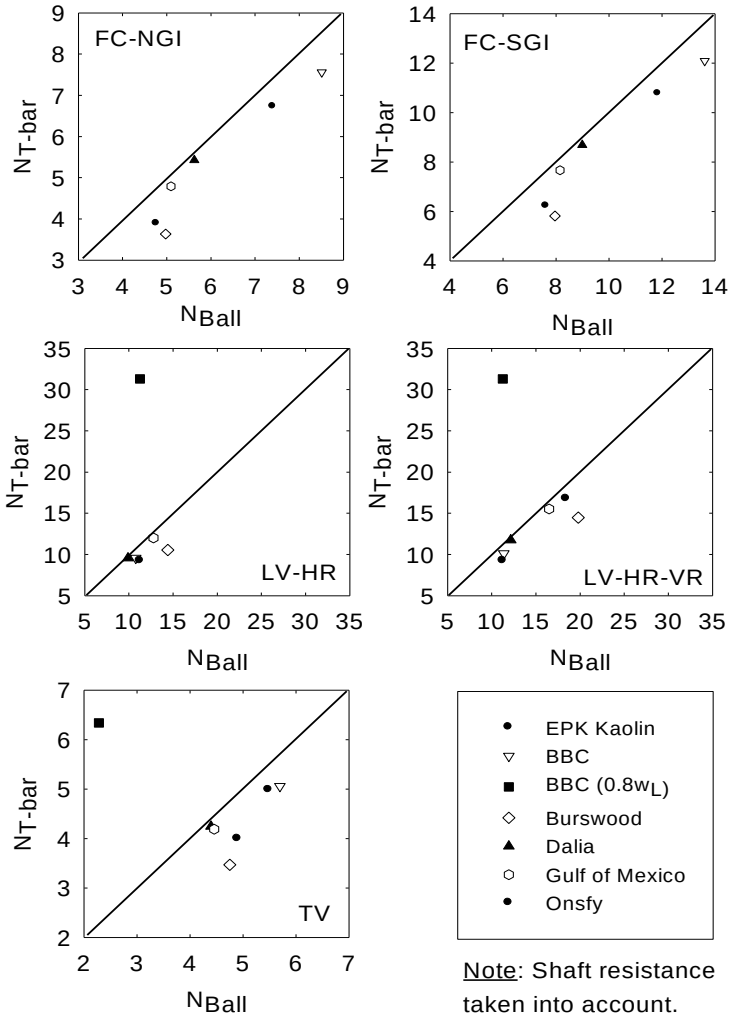

Figure 2.12. Correlations between N_{Ball} and $N_{T\text{-}bar}$ for a given reference test corrected for rod resistance.

CHAPTER 3

RECOMMENDED OFFSHORE BOX CORE TESTING PROTOCOL AND SITE CHARACTERIZATION USING MINIATURE FULL FLOW PENETROMETERS AND MOTORIZED VANE

3.1 Abstract

Full flow penetrometer testing in the box core offers the ability to collect high resolution data on very soft sediments (2-10 kPa) in the upper half meter of the seabed which often influences pipeline behavior starting from construction and continuing throughout the operational life of the pipeline. This study focuses on the development of testing equipment and protocol for box core samples using full flow penetrometers (t-bar and ball) and motorized vane. Recommendations are provided for testing procedure and data evaluation based on sites specific data collected from six pipeline soil investigations.

3.2 Introduction

Development of offshore oil and gas fields in deeper waters is possible due to technological advances. Deep water pipeline design methods continually change to improve safety of pipeline operation, ease pipeline construction, and reduce costs. Controlled lateral buckling is a method of pipeline design that has become increasingly popular for offshore pipeline construction because it addresses the above three concerns.

Controlled lateral buckling design allows the pipeline to move along the seabed. Design of these pipelines takes into account movement during construction and operation of the pipeline. Often, only the first half meter of the seabed is engaged. Therefore, assessing soil strength and predicting soil behavior is important for safe and effective design and operation.

Many deep water pipeline routes are located in areas consisting of very soft fine-grained sediments. Common testing and sampling practices often miss or distort this zone. The

combination of box core sampling with miniature full flow penetrometer and motorized vane testing has proven effective for characterizing very soft sediments in the upper half meter of the seabed. The box corer is able to collect large diameter samples of soft sediments with little disturbance to the sample, while miniature full flow penetrometers are sensitive to small strength changes which help better understand soft sediment transformation from intact to remolded states through cyclic testing. This paper discusses equipment development and test protocol recommendations for box core testing using miniature full flow penetrometers and motorized vane based on experience collecting and interpreting box core data from six offshore pipeline soil investigations.

3.3 Background

The upper half-meter of the seabed is of particular interest for pipeline design. Soil strengths in this zone are typically 2-10 kPa for fine-grained sediments, which is very difficult to accurately characterize using conventional *in situ* testing and sampling methods. Therefore, new sampling and testing techniques needed to be developed to accurately characterize this upper zone of the seabed.

Full flow penetrometers were first developed in the early 1990s to obtain more accurate measurements of undrained and remolded shear strengths of soft offshore sediments (Stewart & Randolph 1991). The large ratio of the projected probe area to rod area of the full flow penetrometers increases penetrometer sensitive and allows for identification of small strength changes with depth. The full flow failure mechanism almost eliminates an overburden pressure correction (commonly applied to CPTs) because soil flowing around the probe theoretically ends in the same position it started, eliminating the correction. Undrained shear strength, s_u, is calculated as (Stewart & Randolph 1991):

$$s_u = q/N \quad (3.1)$$

where:

q = t-bar or ball resistance

N = bearing capacity factor

The box core, initially used for ecological studies, was adapted for geotechnical pipeline site investigations by Low & Randolph (2008) to collect a large sample (50 x 50 x 50 cm) of soft sediments. Compared to a 3" Shelby tube (7.6 cm diameter) and Jumbo piston sampler (10 cm diameter), the cross-sectional are of the box corer is 55 and 31 times greater, respectively. As sampler diameter increases, the volume of soil that remains intact increases. Box core samples are difficult and costly to transport because of their large size and is the drive for development of new testing equipment that can be easily deployed offshore, tested directly in the box core sample, and is sensitive to small strength changes and low resistances.

The DMS was the first full flow penetrometer testing equipment designed for box core testing by the University of Western Australia in collaboration with TDI Brooks Instrumental (Randolph et al. 2007). The DMS uses a miniature t-bar or ball to measure intact and remolded s_u by measuring probe resistance using a load cell located behind the probe (Hill & Jacob 2008). The DMS is self-contained, has a built-in microcomputer, operates manually, and uses a digital tape to measure probe depth and penetration rate (Dingle et al. 2008). Because the probe is operated manually, the consistency of push rate is operator dependent. A temperature correction is also applied to DMS data due a zero shift in the load cell due to calibration at ambient temperature, but operated in sample temperature (often 10^{o}C).

The Fugro DECKSCOUT^{TM} was developed to test soft sediments collected by a 0.5 x 0.5 x 0.5 m box corer using a 12 mm diameter and 75 mm length t-bar with a test rate of 0.01-20

mm/s (Puech et al. 2011). With its current configuration, testing using the DECKSCOUT^{TM} can only take place along the edge of the box corer.

Laboratory testing using the DECKSCOUT^{TM} was also performed on reconstituted Gulf of Guinea soil and an artificial soil (50/50 bentonite and kaolin) with a water content of 110-150%. Laboratory testing was performed at 2-20 mm/s. To observe the failure mechanism around the t-bar with depth, cyclic t-bar tests were performed against a glass plane. From this testing Puech et al. (2011) observed two failure mechanisms, shallow and deep. Shallow failure occurred until approximately 12-15 probe diameters at which time flow transition to the deep mechanism which matched numerical modeling by Barbosa-Cruz & Randolph (2005), Zhou & Randolph (2009), and White et al. (2010).

Currently based on laboratory, field, and numerical analysis, there is much discussion on selection of N to convert t-bar and ball resistance to s_u. Initially N was believed to have a unique solution of 10.5 (Randolph & Houlsby 1984). Later Stewart & Randolph (1991) found N to deviate up to 13% and further studies by found greater variation (Randolph et al. 2000; Lu et al. 2001; Lunne et al. 2005; Randolph & Andersen 2006; Low & Randolph 2010; Low et al. 2010; DeJong et al. 2011). For example, Low & Randolph (2008) compared t-bar and field vane testing in the box core, finding N to fall between 9.5 and 13.5 in reference to the field vane. Based on empirical and theoretical studies, $N_{T\text{-}bar}$ is typically taken as 11.5 and 13.5 for intact and remolded testing, respectively. Further research of cause behind variation in N is needed.

3.4 Equipment Development

One of the major goals of this study was the development of computer automated strength tests for soft to very soft sediments sensitive to small strength changes. Two types of box corers were used in this study for collection of seabed sediments: a large (50 x 50 x 50 cm)

and small (25 x 25 x 50 cm) box. The large box core consisted of a seabed frame, weights, and box with a spade cutting shoe. The small box also includes a seabed frame, weights, and box. Instead of a spade cutting shoe, jaws close over the bottom of the box (Boland & Rowe 1991). The small box was only used in Maine.

Box core sample were collected by deploying a seabed frame with box and open cutting shoe off the side of the boat using a winch and A-frame. Once the frame was in contact with the seabed, weights were released, and the box penetrated the seabed under its own self weight. The cutting shoe closed over the bottom of the box after sampler penetration stopped and the frame was pulled up on deck for characterization and strength testing.

After the box core was removed from the box core frame, miniature full flow penetrometer testing (t-bar and ball) was performed on the sample to obtain intact and remolded undrained shear strength (s_u and s_{ur}) profiles. Both the t-bar and ball were made of stainless steel with a smooth polished finish. Only probes with a smooth surface finish were tested because previous studies by Boscardin (2007) found that smooth probes tended to stabilize on a minimum strength value in fewer strokes than rough. Though smooth and rough probes tended to measured similar s_u and s_{ur} values. The t-bar has a length of 49.3 mm and diameter of 7.9 mm. The diameter of the ball is 22.2 mm (Table 3.1). Both probes attach to a 6.35 mm push rod in which the projected area of the probe to rod was the recommended 10:1 (Einav & Randolph 2005).

Miniature full flow penetrometers were pushed at a constant rate of 2 mm/s using a GeoJac load frame controlled by a computer automated data acquisition. Probe resistance was measured using a low capacity Interface load cell located at the top of the push rod as shown in Figure 3.1.

Motorized vane (MV) testing with friction reducer was performed after full flow penetrometer testing to obtain a second measure of s_u and s_{ur} and assess the bearing capacity factor, N, for a given site for the t-bar and ball. A vane with a height and diameter of 38.1 mm and 19.1 (H/D =2) was used. The friction reducer is a Teflon cone located 100 mm above the center of the vane blade to reduce rod length in contact with the soil during testing.

Two types of MV were used. First, a motor attached to an ELE laboratory vane in which peak shear strengths were recorded. Second, a computer automated MV using GeoJac load frame for vertical displacement, a MicroMo motor controlling rotation, and an Interface torque transducer measured resistance during rotation.

Simplicity and durability were two driving forces behind equipment design. Simplicity, meaning easy equipment repairs minimizing downtime. Because the equipment is often tested in saltwater environments, part and material were selected and designed to reduce maintenance.

3.5 Methods

A standard set of procedures was followed during box core testing. This section focuses specifically on full flow penetrometer and motorized vane testing. The recommended protocol section presents recommended testing procedures for the entire box core testing program.

All penetrometer testing (t-bar, ball, and vane) was performed in the center 100 cm^2 of the box spaced 10 cm apart (Figure 3.2) to prevent interference between tests (Randolph & Anderson 2006). Rod testing was conducted first to identify stiff layers that may cause the t-bar or ball to exceed the load cell capacity. The rod's diameter is the same as the rod connected to the t-bar and ball with a smooth polished surface finish coming to a 60^o apex. T-bar testing followed rod testing preceded ball and motorized vane testing.

Intact and remolded shear strength was evaluated using Equation 3.1 first presented by Stewart & Randolph (1991). Because the load cell was located at the top of the rod as shown in Figure 3.1, two corrections were applied to the penetrometer resistance. First, the total measured resistance was corrected for rod resistance by taking the difference of the measured probe (t-bar or ball) resistance and the up-stroke resistance of the rod (to isolate side friction). Second, penetrometer resistance was corrected for overburden pressure displaced by the rod during testing by:

$$q_{net} = q_c - \frac{A_s}{A_p}\gamma d \quad (3.2)$$

where:

q_{net} = net penetrometer resistance

q_c = corrected penetrometer resistance

A_s = projected rod area

A_p = projected penetrometer area

γ = total unit weight

d = penetrometer depth at apex

The overburden correction was based on total unit weight because these probes cannot measure pore water pressure. Additionally, the overburden pressure was reduced by approximately 1/10th corresponding to the ratio of projected rod to penetrometer area (A_s/A_p). The combination of these two corrections generally amounted to an average decrease in resistance of 16% and 22% for the t-bar and ball.

Penetrometer testing was split into two phases: (1) profile, and (2) cyclic testing. A strength profile test was performed first in the box corer at a rate of 2 mm/s. A profile consists of a down- and up-stroke over the full sample depth. Next, the probe was lowered to the first

cyclic test depth. Depending on sample recovery, one to three cyclic tests were performed in each sample generally centered around 15, 30, and 45 cm depth (for a 50 cm recovery). A cyclic test consisted of 10 down- and up-strokes over a 5 cm length at the rate of 2 mm/s. The remolded shear strength is the soil strength measured at mid-depth of the 10th cycle. Figure 2.9 presents an example of a cyclic test and corresponding force degradation curve.

Profile and cyclic testing was first performed using the t-bar in a single location followed by rod testing in the same hole to estimated rod resistance. Ball testing with rod testing down the same hole followed. Generally, only cyclic testing was performed using the t-bar due to time constraints with the sample.

Motorized vane testing in the box core served as a secondary measure of s_u and s_{ur} and as a reference value for evaluating intact and remolded N (N and N_{rem}). The large vane was used for all MV testing. The vane was rotated at 6^o/min in accordance to the British Standard (BS1377-7:1990). The vane test was performed at 10 cm intervals starting at a depth of 10 cm in box core collected in Egypt. For all other sites, testing was performed at mid-depth of cyclic tests for easy assessment of N_{rem}. Assessment of s_u and s_{ur} followed that of ASTM D4648 (2002) for SI units:

$$s_u \text{ or } s_{ur} = \frac{2T}{\pi D^2\left(H-\frac{D}{3}\right)} \quad (3.3)$$

where:

s_u = intact undrained shear strength

s_{ur} = remolded undrained shear strength

T = peak torque

D = vane diameter

H = vane height

Soil was remolded by rotating the vane at a rate of 2700°/min for 10 revolutions before remolded MV testing.

The main purpose of MV testing in the box core was to obtain a reference value to evaluate N and N_{rem} for the t-bar and ball at a given site. Therefore, for a given site, four N-values were evaluated: $N_{t\text{-}bar}$, N_{ball}, $N_{rem,t\text{-}bar}$, and $N_{rem,ball}$. The bearing capacity factor was calculated as:

$$N = \frac{q}{s_{u,vane}} \tag{3.4}$$

where:

q = t-bar or ball resistance

$s_{u,vane}$ = shear strength measured by the vane

Bearing capacity factors were calculated for each box core over a range of depths. But to convert q to s_u, an average N was used across the site for the ball and t-bar. Additionally, N was adjusted for changing flow mechanisms around the probe following methodology by White et al. (2010). The flow of soil around the t-bar and ball is either a shallow or deep flow mechanism. For shallow flow, N incorporates change in soil strength and soil buoyancy as it relates to surface heave and cavity opening. Deep flow refers to the full flow failure mechanism.

3.6 Test Sites

Box core sampling with miniature penetrometer testing was collected and performed at six offshore sites – two sites in Norway (Norway-L and -O), three sites in Egypt (Egypt-G, -R, and -T), and at one site in Maine. A summary of soils properties at each site is presented in Table 3.2.

Norway-O and Norway-L generally consist of very soft clay in the upper half meter of the seabed with average undrained shear strengths, s_u, of 2.0-4.5 kPa in reference to the t-bar ($s_{u,t\text{-}}$

$_{bar}$). Seven box core samples were collected and tested at Norway-O in 2010 and 16 at Norway-L in 2009. Water depths at Norway-O are 850-920 m and 1230-1320 m at Norway-L.

The Egypt soil investigations occurred in 2008. Water depth among Egypt-G, -R, and -T vary between 150 m and 800 m. The test sites are located in deltaic deposits and are still undergoing deposition. Geophysical studies show evidence of small landslides. The upper half meter of the seabed generally consists of very soft olive brown clay with average $s_{u,t\text{-}bar}$ of 1.5-3.0 kPa. A total of 57 box corers were collected among the three sites. Thirteen box corers were collected at Egypt-R, 12 at Egypt-G, and 32 at Egypt-T.

Four box core samples were collected as part of a preliminary soil investigation for Maine Wind in collaboration with the University of Maine in 2010. The site was located approximately 3 miles off Monhegan Island in Maine waters. The site consisted of undulating bedrock. Troughs were filled with fine-grained sediment in which all soil samples were collected. Box core samples of the upper half meter of the seabed consisted of very soft brown clay with average $s_{u,t\text{-}bar}$ of approximately 4.5 kPa.

3.7 Results and Discussion

3.7.1 Motorized Vane Testing

Two types of motorized vanes were developed and used in this study: (1) an ELE vane head attached to a speed controlled motor (alpha), and (2) a computer automated motorized vane (beta). The motorized vane was used to obtain a secondary shear strength profile and as a reference strength to assess N for a given site.

The alpha vane was used at all test sites except Norway-O and Maine. In general, motorized vane intact and remolded shear strength profiles were greater than t-bar and ball

profiles. This behavior is most likely related to the different failure mechanisms: a cylindrical shear failure (MV) verses full flow mechanism (t-bar and ball).

The beta motorized vane continually measures resistance throughout the duration of the test giving a better understanding of soil behavior before and after failure. The typical failure curve of an intact soil increases in strength to a peak strength before failing and stabilizing on a residual strength. Since remolded strength is soil strength at its weakest state, the remolded strength curve increases and asymptotically approaches s_{ur}, which tends to be equal or be less than the residual strength of the intact soil (Figure 3.3).

Table 3.3 presents average intact and remolded shear strengths measured by both vanes. The average intact shear strengths measured by the alpha and beta vane tend to be similar for soils of similar strength range.

3.7.2 Stress Profiles

Results from full flow penetrometer testing were first analyzed as stress, q, profiles to observe change of strength with depth and layering within the box core sample. Stress profiles were converted to s_u profiles in reference to the motorized vane. Profiles across a given site were compiled into recommended upper and lower bound strength profiles for use in pipeline design.

The t-bar and ball stress profiles across all sites were of similar shape of increasing stress with depth (Figure 3.5). The t-bar tended to measure higher resistance then the ball. Similar observations were made by Low & Randolph (2010) using miniature penetrometers on laboratory consolidated box core specimens and by Yafrate & DeJong (2006) at the Burswood site in Western Australia at depths less than 11 m using *in situ* t-bar and ball. Though, in general DeJong et al. (2011) found the *in situ* ball resistance to be 5-16% greater than the t-bar. Two

relationships were investigated further to understand discrepancies between t-bar and ball resistance measurements: (1) the ratio of the down- and up-stroke resistance, q_{down}/q_{up}, with depth, and (2) the measured t-bar and ball resistance with depth.

The ball showed a general increase in q_{down}/q_{up} with depth while the t-bar remained fairly constant (Figure 3.6). Randolph et al. (2006) observed that q_{down}/q_{up} tended to fall between 1.25 and 1.67 based on t-bar field testing. DeJong et al. (2011) found that q_{down}/q_{up} fell between 1.67 and 3.33 using the *in situ* t-bar and ball. In this study, the ratio of q_{down}/q_{up} for the t-bar generally fell between 1 and 2 and remained fairly constant with depth. The ball showed an increase in q_{down}/q_{up} with depth from 1 to 2.5 which may indicate a change in failure mechanism with depth. At shallow depths, soil was observed to be displaced by the probe forming an open cavity behind, and eventually at deeper depths, soil collapsed behind the probe. This observation suggests that the failure mechanism may not necessarily be full flow, but rather a sort of deep flow as described by Tho et al. (2012). Most of the samples tested were of uniform composition and showed very little layering.

A linear relationship exists between the ball and t-bar resistance ($q_{t\text{-}bar}/q_{ball}$). Comparing discrete depths, the slope of the linear fit increases between 10 cm to 20 cm depth of 1.30 to 1.60 and, thereafter, remains fairly constant at 1.60 with the exception of 30 cm depth in which the slope decreased slightly to 1.46. After applying a rod resistance correction, the slope increased slightly to 1.60-1.70. The slope remained at 1.30 between 10 and 20 cm depth. DeJong et al. (2011) found the relationship to be closer to 1.0 (ranging from 1.0 to 1.2 for $q_{ball}/q_{t\text{-}bar}$) for the *in situ* penetrometers.

The linear fit between the t-bar and ball was compared for all test depths: (a) uncorrected, (b) corrected for rod resistance, (c) corrected for rod resistance for depths greater than 20 cm, and (d) corrected for overburden pressure (Figure 3.7). The slope of the linear fit

increased when corrected for rod resistance. The slope of the linear regression also increased after isolating data collected from greater than 20 cm depth (full flow engaged). The overburden correction caused the slope of linear fit to increase. The slopes of plots (c) and (d) were almost equivalent of approximately 1.61 and the highest of the four plots. Note that plot (d) is in terms of stress, not force. The relationship of the t-bar and ball resistance is similar to $N_{t\text{-}bar}/N_{ball}$ of 1.5 taking the average N across all sites.

The linear relationship between t-bar and ball resistance is most likely the result of different flow conditions around each probe. Even though full flow is believed to eventually develop behind the penetrometers with depth, the linear relationship between the t-bar and ball suggest that perhaps full flow is not developing behind the ball. Instead, a void may be forming behind the ball. During testing, open cavities behind both probes were observed at the surface, with the cavity closing at a deeper depth for the ball than the t-bar. The void behind the ball is suspected to be present at deeper depths (Figure 3.8), otherwise q_{ball} would equal $q_{t\text{-}bar}$ and N_{ball} would equal $N_{t\text{-}bar}$. The formation of void behind the ball may result from soil collapsing behind the ball and adhering to the rod preventing soil from filling behind the probe. Therefore, only partial flow instead of full flow occurs around the ball. Tho et al. (2012) has observed similar behavior with FE modeling of soft seabed sediments flow around the t-bar with for diameters of 4-40 cm. Puech et al. (2011) observed similar void formation during t-bar testing against a glass plate. The diameter of the miniature t-bar used in this study is very small (< 8 mm) and likely to be mainly engaged in full flow.

The surface area of the ball is 1.25 times greater than the t-bar and is therefore expected to be greater as observed in field testing (Yafrate & DeJong 2006). If flow is only occurring around the bottom half of the ball, then the surface area of the t-bar in contact with the soil becomes greater than the ball by 1.6 which corresponds to $q_{t\text{-}bar}/q_{ball}$ (Figure 3.7).

Miniature penetrometer stress profiles were also compared with *in situ* CPTu, t-bar, and ball testing. Often the miniature t-bar and ball profiles were bounded between the *in situ* ball or t-bar and the CPTu. The *in situ* ball and t-bar makes up the lower bound and the CPTu is the upper bound. Figure 3.9 presents representative curves at a given site. Miniature t-bar profiles most closely resemble CPTu profiles in shape and resistance, but with higher resolution detecting small strength changes. *In situ* t-bar and ball results may be affected by seabed disturbance from load frame touchdown (Lunne et al. 2005) and/or uncertainty of probe positioning in relation to the seabed resulting in a lower bound strength profile. Lunne et al. (2011) gives recommendations for reducing measurement error when using the *in situ* t-bar and ball offshore.

3.7.3 Cyclic Penetrometer Testing

For each box core, at least one cyclic profile was performed with the t-bar, and when time permitted with the ball. Cyclic testing was not performed in boxes containing sand or of low recovery (< 20 cm). The stress at the mid-depth of each cycle was normalized by the intact stress, q_{ult}, at that depth to develop force degradation curves. In all curves, normalized stress decreases with each penetrometer stroke until stress stabilized on a minimum resistance which often occurred within 3-6 cycles. The down-stroke $q_{(n)}/q_{ult}$ was generally higher than the up-stroke and both tended to stabilized between 0.2-0.5.

3.7.4 Shear Strength and Sensitivity Profiles

In general, stress was converted to shear strength using a bearing capacity factor, N (Equation 3.1). For initial evaluation of s_u and s_{ur} for a given site, N was selected based on the literature of 11.5 for the t-bar and 9 for the ball. Finial selection of N for a given site was based

on N and N_{rem} in reference to MV and literature. Calculation of N and general trends are discussed in the proceeding section.

Overall, $s_{u,t\text{-}bar}$ tends to be greater than $s_{u,ball}$ and most likely related to the changing flow conditions around the probes with penetration depth. Shear strength profiles were similar in shape to stress profiles. On average $s_{u,t\text{-}bar}$ was 2.0-4.5 kPa and between 1.5-3.5 kPa for the ball (Table 3.3). The average ball and t-bar s_{ur} was 0.3-1.5 kPa.

3.7.5 Comparison of Motorized Vane and Full Flow Penetrometers

The shear strength measured with the motorized vane follows the general shape of the t-bar and ball profile and is often greater than $s_{u,t\text{-}bar}$ and $s_{u,ball}$. The average $s_{u,MV}$ was 2.3-4.5 kPa and the average $s_{ur,MV}$ was 0.5-1.9 kPa (Table 3.3). Likewise, the sensitivity of the MV is greater than the ball and often the t-bar. Differing failure mechanisms of the penetrometers and MV may be the cause of strength measurement discrepancies.

3.7.6 Comparison of Strength Testing in Box Corer to Sub-samples

Strength testing was also performed on subsamples collected from the box corer in either the onshore or offshore lab (Table 3.4). Sub-samples were collected with 76.2 mm OD and 72.6 ID Shelby tubes. Intact and remolded shear strength in the laboratory was measured using the fall cone (FC) and lab vane (LV). The average shear strength measured using the FC was 2.0-5.4 kPa, and 2.3-2.6 kPa using the LV. The average $s_{ur,FC}$ was 0.7-1.7 kPa and 0.6-0.7 kPa with the LV. Average FC sensitivity was 2.8-5.8, and the LV sensitivity was 4.0-4.5.

The average FC intact and remolded s_u generally measured higher than the average miniature t-bar, ball, and MV. The average $s_{u,FC}$ was lower than the MV at Egypt-R and Norway-

O. The remolded FC shear strength was lower than the t-bar, ball, and MV at Norway-L, and lower than the t-bar and MV at Norway-O.

The average intact and remolded LV shear strength were generally higher than the t-bar, ball, and MV. Though at Egypt-G, the intact and remolded shear strength of the LV matched the MV, and at Egypt-T, the intact LV shear strength was lower than the t-bar.

The process of sampling, transportation, and specimen preparation affect intact shear strength measurements (Ladd & DeGroot 2003). Limiting straining of the sample during the sampling process preserves sample quality. Theoretically, shear strength measured in the box corer should be higher than laboratory measurement because disturbance caused by sub-sampling, transportation and sample preparation are avoided. Soil layers tended to compress during sub-sampling because the soil was apt to adhere to the container walls. This consolidation may have caused an increase in density and consequently an increase in shear strength. Other measurement discrepancies are the result of differing failure mechanism for each type of test from full flow for the ball and t-bar to cylindrical for the MV and LV to conical using the FC.

Theoretically, the remolded shear strength measured in the box corer and sub-sample should have been equivalent. Remolded shear strength is the minimum soil strength at constant water content. Therefore, loss in water may explain a higher s_{ur} of the sub-samples verses the box corer. Again, these discrepancies may be the result of differing test failure mechanisms.

Fall cone testing was also performed on two small samples collected from a box corer at Norway-L. Samples were collected by carefully digging to the test depth, pushing a 45 mm long Shelby tube into the soil, slipping a thin metal sheet under the bottom of the tube, and removing the tube by digging soil out around it. The intact shear strengths using FC were 7.7 and 3.7 kPa, both measured at 15 cm depth. Laboratory fall cone testing of the sub-sample taken

from the same box and depth measured s_u of 5.8 kPa. In comparison, the t-bar, ball, and MV measured s_u of 4.3, 3.6, and 4.8 kPa respectively, in the same box and depth. The differences between the two box core FC tests were either the result of a local disturbance in the box core or a localized change in layering. The shear strengths measured by the t-bar, ball, and MV were similar to the lower of the two fall cone tests making evident that the $s_{u,FC}$ of 7.7 kPa was due to some localized anomaly. No conclusion about general behavior of box core fall cone testing can be made because the data set is too small.

3.7.7 N-values

Stress was converted to shear strength using Equation 3.3 in which N was taken as the average N for a given site. Average N-values were calculated in reference to the MV using Equation 3.4. Table 3.5 presents average intact ball and t-bar N-values at each site. Table 3.6 presents average remolded N-values.

The average N across all sites is $N_{t\text{-}bar}$ = 11.6, N_{ball} = 7.7, and N_{rem} = 12. This gives a ratio of $N_{t\text{-}bar}/N_{ball}$ = 1.5. To depths of 20 cm, N tends to increase with depth and remain constant thereafter. In comparison to published N-values, N derived in this study falls on the lower end of the range (Stewart & Randolph 1994; Randolph et al. 2000; Lu et al. 2001; Einav & Randolph 2005; Lunne et al. 2005; Randolph & Andersen 2006; Yaftrate & DeJong 2006; Low & Randolph 2010; DeJong et al. 2011).

The confidence in N_{ave} was assessed by fitting probability curves to histograms. Only data collected from Egypt had a large enough sample size for statistical analysis. As shown in Figure 3.10, there was no correlation between sample size and standard deviation. The standard deviation of the ball tended to be fairly uniform, averaging 3.4, across the Egypt test sites. The average standard deviation of $N_{t\text{-}bar}$ was 5.9. Remolding caused the standard deviation to

increase. To compare the standard deviation of the ball and t-bar, the standard deviation was normalized by the average N (e.g., $\sigma_{t\text{-}bar}/\mu_{t\text{-}bar}$ and σ_{ball}/μ_{ball}). The normalized standard deviation of the t-bar tended to be less than the ball. This suggests that the t-bar is a more reliable measure of s_u and s_{ur}.

Intact N typically falls between 8 and 16. Three causes of N deviating beyond this range were identified. High N-values were obtained (N>16) when $s_{u,MV}$ readings were low, often less than 1.5 kPa. N-values were low (N<8) when q was low compared to $s_{u,MV}$. These low N-values were generally found at shallow depths (z<10 cm). N_{ball} was much less than $N_{t\text{-}bar}$ when q_{ball} was much less than $q_{t\text{-}bar}$ (often when $q_{ball} = 0.5q_{t\text{-}bar}$).

Remolded N-values tend to be less than N_{int} for the t-bar. Often when N was out of range, N was very high (>17) due to low $s_{u,MV}$ (<0.3 kPa). Results for all tests sites are presented in Table 3.5 and Table 3.6.

A differing flow condition from full flow is suspected to be a major factor of low stress measurements. Initially, the full flow mechanism of soil around the t-bar and ball was thought to be independent of depth (Stewart & Randolph 1991; Randolph & Andersen 2006). Boscardin (2007), Puech et al. (2011), and Tho et al. (2012) observed that full flow does not occur instantly, but develops with depth. Soil tends to close behind the ball at 5-10 cm depth and from 1-5 cm around the t-bar. White et al. (2010) developed a model to correct N at shallow depths to account for changing flow mechanisms from shallow to deep. Figure 3.11 illustrated the transition of N from shallow to deep flow in which N increases with depth until the failure mechanism changes to deep. The critical depth refers to this transition point. Figure 3.11 also compares profiles corrected and uncorrected for shallow flow. Since $N_{shallow}$ is lower than N_{deep} until critical depth, s_u increases in the zone of shallow flow.

The critical depth of the t-bar was compared to the ball for all Egypt sites. Note that White et al. (2010) developed this correction for the t-bar, but this study also applied the correction to the ball to get an estimate of ball critical depth. Since critical depth is a function of depth and probe diameter, the average critical depth of the t-bar of 12.4 cm is lower than the ball of 20.2 cm (White et al. 2010). This indicates that the flow mechanism around the ball at the first cyclic test depth needs further investigation as to the flow mechanism actually engaged. Otherwise ball cyclic testing should be performed at a deeper depth within the sample. T-bar cyclic testing is generally unaffected because the critical depth is generally located above the first cyclic test depth.

3.8 Recommended Testing Protocol

Box core characterization followed a standardized set of procedures for soil classification and strength testing. Once the box is removed from the test frame the procedures are as follows:

1. Describe soil noting any special sample characteristics (including recovery, degree of surface slope, undulations, marine life, etc.)
2. Photograph top of sample with unit and color scale for future reference.
3. Obtain a profile with the push rod.
4. Perform profile and cyclic testing with the t-bar to obtain s_u and s_{ur} profiles. Run the push rod down the t-bar hole to estimate rod resistance.
5. Perform profile and cyclic testing with the ball to obtain s_u and s_{ur} profiles. Run the push rod down the ball hole to estimate rod resistance. Ball testing may be skipped if time with sample is limited.

6. Obtain s_u and s_{ur} profiles using the motorized vane.
7. Collection sub-samples for laboratory index and strength testing.
8. If requested, bag remaining offshore sample for future laboratory testing (e.g., reconstituting samples in the laboratory).

Before further elaboration on testing protocol, it is suggested to take care when moving the box corer on deck after removal from the seabed frame by moving the sample gently as possible avoiding excessive vibrations and disturbances, ideally using a handcart, to maintain sample quality.

Soil descriptions should consist of a visual description of the sample surface including color, soil type, slope of surface, any unusual features, undulations, marine life, etc. A more detailed description of soil layering may be noted after testing and sub-sampling of the box corer. A photograph of the top of the sample should follow visual surface soil description with color scale and tape measure. If sample recovery is less than 250 mm, a second attempt at collecting a box core sample is recommended. Only one cyclic test is recommended for recoveries less than 300 mm and no cyclic testing for recoveries less than 200 mm due to edge effects.

It is recommended to use the lowest capacity load cell possible during full flow penetrometer testing to obtain higher resolution data. A profile with the push rod is performed first to locate any potential “stiff” layers of which may exceed the capacity of the load cell during t-bar or ball testing. If a “stiff” layer is present that may exceed load cell capacity, a lager capacity load cell should be used for t-bar and ball testing.

A t-bar profile follows push rod testing 10 cm from the push rod location. The t-bar is advanced to the first cyclic test depth after obtaining a profile. Between 1 and 3 cyclic tests may be performed in a sample depending on sample recovery. Generally 3 cyclic test can be

performed in samples with recoveries greater than 450 mm, and 2 cyclic tests in samples with recoveries between 300-450 mm, one cyclic test in samples with recoveries less than 300 mm, and no cyclic testing in samples less than 250 mm recover due to edge effects.

The push rod should be performed down the same hole as the t-bar hole after cyclic testing and used for rod resistance correction. A rate of 2 mm/s is suggested for all penetrometer testing (push rod, t-bar, ball). If the operator decides to use a different rate or probe, the rate of penetration should not exceed two probe diameters per second.

Ball testing should follow the same procedures as the t-bar. If time with the box is limited, ball cyclic testing or complete ball testing may be omitted. The t-bar is recommended as the preferred test because of greater certainty in development of the full flow mechanism at shallower depths. The ball test should be performed 10 cm away from t-bar and push rod test locations.

Motorized vane testing is generally performed after ball testing 10 cm away from all other penetrometer tests. The suggested test rate is 6^{o}/min following the BS1377-7:1990. Before testing, the MV should sit at test depth for 1 minute to allow dissipation of excess strains from insertion of the blade. Remolded testing used the same test rate. Soil is remolded by rotating the blade 10 times at a fast rate (2700^{o}/min is suggested). No wait time is needed between soil remolding and the start of the test. It is recommended to test the MV at mid-cyclic depth for easy evaluation of N_{intact} and N_{rem}.

Up to 4 sub-samples can be collected from the large box core and 2 for the small box. Ideally, thin walled, stainless steel Shelby tubes with a 10^{o} cutting edge should be used. Tubes may be pushed in by hand and carefully dug out. Before removing the tube, a flat metal or plastic plate should be inserted under the sampler to prevent loss of sample.

Bagged samples may be collected from the box core using a shovel and storing the samples in a sealed plastic bags or containers. Double bagging the samples is recommended to prevent water loss.

3.9 Conclusions

Miniature full flow penetrometer and motorized vane testing are useful for obtaining high resolution strength profiles of box core samples. In general, the t-bar measured higher resistance than the ball which implies that full flow may not be forming around the ball. With depth, q_{in}/q_{out} remained fairly constant for the t-bar and increased with depth for the ball. The increase of q_{in}/q_{out} for the ball also suggests changing flow conditions with depth. An open cavity was observed behind the ball at shallower depths and at deeper depth a void behind the probe is suspected. Further investigation into void formation behind the ball is recommended.

In general, $N_{t\text{-}bar}$ tends to be greater than N_{ball}. Based on this study's findings in reference to the motorized vane, $N_{t\text{-}bar} = 11.5$, $N_{ball} = 8$, and $N_{rem} = 12$ are recommended. Field testing indicates that N_{ball} should be greater than $N_{t\text{-}bar}$ by 10%. Since visual evidence during testing suggests flow conditions other than full flow around the ball and lower resistance measurements of the ball than t-bar, the t-bar is likely to be the more reliable probe for profiling shear strength in very soft seabed sediments.

It is therefore recommended to perform at least a t-bar test (consisting of profile and cyclic testing) with rod correction if time is limited for box core testing. Motorized vane should also be tested to obtain a secondary shear strength profile and to evaluate a site specific N.

Index testing in sub-samples using the laboratory vane and fall cone generally measured higher shear strengths than miniature penetrometer and motorized vane testing in the box

corer. Either the sub-samples gained strength because soil was compressed during the sampling process or there was a loss in water content.

Acknowledgements
This work was supported in part by the National Science Foundation under grant OISE-0530151.

3.10 References

ASTM Standards (2002). *Annual Book of Standards*, vol 4.80, Soil and Rock (I): D420-D5779. West Conshohocken, PA, USA.

Barbosa-Cruz, E.R., and Randolph, M.F. (2005). "Bearing capacity and large scale penetration of a cylindrical object at shallow embedment." *Proc., 1st International Symposium on Frontiers in Offshore Geotechnics*, ISFOG 2005, Perth, WA, 615-621.

Boscardin, A.G. (2007). "Evaluation of miniature full flow penetrometers and push cone for laboratory measurement of remolded undrained shear strength of soft clays." *Masters of Science Thesis*, Univ. of Massachusetts Amherst, Amherst, MA.

Boyland, G.S., and Row, G.T. (1991). "Deep-sea benthic sampling with the GEOMEX box corer." *American Society of Limnology and Oceanography*, 36(5), 1015-1020.

British Standards Institute (BSI) (1990). *Soils for civil engineering purposes – Part 7: Shear strength tests (total stress)*, Standard BS1377-7, London, BSI.

DeJong, J.T., Yafrate, N.J., and DeGroot, D.J. (2011). "Evaluation of undrained shear strength using full-flow penetrometers." *ASCE Journal of Geotechnical and Geoenvironmental Engineering*, 137(1), 14-26.

Dingle, H.R.C., White, D.J., and Gaudin, C. (2008). "Mechanisms of pipe embedment and lateral breakout on soft clay." *Canadian Geotechnical Journal*, 45(5), 636-652.

Einav, I., and Randolph, M. F. (2005). "Combining upper bound and stain path methods for evaluating penetration resistance." *International Journal for Numerical Methods in Engineering*, 63, 1991-2016.

Hill, A.J., and Jacob, H. (2008). "In-situ measurement of pipe-soil interaction in deepwater." *Proc., Offshore Technology Conference*, Huston, Texas, OTC19528.

Ladd, C.C., and DeGroot, D.J. (2003). "Recommended practice for soft ground site characterization." Proc., 12th *Panamerican Conference on Soil Mechanics and Geotechnical Engineering*, Boston, Massachusetts, 1, 3-57.

Low, H.E., and Randolph, M.F (2010). "Strength measurement for near-seabed surface soft soils using manually operated miniature full-flow penetrometers." *ASCE Journal of Geotechnical and Geoenvironmental Engineering*, 136(11), 1565-1573.

Low, H.E., and Randolph, M.F (2008). "Characterization of near seabed surface sediments." Proc., Offshore Technology Conference, Huston, Texas, OTC19149.

Lu, Q., Hu, Y., and Randolph, M.F. (2001). “Deep penetration in soft clays with strength increasing with depth.” *Proc., International Offshore and Polar Engineering Conference*, Stavanger, Norway, 2, 453-458.

Lunne, T., Andersen, K.H., Low, H.E., Randolph, M.F., and Sjursen, M. (2011). “Guidelines for offshore in situ testing and interpretation in deepwater soft clays.” *Canadian Geotechnical Journal*, 48, 543-556.

Lunne, T., Randolph, M. F., Chung, S. F., Andersen, K. H., and Sjursen, M. (2005) “Comparison of cone and t-bar factors in two onshore and one offshore clay sediments.” *Frontiers in Offshore Geotechnics*, 981-989.

Puech, A., Orozco-Calderon, M., and Foray, P. (2011). “Mini t-bar testing at shallow penetration.” *Proc., Frontiers in Offshore Geotechnics II*, London, UK.

Randolph, M. F. (2004). “Characterisation of soft sediments for offshore applications, keynote lecture.” *Proc., 2nd Int. Conf. on Site Characterisation*, 1, Porto, Portugal, 209–231.

Randolph, M.F., and Andersen, K.H. (2006). “Numerical analysis of t-bar penetration in soft clay.” *ASCE International Journal of Geomechanics*, 6(6), 411-420.

Randolph, M.F., and Houlsby, G.T. (1984). “The limiting pressure on a circular pile loaded laterally in cohesive soil.” *Geotechnique*, 34(4), 613-623.

Randolph, M.F., Low, H.E., and Zhou, H. (2007). “In situ testing for design for pipeline and anchoring systems.” *Proc. of 6th Int. Conf. on Offshore Site Investigation and Geotechnics: Confronting New Challenges and Sharing Knowledge*, SUT, London, UK, 251.

Randolph, M.F., Martin, C.M., and Hu, Y. (2000). “Limiting resistance of a spherical penetrometer in cohesive material.” *Geotechnique*, 50(5), 573-582.

Stewart, D.P., and Randolph, M.F. (1991). “A new site investigation tool for the centrifuge.” *Proc., Int. Conf. Centrifuge 1991*, Boulder, CO, 531-538.

Stewart, D.P., and Randolph, M.F. (1994). “T-bar penetration testing in soft clay.” *Journal of Geotechnical Engineering*, 120(12), 2230-2235.

Tho, K.K., Leung, C.F., Chow, Y.K., and Palmer, A.C. (2012). “Deep cavity flow mechanism of pipe penetration in clay.” *Canadian Geotechnical Journal*, 49, 59-69.

White, D.J., Gaudin, G., Boylan, N., and Zhou, H. (2010). “Interpretation of t-bar penetrometer tests at shallow embedment and in very soft soils.” *Canadian Geotechnical Journal*, 47, 218-229.

Yafrate, N.J., and DeJong, J.T. (2006). “Interpretation of sensitivity and remolded undrained shear strength with full flow penetrometer.” *ISOPE-06: International Society for Offshore and Polar Engineering*, San Franciso, CA.

Zhou, H., and Randolph, M.F. (2009). “Numerical investigation into cycling of full-flow penetrometers in soft clay.” *Proc., 3rd Australian-New Zealand Younge Geotechnical Professionals Conf.*, 151-156.

Table 3.1. Miniature penetrometer dimensions.

Probe	D (mm)	L (mm)	A_p (mm^2)	A_s (mm^2)	A_p/A_s (-)	Comments
Ball	22.2	-	388	32	12.1	
T-bar	7.9	49.3	389	32	12.1	L/D = 6.25
Rod	6.35	-	-	32	1	60° tip

Table 3.2. Summary of average soil properties at each test site.

	w_c	γ_T	PL	LL	PI	LI	Grain Size Distribution			$s_{u,fc}$ +		$s_{u,t\text{-}bar}$	
							clay	clay+silt	clay+silt +sand				
							< 2 µm	< 0.063 mm	< 2 mm	ave.	max.	ave.	max.
Site	%	kN/m^3	%	%	%	%	%	%	%	kPa	kPa	kPa	kPa
Egypt-G	100.2 (35.7-157)	15.36 (13.61-17.80)	38.7 (34.6-41.6)	79.6 (67.1-87.1)	41.0 (32.5-47.9)	1.52 (0.60-2.78)	46.0 (29.9-60.7)	94.4 (76.0-99.5)	99.0 (92.0-100)	3.2	12.0	2.1	5.5
Egypt-R	118.8 (76.5-181.3)	14.36 (13.52-16.3)	39.4 (33.6-42.1)	83.4 (74.3-91.4)	44.0 (36.5-49.3)	1.71 (1.22-2.34)	48.6 (37.9-60.7)	96.1 (76.0-100)	99.3 (92.0-100)	2.0	5.2	1.9	5.4
Egypt-T	100.3 (64.2-192.4)	14.14 (11.81-16.30)	40.3 (34.6-43.9)	86.3 (67.1-109.2)	46.1 (32.5-66.2)	1.57 (0.60-3.81)	15.2 (3.9-52.8)	51.2 (29.9-67.0)	96.7 (76.0-100)	4.3	17.0	3	41.3
Norway-L	84.5 (35.2-116.7)	15.30 (13.89-18.55)	25.9 (16.0-31.3)	66.2 (37.0-88.4)	40.3 (21.0-49.1)	1.45 (0.91-1.99)	46.3 (32.2-60.8)	85.6 (64.3-97.1)	98.1 (82.9-100)	5.4	9.6	4.4	7.6
Norway-O	166.6 (151.9-176.0)	12.88 (12.70-13.13)	43.2 (38.6-47.7)	95.5 (87.8-103.0)	52.2 (40.1-63.8)	2.47 (2.11-2.79)	48 (46-50)	97 (96-98)	100	4.0	6.4	2.7	3.8
Australia*	-	-	-	-	-	-	-	-	-	9.8	10	9.2	13.8
Maine	-	-	-	-	-	-	-	-	-	2.5	5.3	2.4	4.6
(min.-max.)													
*sandy													
+onshore lab													

Table 3.3. Summary of average intact and remolded shear strengths in box corers.

	Shear Strength						
	Motorized Vane		T-bar		Ball		
	Intact	Rem	Intact	Rem	Intact	Rem	MV
Site	kPa	kPa	kPa	kPa	kPa	kPa	Version
Egypt-G	2.45 (0.99-4.94)	0.64 (0.28-1.24)	2.05 (1.07-5.54)	0.36 (0.03-0.60)	2.07 (0.91-6.84)	NA	alpha
Egypt-R	2.32 (0.96-4.48)	0.61 (0.14-1.35)	1.89 (1.06-5.37)	0.41 (0.18-0.99)	1.57 (0.12-4.23)	NA	alpha
Egypt-T	2.44 (0.99-7.81)	0.55 (0.25-1.21)	3.02 (1.05-41.34)	0.64 (0.09-2.52)	2.17 (0.22-10.18)	NA	alpha
Norway-L	4.51 (2.38-12.36)	1.35 (0.79-2.95)	4.39 (1.03-7.56)	1.18 (0.64-2.40)	3.63 (1.85-7.49)	1.41 (0.82-2.58)	alpha
Norway-O	4.19 (1.32-7.70)	2.07 (0.37-4.43)	2.74 (1.53-3.78)	0.77 (0.47-1.13)	2.09 (1.27-2.91)	0.62 (0.38-0.82)	beta
Australia*	9.84 (9.27-10.41)	1.85 (1.60-2.10)	9.20 (6.30-13.80)	1.60	NA	NA	alpha
Maine	2.49 (0.61-5.33)	1.09 (0.53-1.79)	2.42 (0.69-4.55)	1.18 (0.30-2.55)	NA	NA	beta
(min.-max.)							
*Only one box tested							

Table 3.4. Summary of average intact and remolded shear strength testing in sub-samples.

	Shear Strength					
	Fall cone			Lab Vane		
	Intact	Rem	S_t	Intact	Rem	S_t
Site	kPa	kPa	-	kPa	kPa	-
Egypt-G	3.17 (1.10-12.0)	0.96 (0.50-2.30)	3.11 (1.00-6.32)	2.42 (0.99-4.94)	0.62 (0.28-1.24)	3.99 (1.26-7.04)
Egypt-R	2.02 (0.90-5.20)	0.76 (0.40-1.30)	2.80 (1.29-4.73)	2.35 (0.96-4.48)	0.63 (0.14-1.35)	4.47 (1.39-12.0)
Egypt-T	4.32 (1.00-17.0)	1.68 (0.40-7.30)	2.92 (0.46-8.33)	2.54 (0.50-7.81)	0.68 (0.25-3.84)	4.40 (1.33-9.80)
Norway-L	5.38 (2.50-9.60)	1.14 (0.50-2.10)	4.70 (2.33-6.18)	NA	NA	NA
Norway-O	4.0 (1.5-6.4)	0.7 (0.4-0.8)	5.8 (3.8-8.0)	NA	NA	NA
Australia*	NA	NA	NA	NA	NA	NA
Maine	NA	NA	NA	NA	NA	NA
(min.-max.)						
*Only one box tested						

Table 3.5. Summary of intact N-values.

		N								Count
		T-bar				Ball				
Site		min-max	ave μ	st dev σ	σ/μ	min-max	ave μ	st dev σ	σ/μ	intact
Egypt	R	3.6 - 20.7	10.3	3.9	0.38	0.7 - 17.0	6.8	2.8	0.41	45
	G	3.4 - 20.0	10.4	4.2	0.40	3.4 - 14.2	7.8	3.3	0.42	28
	T	3.8 - 121.7	12.7	12.7	1.00	0.5 - 24.5	8.2	3.8	0.46	97
Norway	O	4.8 - 16.3	9.6	4.2	0.44	2.5 - 13.0	6.5	4.4	0.68	7
	L	3.9 - 18.7	12	4.3	0.36	3.7 - 13.0	7.8	2.8	0.36	16
Maine		7.2 - 14.1	11.6	na	na	na	na	na	na	2

Table 3.6. Summary of remolded N-values.

		N_{rem}								Count
		T-bar				Ball				
Site		min-max	ave μ	st dev σ	σ/μ	min-max	ave μ	st dev σ	σ/μ	rem
Egypt	R	4.4 - 26.1	11.3	6.7	0.59	na	na	na	na	12
	G	0.4 - 15.5	7.3	4.2	0.58	na	na	na	na	10
	T	4.8 - 62.2	15.5	13.8	0.89	na	na	na	na	29
Norway	O	1.7 - 16.5	6.8	5.3	0.78	1.4 - 17.0	5.7	5.5	0.96	7
	L	6.2 - 27.6	13.5	6.2	0.46	7.6 - 29.6	14.9	6.6	0.44	15
Maine		3.0 - 13.1	7.2	na	na	na	na	na	na	2

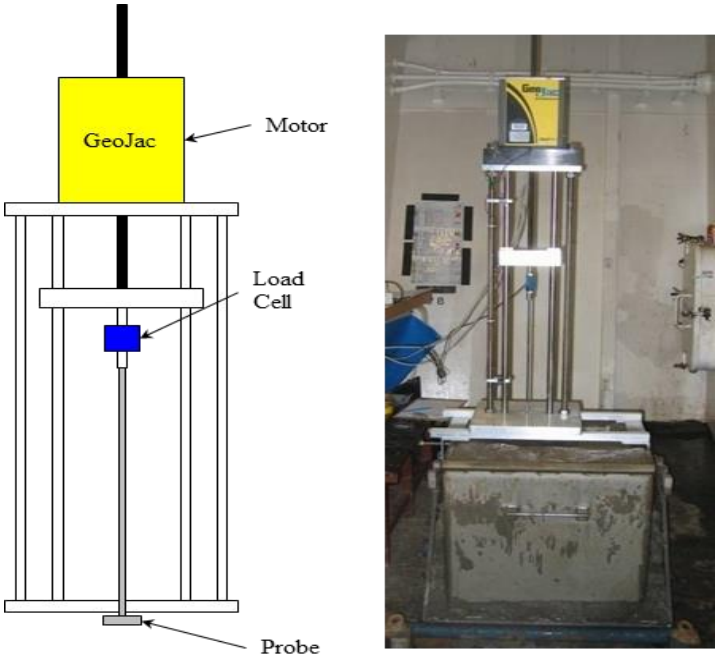

Figure 3.1. Box corer load frame schematic and testing a sample.

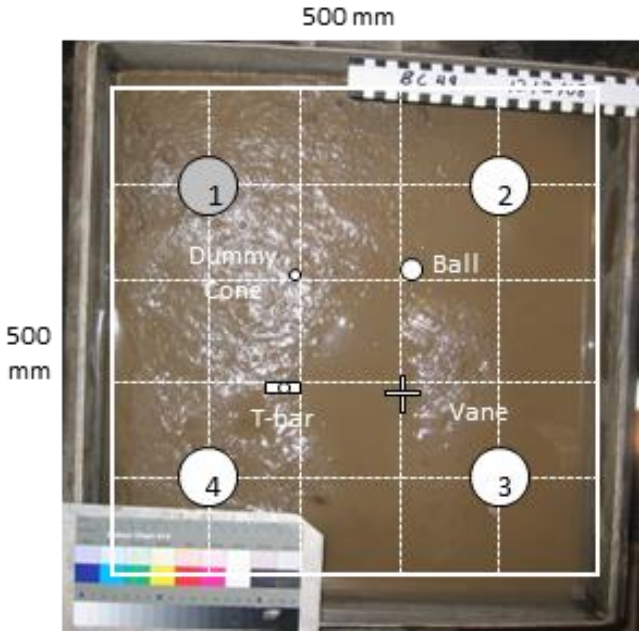

Figure 3.2. Miniature full flow penetrometer and motorized vane spacing with sub-sample locations.

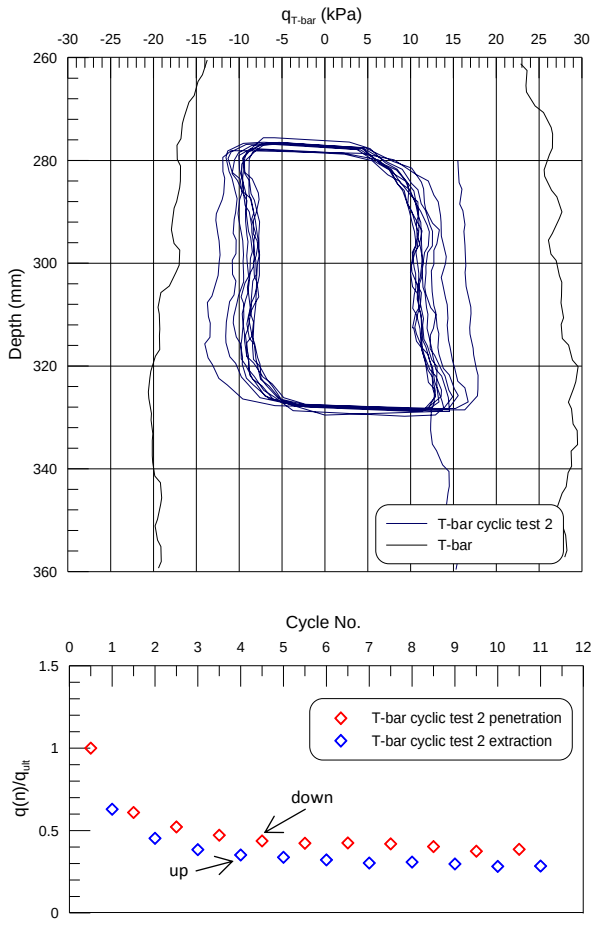

Figure 3.3. Example results from a cyclic test and force degradation curve taken from Egypt-G (BC59).

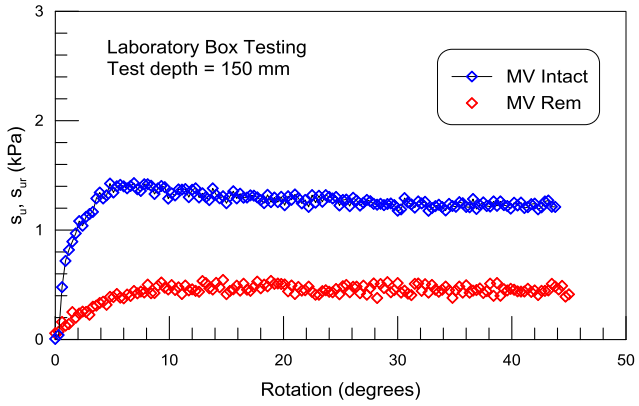

Figure 3.4. Example of intact and remolded motorized vane testing on a laboratory prepared box core sample of Kaolin.

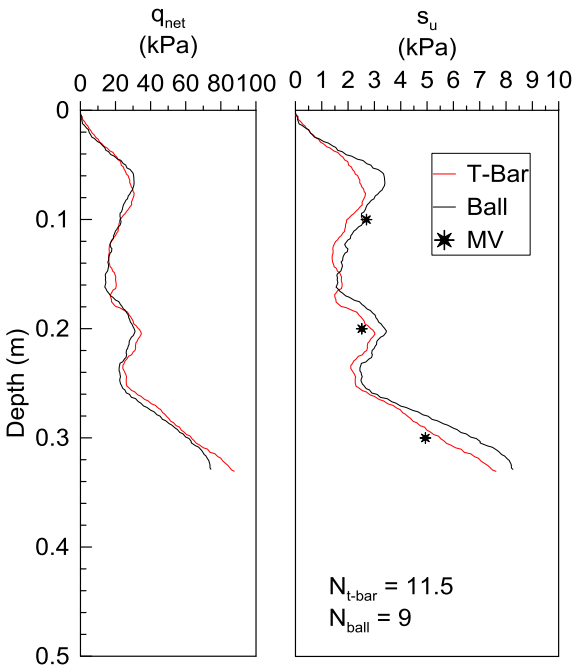

Figure 3.5. Example stress, q, and undrained shear strength, s_u, profile with depth at Egypt-G (BC257).

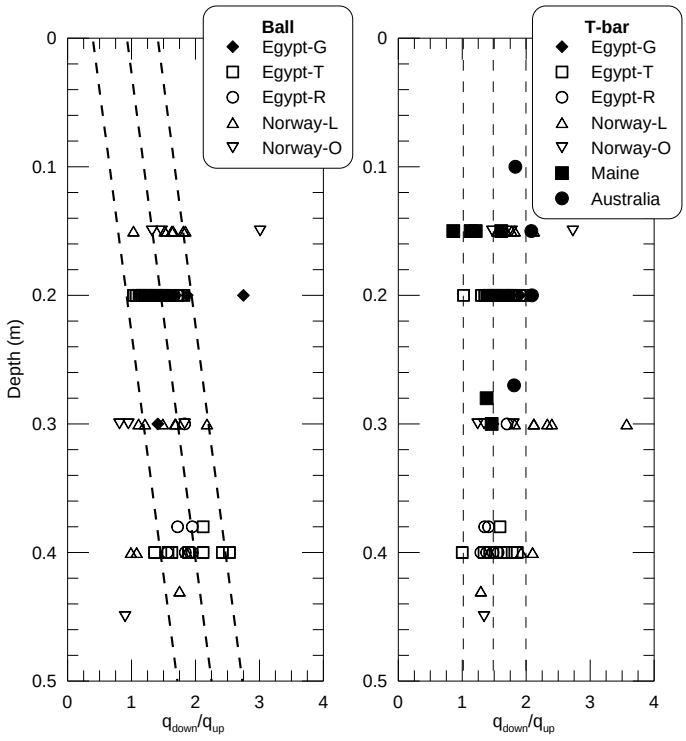

Figure 3.6. Behavior of q_{down}/q_{up} with depth for the ball and t-bar.

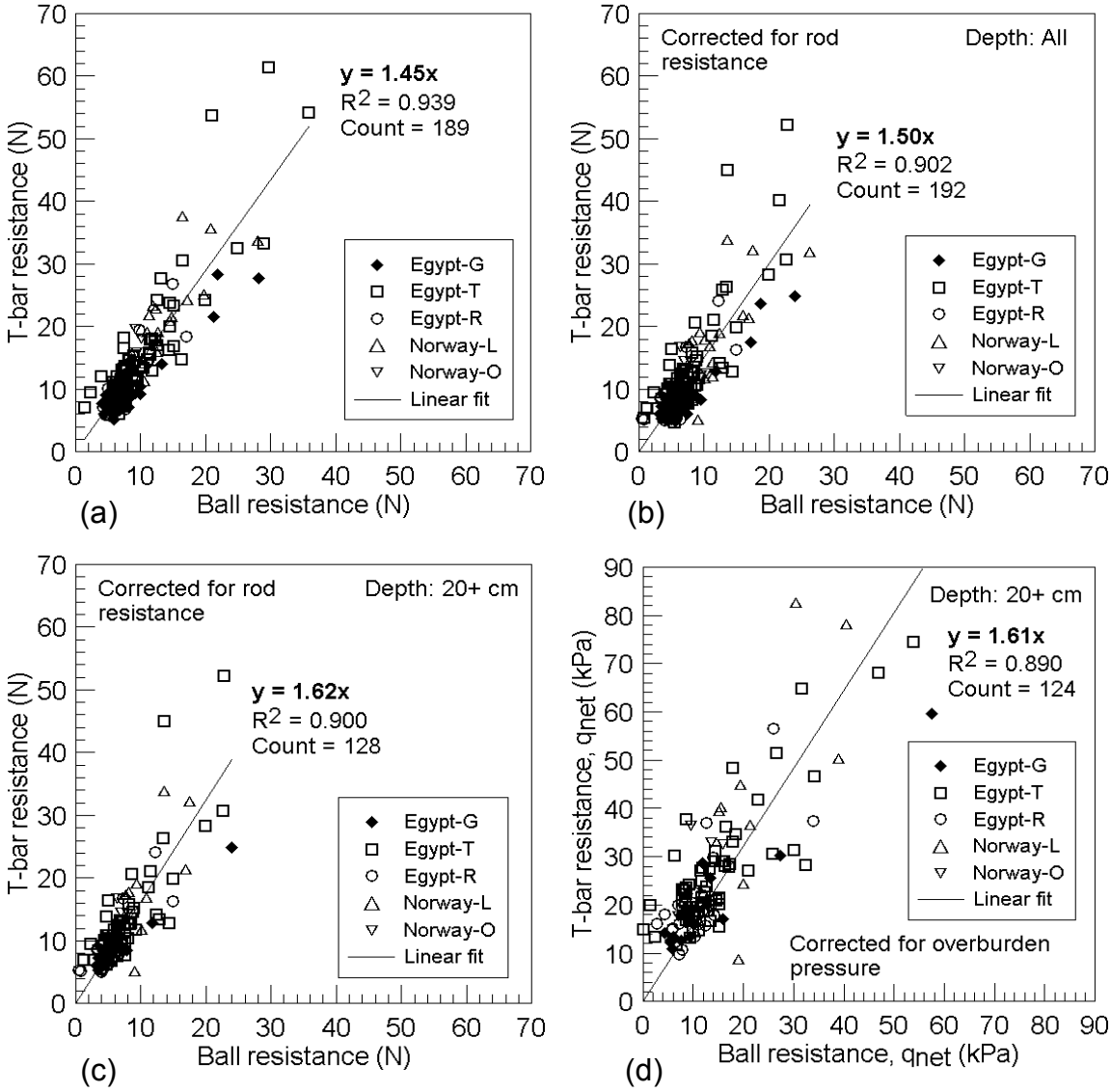

Figure 3.7. Relationship of t-bar and ball resistance at equivalent depths (a) uncorrected, (b) corrected for rod resistance, (c) corrected for rod resistance at depths < 20 cm, and (d) corrected for overburden pressure at depths < 20 cm.

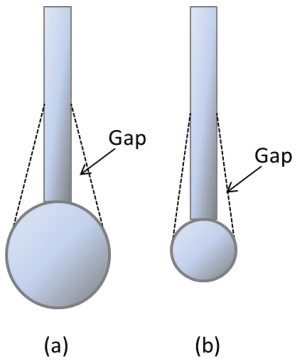

Figure 3.8. Side view of gap development around (a) ball and (b) t-bar.

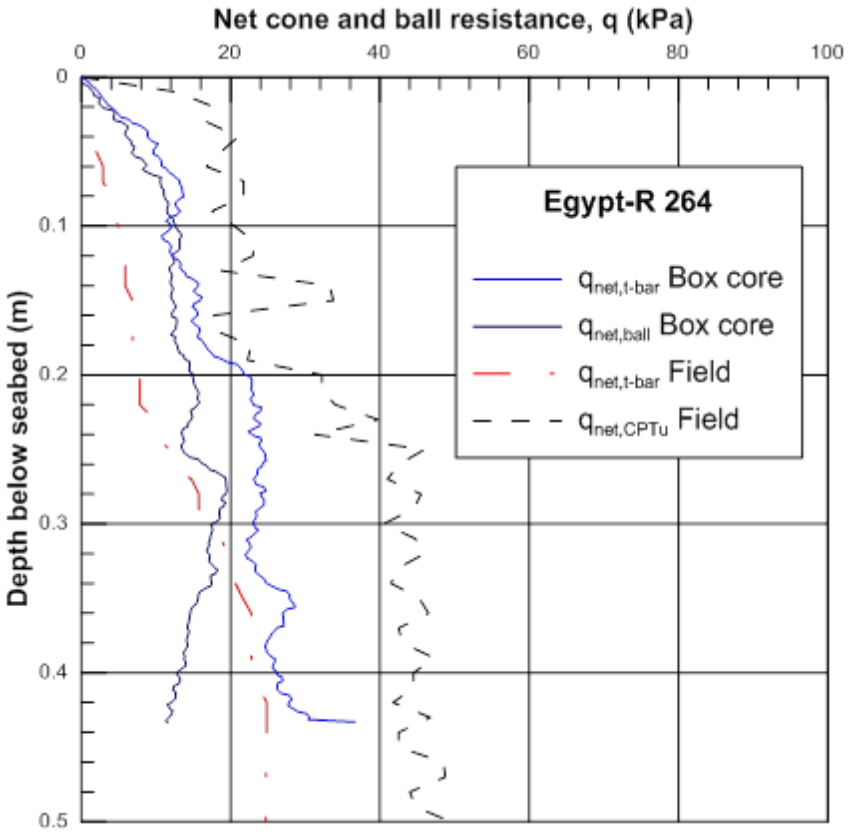

Figure 3.9. *In situ* CPT and t-bar testing verses box core miniature penetrometer testing (Egypt-R BC264).

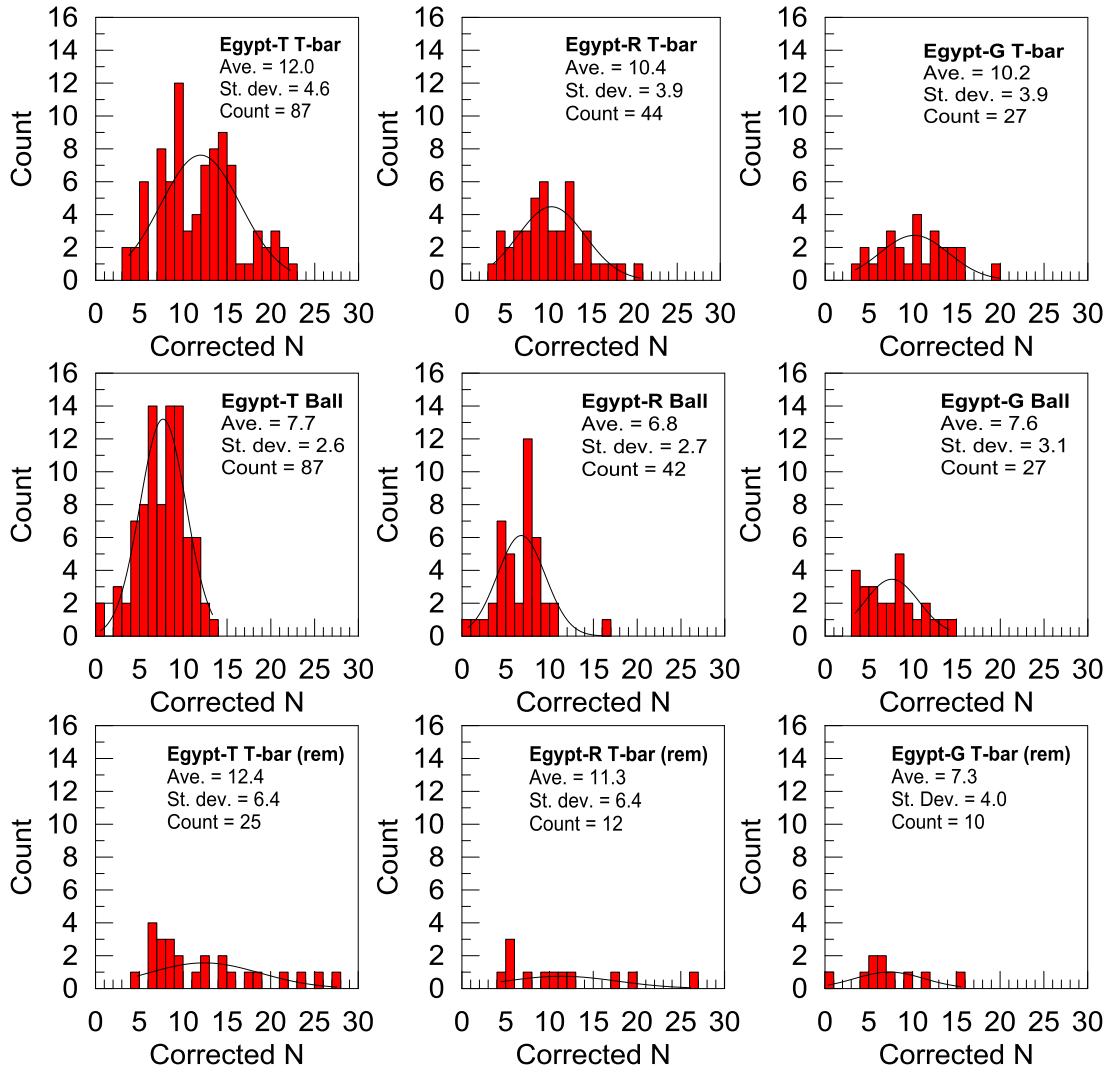

Figure 3.10. Histograms of t-bar, ball, and remolded t-bar N-values for each site at Egypt (boxes containing sand omitted).

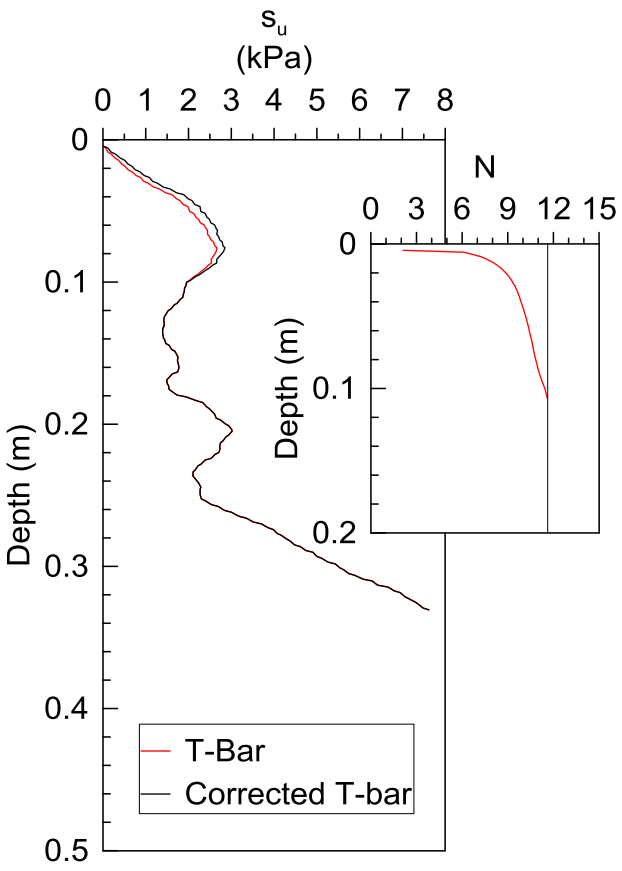

Figure 3.11. Shallow flow correction applied to the t-bar and N.

CHAPTER 4

LABORATORY EVALUATION OF A TOROID FOR MODEL PIPELINE TESTING OF VERY SOFT OFFSHORE BOX CORE SAMPLES

4.1 Abstract

Model pipeline testing helps better understand pipe-soil interaction during various scenarios encountered during the service life of a pipeline. The toroid is a probe which can be used to study soil response during embedment and axial movement. This study focused on investigating the toroid as a tool for box core testing to collect pipe-soil interaction data on intact seabed samples. Several types of tests including (1) vertical displacement after initial penetration (e.g., consolidation), (2) vertical stress, (3) embedment depth, (4) rate of rotation, and (5) episodic shearing and consolidation were performed on laboratory prepared samples to assess toroid performance and develop a recommended testing protocol for the toroid in the box corer. Results, specifically friction factor, were compared to previous field and laboratory model pipeline studies and found to fall within the typical range of 0.2-0.6.

4.2 Introduction

With offshore oil and gas development moving further offshore and into deeper waters, where the surficial sediments are typically very soft cohesive soils, the difficulty and cost of construction increases. Controlled lateral buckling is becoming a common design method for deep water pipelines, which allows the pipeline to move axially and laterally along the seabed. Based on observations taken of operating deep water pipelines, typical pipeline displacements are 10 to 20 pipe diameters (2 to 10 m) laterally and over 100 to 300 m axially (Bruton et al. 2009). To accurately predict pipeline behavior, including the extent of lateral and axial movement and buckle formation, all forces acting on the pipeline must be estimated. This can

be a significant challenge since the very soft sediments located within the upper half meter of the seabed, the depth within which most offshore unburied pipelines are located, are very difficult to characterize and to obtain geotechnical pipeline design parameters using common sampling and testing techniques. As a result, new in situ testing and sampling methods are being developed to address this challenge including full-flow penetrometers, box core sampling and testing, and in situ model pipeline test systems.

This paper describes a new set of equipment for testing box core samples, offshore, immediately after sampling, to collect preliminary soil-pipeline interaction data for very soft intact sediments. The equipment includes using a toroid instrument coupled to a computer controlled load frame that mounts directly on a box core sample. The toroid penetrometer was originally developed by Yan et al. (2011) for model pipeline testing in the centrifuge. The advantage of the toroid configuration (i.e., donut shape) to simulate axial soil-pipe interaction is that end effects, as with regular finite length model pipes, are eliminated and furthermore, the rotatory motion of the toroid readily allows for large deformation behavior to be measured. The paper first describes design considerations for offshore pipelines in soft seabed sediments and reviews existing laboratory and in situ methods for evaluating soil-pipeline interaction. Design and fabrication of the torrid test system is described and test procedures used to evaluate, in the laboratory, the developed prototype system are presented. Results obtained from the evaluation test program are presented and discussed and based on these outcomes the papers concludes with a recommended protocol for performing toroid testing of box core samples offshore.

4.3 Background

Model pipeline testing is a useful method for assessing soil resistance and predicting behavior of deep water pipelines. Better understanding of pipeline behavior from the start of construction throughout its service life improves design safety and reduces construction cost. Pipeline movement is generally the result of excessive force development during pipeline laying, stress buildup within the pipe due to the formation of thermal gradients from alternating between startup and shutdown cycles, tension development at touchdown points of steel catenary risers (SCR), sloping seabed, landslide events, soil erosion, etc. Accurately estimating the necessary soil properties for predicting pipeline movement is an ongoing challenge because of the continuously changing stresses within the pipeline and between the soil and pipeline due to changing operating and environmental conditions.

Pipeline movement generally consists of three phases: (1) initial pipe embedment, (2) lateral, or buckling, and (3) axial, or 'walking' (Bruton et al. 2008). Initial pipeline embedment occurs during installation at which time the greatest amount of settlement typically occurs. Embedment of the pipeline affects subsequent movement, degree of thermal insulation, exposure to turbidity (water currents), and provides protection against submarine landslides and trawl gear (Bruton et al. 2009; Yan et al. 2010). The initial installation embedment typically remains throughout subsequent operation of the pipeline, although the depth may vary, which affects lateral and axial movements that develop during operation.

Pipeline buckling and walking typically occur throughout pipeline operation. Pipelines tend to buckle and move as a mode of internal stress release which develops due to the formation of thermal gradients from start-up and shut-down cycles resulting in movement towards the cold end of the pipeline or down slope (Bruton et al. 2008). Initial resistance against

lateral or axial movement has been observed to depend on embedment depth and pipe-soil interface interaction (Oliphant & Maconochie 2006, Yan et al. 2010). Embedment depth can increase or decrease throughout the service life of the pipeline depending on the relation of the pipe weigh, pipe geometry, and soil shear strength. Bruton et al. (2008) classifies pipelines as either 'light' ($V/s_uD < 1.5$) or 'heavy' ($V/s_uD > 2.5$). 'Light' pipelines tend to uplift and 'heavy' tend to settle throughout the service life.

The available soil resistance against axial movement changes throughout the life of a pipeline because excess pore water pressures develop, and dissipate, as a function of duration and rate of loading events. Thixotropic hardening of clay remolded at the pipe interface also plays a role. Excess pore water pressures initially develop during pipeline installation because of vertical and lateral (if embedded) loading from the pipe and these are generally greater than pore pressures that developed during subsequent pipeline operation (Yan et al. 2011). Hill et al. (2012) noted that in fact the soil state around the pipe fluctuations between drained and undrained throughout its service life. Axial movement caused by buckle initiation, downslope movement, and landslide events can create either drained or undrained conditions. Therefore it is important to understand which soil properties govern frictional resistance at various stages of the service life of a pipeline and to break down such responses based on drainage conditions. A clear understanding of these conditions should allow for safer design methods and more cost effective installations if it leads to the ability to use longer pipe segments between supports, choose from a greater selection of tow-in methods, and use a wider array of pipeline construction methods on both flat and sloping seabed (Krost et al. 2011).

4.3.1 Model Pipeline Testing

Various projects have been performed to study the geotechnical challenges associated with designing, installing and predicting the behavior of deep water pipelines, with the Safebuck Joint Industry Projects (JIP) being one of the most notable (Bruton et al. 2008). New laboratory and field test equipment and procedures have been and continue to be developed for assessing soil parameters for offshore pipeline design in soft sediments. Recently developed *in situ* methods include full-flow penetrometers such as the t-bar or ball (Low et al. 2010, DeJong et al. 2010) and the SMARTPIPE which uses a seabed frame to test a model pipe at the seabed (Hill & Jacob 2008; Denis & De Brier 2010; White et al. 2011). The SMARTPIPE is a 255 mm diameter pipe outfitted with transducers for measuring normal load, axial load, and pore water pressure such that changes in load and water pressure during pipeline embedment and axial displacement can be monitored. New developments in testing of soil samples offshore includes the use of miniature full-flow penetrometers and the motorized vane for testing of box core samples (Hill & Jacob 2008; Low et al. 2008; Kelleher et al. 2011; Boscardin et al. 2013). The miniature full-flow probes and motorized vane are used for measuring the intact and remolded undrained shear strength profiles for samples collected from the upper half meter of the seabed with a box core. The advantages of such testing are that they are performed on representative intact samples of the seabed and immediately after they are collected offshore. In the laboratory, model pipeline testing includes performing large scale testing on reconstituted bulk samples as described by Langford et al. (2007) and Bruton et al. (2009). Large samples (approximately 3 to 4 m^3) of seabed sediments are reconstituted and consolidated using a low overburden pressure, which generally takes a month for full consolidation. Similar to the SMARTPIPE, embedment and axial movement is simulated with a segment of pipe. White &

Gaudin (2008) and Gaudin et al. (2011) describe small scale pipeline testing in the centrifuge to simulate and study the behavior of pipeline movement during construction and operational phases. Other laboratory testing of soft soils for pipeline studies includes the tilt table (Pederson et al. 2003; Najjar et al 2007) and low stress shearbox testing (White & Cathie 2011; White et al. 2011). Both of these tests require very little soil and can mimic both drained and undrained conditions by varying the test rate.

4.3.2 Toroid Testing

Axial pipeline movement is mainly governed by development of tension at pipeline ends associated with steel catenary risers, global seabed slope along the length of the pipeline, and development of thermal gradients along the length of the pipe (Bruton et al. 2009). Oliphant and Maconochie (2006) also note that embedment depth and rate and duration of movement affect available axial resistance.

Some of the significant geotechnical aspects affecting pipeline design include: (1) pipeline buckling due to axial feed-in within the free span of the pipeline and thermal and pressure-induced loading, (2) dynamic self-burial at the touchdown location of a steel catenary riser due to oscillation of the floating platform, and (3) pipe-soil interaction in zones at risk of landslides (White & Cathie 2010).

Isolating pipe-soil interaction for an infinitely long pipeline during axial movement is challenging using a model or prototype size pipe segment due to soil interaction at the pipe section ends. Yan et al. (2011) developed the hemi-toroid for centrifuge testing to study pipe-soil interaction without end effects during axial movement. The hemi-toroid is similar in shape to the bottom half of a doughnut. It was fabricated out of aluminum and contains both vertical and torsional actuators and four pore water pressure transducers equally spaced along the

apex. Yan et al. (2010) used finite element analysis to determine the ideal toroid geometry by varying the outer diameter (D_o), diameter (D), and lever arm (L) of a fully rough wished-in-place toroid to assess interference at different depths of embedment in a homogeneous soil. A D/L = 1/2 was found to be sufficient to eliminate interference across the probe and thus Yan et al. (2010) fabricated a toroid with dimensions of D = 16 mm and L = 32 mm to represent a prototype pipe of D = 400 mm and L = 800 mm respectively when tested in the centrifuge.

The friction factor (f_f) is computed as the ratio of the measured shear stress (τ) generated by the applied torque (T) normalized by the vertical stress (σ_v) due to the applied vertical load (V) such that:

$$f_f = \tau/\sigma_v \quad (4.1)$$

Since the projected contact area (A_c) between the soil and the toroid is the same for both τ and σ_v and also that the shear force (F) at the toroid equals T/L, Equation 4.1 can be written as:

$$f_f = T/(VL) \quad (4.2)$$

The shear stress is also often analyzed relative the undrained shear strength (s_u) as measured at the toroid invert such that alpha (α) equals:

$$\alpha = (F/A_c)/s_u = T/(LA_c s_u) \quad (4.3)$$

Offshore pipelines are typically treated as a laterally loaded pile and thus the use of the parameter α (DNV RP-F109 2007). Toroid testing in the centrifuge showed α to decrease from approximately 0.57 to 0.25 with each axial displacement cycle when back calculating α by comparing theoretical resistance to measured resistance (Yan et al. 2011). The most significant decrease in α was observed when axial displacement increased from 0.1 mm/s to 1 mm/s. The highest pore water pressures were measured at the highest axial displacement rates of 1 mm/s.

4.4 Equipment Development

The toroid was developed for this study to investigate pipe-soil interaction during embedment and axial displacement using box core samples. The box corer used for geotechnical investigations typically collects a 0.5 m cubic intact sample from the upper half meter of the seabed. The toroid is used to mimic embedment and axial pipeline movement during pipeline installation and operation. Depending on the degree of stress development, the rate of pipeline movement during a stress relieving event may be 0.001-1 mm/s (Hill & Jacob 2008).

The toroid developed for this study was fabricated from high strength aluminum with a smooth polished finish (Figure 4.1) with a lever arm of L = 40 mm and a diameter of D = 20 mm. A 444 N-6 Nm (100 lbs-50 in-lb) Interface biaxial load cell is located above the toroid to measure both vertical load and torque. Vertical displacement and vertical force is controlled by a GeoJac load frame that uses a ball screw jack and encoder to measure displacement. The toroid is rotated with a separate MicroMo motor that is located directly above the load cell and can rotate at a linear velocity of 0.1-10 mm/s at the toroid center. The load frame is computer controlled providing for either displacement or force control. All load, torque and displacement transducers can be recorded at any specified frequency.

The toroid is attached to the same load frame developed by Boscardin et al. (2013) for miniature t-bar, ball, and motorized laboratory vane (MV) testing of box core samples and is designed to withstand commonly encountered offshore environmental conditions and all parts are easily accessible for repair. The toroid itself is designed to be interchangeable such that different test geometries and surface roughness can be used. Furthermore, probes outfitted with pore water pressure transducers could be incorporated in the system but was not done for this research.

As part of the overall box core test system, the same GeoJac load frame is used for t-bar and MV testing. During t-bar testing, a load cell located at the top of the penetrometer rod is used to measure load during testing and displacement is recorded using the GeoJac encoder. A second MicroMo motor and Interface torque transducer is attached to the GeoJac load frame for performing MV testing and measuring torque.

4.5 Test soil

Evaluation of the toroid system was performed in the laboratory on samples of Prestige Kaolin D-6 with a liquid limit (LL) equal to 53%, plastic limit equal to 30%, for a plasticity index equal to 23%. The goal in preparing the test samples was to produce soil with low undrained shear strength similar to that encountered in deep water sites (e.g., < 5 kPa). Batches were prepared by mixing the kaolin at a water content twice the liquid limit and allowing it to either self-weight consolidate or consolidate under lightly loaded conditions (≤ 10 kPa). Samples were prepared in 28 cm diameter buckets which were modified to provide both top and bottom drainage during consolidation. The surface of the samples were vertically loaded with either a 5 or 10 kPa stress to develop profiles of different undrained shear strength at the end of consolidation. Typical consolidation periods were 1 to 2 weeks. Samples were also prepared in a stainless steel box with inner dimensions similar to a typical offshore box core sampler (0.5 m x 0.5 m x 0.5 m) and lined with geofabric (by Strata Systems) on all sides and bottom to reduce the drainage path and consolidation time. A thin rubber membrane was placed on the top surface of the box sample to prevent formation of a drying crust during consolidation. Typical consolidation time was 1 to 2 months for the box sample. These sample preparation and consolidation procedures resulted in test samples with t-bar undrained shear strengths of about 1 to 6 kPa depending on the applied surcharge prior to testing, drainage paths, and

consolidation time. The coefficient of consolidation, c_v, as determined from constant rate of strain testing is approximately 10^{-7} m^2/s.

4.6 Testing Methods

The prepared bucket and box core samples were all first tested using a miniature t-bar (L = 49.3 mm, D = 7.9mm, A_p/A_s = 12.1) pushed at a rate of 2 mm/s over the full depth of the sample following the test procedures described by Boscardin et al. (2013). The generic equation for converting t-bar resistance q_m to the net resistance q_{net} is:

$$q_{net} = q_m - (\sigma_{v0})A_s/A_p \quad (4.4)$$

and the undrained shear strength is computed as:

$$s_u = q_{net}/N \quad (4.5)$$

where $N_{t\text{-}bar}$ was selected as equal to 11.5 based on full flow penetrometer results by Boscardin (2013) and confirmed using MV. The T-bar profiles were corrected for shallow flow conditions following White et al. (2010) and rod resistance. After t-bar testing was completed, depth specific MV tests were performed along a separate vertical profile using a vane of H = 38.1 mm and D = 19.1 mm and rotated at a rate of 6-10 ^{o}/min (BS1377-7:1990).

Toroid testing was performed using a variety of test conditions so that the experience gained from this test program could be used to develop a recommended test protocol for offshore testing of box core samples. Undrained conditions are typically assumed during pipe laying for which plasticity solutions have been developed for pipeline design by Murff et al. (1989), Aubeny et al. (2005), White & Randolph (2007), and Merifield et al. (2008) and was considered in developing the test program. Test variations evaluated included depth of embedment, vertical stress, episodic interface shearing and consolidation, constant vertical stress or vertical displacement control, and rate of rotation. All tests were performed with some

embedment for which initial embedment was conducted at a rate of 0.1 mm/s which was selected to match typical rates observed in the field and as used in the centrifuge by Yan et al. (2011). The vertical force and displacement during embedment was continuously measured during penetration. The vertical force applied to the toroid was such that the vertical stress, as computed based on the projected area of the embedded section of the toroid, ranged from 2 to 10 kPa among the various tests. This range of stresses used was typical of that for offshore pipelines (Bruton et al. 2009).

Specific test variables investigated included (Table 4.1):

1. Vertical Displacement after Initial Penetration. Tests were performed with vertical stresses of 4, 6 and 8 kPa which were held constant for up to 24 hrs with continuous recording the vertical displacement.
2. Vertical Stress. Soil response to typical pipeline stresses applied to the soil in the field was studied by applying a vertical stress of 4, 6 or 8 kPa and thereafter rotating the toroid at 1 mm/s. Embedment and application of vertical stress took approximately 1 minute and rotation followed immediately.
3. Embedment Depth. Tests were performed with an initial embedment of 0.2D, 0.4D, or 0.5D with constant vertical stress of either 4 or 6 kPa. After the embedment depth was reached, the target constant vertical stress was applied and after approximately 1 min, the toroid was rotated at a rate of 1 mm/s. With the vertical stress held constant, the toroid was free to displace vertically during rotation which was recorded during the test. These tests simulate installation of a pipeline to an initially fixed depth followed by the pipe being free to move vertically under a constant self-weight (vertical stress). For "heavy" pipelines,

the embedment depth increases whereas for "light" pipelines the embedment depth decreases.

4. Rate of Rotation. These tests were performed to evaluate the ability of the toroid test system to evaluate the influence of increasing rate of rotation on the shear resistance. For all tests the toroid was embedded to 0.5D and thereafter subject to a constant vertical stress of 6 kPa. The toroid was rotated at rates of 1, 5 and 10 mm/s with no wait time between a change of rate. Axial resistance and vertical displacement were recorded.
5. Episodic Interface Shearing and Consolidation. The effects of episodic shearing and subsequent consolidation were studied by applying a constant vertical load of 4, 6 or 8 kPa after initially embedding the toroid to 0.5D and periodically rotating the toroid at 1 mm/s . Episodic shearing and subsequent consolidation were observed by measuring shear resistance after rest periods of 15 min, 30 min, 60 min, 120 min, etc. up to end of test period of 4 or 6 hrs periods. Testing over 24 hrs only measured axial resistance at the beginning and end of the 24 hrs.

4.7 Results

Four bucket samples and one box sample of the kaolinite were prepared for testing. Buckets B1 and B2 were loaded to 5 kPa during preparation and buckets B3 and B4 were loaded to 10 kPa. Figure 4.2Figure 4.2 presents the undrained shear strength profiles for each based on interpretation of the t-bar data via Equation 5. Soil strengths averaged 2 kPa and 5.5 kPa in buckets loaded to 5 kPa and 10 kPa, respectively. Water content and t-bar results show a fairly

uniform shear strength profiles with depth and as expected higher s_u profiles and lower water contents for the samples loaded to 10 kPa.

The laboratory box was the only sample with enough space to test both the MV and t-bar. T-bar and a MV test were performed between the toroid footprint and the box edge with at least two probe diameters between all surrounding test locations and container edge. Figure 4.3 presents results from intact and remolded MV testing performed at 150 mm depth in the box and the corresponding s_u(MV) value is plotted in Figure 4.2.

4.7.1 Vertical Displacement after Initial Penetration

Figure 4.3 plots embedment depth versus time for three successive vertical stresses applied to the toroid; 4 kPa, followed by 6 kPa and then 8 kPa. As expected, the excess pore pressures generated during initial penetration of the toroid took greater than several hundred minutes to dissipate given the low c_v of the test soil. This has significant practical implications for offshore testing of box core samples since during production sampling the time available to test a given box core sample is often limited (i.e., less than 4 to 5 hrs; although the actual duration depends on the water depth at which sampling is taking place and other sampling activities). As such, there will often be no opportunity to allow the soil to fully consolidate after initial penetration of the toroid before commencement of rotation. With this practical limitation in mind, most of the testing performed in this research involved rotating the toroid immediately after initial penetration. If needed, the toroid test system can be readily used offshore to allow for full consolidation after initial penetration before rotating if such time were provided for in the sampling schedule.

4.7.2 Vertical Stress and Embedment Depth

Figure 4.5 plots data from tests performed in the box with vertical stress equaling 4, 6, and 8 kPa. These figures show that with increasing vertical stress the shearing resistance increases. The embedment depth remains fairly constant for vertical stresses of 4 and 6 kPa during shearing whereas it increases significantly for the 8 kPa test. The 8 kPa test showed greatest displacement during shearing because the soil became too weak to support the 8 kPa vertical stress. Had this test continued, the toroid would continue to sink. The most significant increase of embedment depth typically occurred during shearing as a result of soil remolding. Figure 4.6 presents a summary of these test results together with data from all such constant stress tests performed in the box and also results from the embedment depth tests. The collective data set shows that both T/L and α increase with increasing vertical stress. Similar trends were measured for tests performed in the buckets as plotted together with the box data in Figure 4.7, although the α-data do show significant scatter. Tests performed in the higher s_u soil (Buckets B2 and B3) plot much lower upon normalization by s_u for computing α.

Shear resistance was expected to increase with initial depth of embedment, but no increase was observed. This behavior is most likely related to the small scale of the probe in which there is a small increase in A_c with embedment depth.

Figure 4.8 plots the change of embedment depth from the application of the target vertical stress to the end of rotation versus the normalized maximum embedment stress, which is the maximum vertical stress required to achieve a target embedment depth divided by the target vertical stress that was maintained after the embedment depth was reached. As this ratio becomes greater than about 2 the toroid embedment depth remains essentially constant

whereas for values less than 2, the toroid tends to embed (i.e., acts similar to a 'heavy' pipeline as described by Bruton et al. 2008).

4.7.3 Rate of Rotation

In the tests performed to study the influence of rate of rotation, three rates used were between 1-10 mm/s. The shearing response for these tests was expected to be undrained; as noted by Hill and Jacob (2008), axial displacement rates of 0.1-10 mm/s typically result in undrained soil conditions for fine-grained soils. Figure 4.9 plots the friction factor versus rate of rotation and the normalized velocity. The data show a clear trend of increasing friction factor with increasing rate and represent an approximately 12% increase in friction factor per decadal increase in rate. This rate is similar to that observed for undrained shear strength of clays based on field and laboratory tests (e.g., Lunne et al. 2011; DeGroot et al. 2012).

From a practical perspective the test results were most stable for a rotation rate of 1 mm/s and accordingly this rate is recommended for toroid tests of field box cores.

4.7.4 Episodic Interface Shearing and Consolidation

Figure 4.10 and Figure 4.11 plot f_f and α versus time for the episodic interface shearing and consolidation tests. Both f_f and α increase with time as a result of soil consolidation and perhaps thixotropic hardening of the soil around the toroid. Krost et al. (2011) explains this increase of resistance as a function of partial consolidation due to dissipation of excess pore water pressures between rest periods using FE analysis and field testing results. When the toroid was removed from the sample a cone of soil was found adhered to the bottom as shown in Figure 4.12 which Krost et al. (2011) described as the "wedging effect". This cone

development likely also contributes to increased shearing resistance because it increases the total contact area with the shear surface.

The increase of f_f with time was between 1.5×10^{-4} - 7.0×10^{-4} min^{-1}. 'Alpha' increased at the rate of $10^{-4} – 10^{-3}$ min^{-1}. Friction factor is generally higher for lower vertical stresses, but when T is normalized by s_u, such as in terms of α (Figure 4.11), lower applied vertical stresses plot below higher stresses. This type of episodic interface shearing testing can potentially be used for simulation of changes in pipeline resistance throughout a series of start-up and shut-down cycles.

4.7.5 General Toroid Testing Observations

In general, the shearing resistance of the toroid reached a steady, approximately constant value within 5-10 minutes after the start of rotation. The friction factors measured for this testing (e.g., Figure 4.9, Figure 4.10, Figure 4.11) are similar to those measured with a toroid in the centrifuge by Yan et al. 2011 and that in situ measured using the SMARTPIPE by Bruton et al. 2009. The values are also within the range of 0.2 to 0.6 recommended by DNV (2007) for pipeline design.

4.8 Recommended Testing Protocol

Based on the above testing observations and experiences, the following test procedures are recommended for offshore box core testing with the toroid:

1. Use the t-bar and motorized vane to obtain shear strength profiles of the sample.

2. Select an undisturbed area of the sample, preferably two probe diameters (D) away from any other test and the box edge (Yan et al. 2011) ideally in the center of the box, for toroid testing.
3. Embed the toroid between 0.4D to 0.5D at a rate of 0.1 mm/s measuring normal load on the toroid. Record the maximum embedment load on the toroid.
4. Maintain a continuous load on the toroid representative of the designed pipe weight. If this weight is unknown either reduce the load to 6 kPa corresponding to an average pipe weight or to half the maximum embedment load (following methodology by Yan et al. 2011).
5. Once the normal load on the toroid reduces to the desired pipe weight, rotate the toroid at 1 mm/s until the measured torsional resistance has stabilized on a minimum resistance. Resistance typically stabilizes within 5-10 min.
6. Stop rotation and remove the toroid from the soil at a rate of 0.1 mm/s.
7. Clean off the toroid.
8. Carefully remove soil to the next test depth. Maintain a minimum vertical distance of 5 cm between test locations.
9. Repeat steps (3) – (8) until the complete of testing at the final test depth.

For stable transducer readings it is recommended to allow the transducer to sit under no load with all electronic and control program on and for 15-30 min before testing. It is also strongly recommended to obtain a shear strength profile first with the miniature t-bar and motorized vane. Total stress analysis is only possible with the shear strength. For more on recommended test procedures using miniature penetrometers in the box corer see Boscardin (2013).

Before starting toroid testing, removing the upper 5 cm of soil is recommended. This top layer which tends to be muddy (<1 kPa) and toroid testing on a flat surface is preferable. Testing at multiple depths should be performed to profile friction factor and total stress with depth. A minimum distance of 5 cm is recommended between tests depths to minimize soil disturbance from the previous test.

4.9 Conclusions

This study focused on the development of the toroid for offshore box core testing. Both equipment and soil behavior were observed to develop a testing protocol to study pipe-soil interaction of very soft sediments by performing a sequence of tests on laboratory prepared samples of Kaolin including vertical displacement, vertical stress, initial embedment depth, rate, and episodic shearing.

Soils were still undergoing primary consolidation after 24 hrs under applied vertical stress of 4, 6, and 8 kPa on the toroid. Therefore, it is recommended to apply torque immediately after apply consolidation load to ensure maintenance of undrained conditions during testing.

An increase in resistance was observed with increasing vertical load. Resistance was not affected by initial embedment depth. The direction of vertical displacement of the toroid was related to the ratio of the maximum embedment load to vertical stress. Embedment depth increased for a ratio less than 2 and stabilizes at a ratio greater than 2.

Torsional resistance increased with rotational rate. The rate of 1 mm/s is recommended for toroid testing in the box core to maintain undrained conditions and collect stable resistance measurements within a reasonable time period of 5-10 minutes per torque episode.

An increase in f_f and α was observed after episodic periods shearing and consolidation. Such testing may be used to simulate soil response to start-up and shut-down cycles during pipeline operation. The slopes of f_f and α generally fell between 10^{-4}-10^{-3} min^{-1}.

This study shows that toroid testing in the box corer is a feasible method of model pipeline testing. Testing in the box core allows for collection of pipe-soil interaction data directly on intact seabed samples. Pipe weight, embedment depth, and embedment and axial displacement rates can be adjusted to meet project specifications or anticipated soil behavior to understand and predict pipe-soil interaction during axial pipeline movement and initial pipeline embedment. Such information supports in selection of pipeline feed-in lengths for safe expansion of pipelines, selection of laying methods to retrain or assist pipeline embedment, and predict stress development and relief in the pipeline throughout its service life.

Acknowledgements
This work was supported in part by the National Science Foundation under grant OISE-0530151. The authors thank Professor Mark Randolph of the University of Western Australia for suggesting the idea of developing a toroid for box core testing.

4.10 References

Aubeny, C.P., Shi, H., and Murff, J.D. (2005). "Collapse loads for a cylinder embedded in trench in cohesive soil." *International Journal of Geomechanics*, 5(4), 320-325.

Boscardin A.G., DeGroot D.J., and Lunne T. (2013). "Measurement of remolded undrained shear strength of soft clays using cyclic miniature penetrometers and push cone." *Geotechnical Testing Journal* (in review).

British Standards Institute (BSI) (2007). *Soils for civil engineering purposes – Part 7: Shear strength tests (total stress)*, Standard BS1377-7, London: BSI.

Bruton, D.A.S., White, D.J., Carr, M.C., and Cheuk, C.Y. (2008). "Pipe-soil interaction during lateral buckling and pipeline walking: The SAFEBUCK JIP." *Proc., Offshore Technology Conference*, Houston, Texas, OTC19589.

Bruton, D.A.S., White, D.J., Langford, T., and Hill, A.J. (2009). "Techniques for the assessment of pipe-soil interaction forces for future deepwater developments." *Proc., Offshore Technology Conference*, Houston, Texas, OTC20096.

DeGroot, D.J., Lunne, T., Andersen, K.H., and Boscardin, A.G. (2012). "Laboratory measurement of the remoulded shear strength of clays with application to design of offshore infrastructure." *Proc., 7th Int. Conf. Offshore on Site Investigation and Geotechnics*, London.

Denis, R., and de Brier, C. (2010), "Deep water tool for in-situ pipe-soil interaction measurement: recent developments and system improvement." *Proc., Offshore Technology Conference*, Houston, Texas, OTC 20630.

Det Norske Veritas (2007). "On-bottom stability of submarine pipelines." *Recommended Practices DNV RP-F109*.

Gaudin C., Clukey E.C., Garnier J., and Phillips R. (2011). "New frontiers for centrifuge modeling in offshore geotechnics." *Proc. 2nd Int. Symposium on Frontiers in Offshore Geotechnics*, Perth, 155–188.

Guo, B., Song, S., Chacko, J., and Ghalambor, A. (2005). *Offshore Pipelines*, Amsterdam.

Hill, A.J., White, D.J., Bruton, D.A.S., Langford, T., Meyer, V., Jewell, R., and Ballard, J-C. (2012). "A new framework for axial pipe-soil resistance, illustrated by a range of marine clay datasets." *Proc., 7th Int. Conf. Offshore on Site Investigation and Geotechnics*, London, 367-377.

Hill, A.J., and Jacob, H. (2008). "In-situ measurement of pipe-soil interaction in deepwater." *Proc., Offshore Technology Conference*, Huston, Texas, OTC19528.

Kelleher, P., Low, H.E., Jones, C., Lunne, T., Strandvik, S., and Tjelta, T.I. (2011). "Strength measurement in very soft upper seabed sediments." *Proc. 2nd International Symposium on Frontiers in Offshore Geotechnics*, Perth. 283–288.

Krost, K., Gourvenec, S.M., and White, D.J. (2011). "Consolidation around partially embedded seabed pipelines." *Geotechnique*, 61, 167-173.

Langford, T.E., Dyvik, R. and Cleave, R. (2007). "Offshore pipeline and riser geotechnical model testing: practice and interpretation." *Proc. Conf. on Offshore Mech. and Arctic Eng*., San Diego.

Low, H.E., and Randolph, M.F. (2008). "Characterization of near seabed surface sediments." *Proc., Offshore Technology Conference*, Huston, Texas, OTC19149.

Lunne, T., Andersen, K.H., Low, H.E., Randolph, M.F., and Sjursen, M. (2011). "Guidelines for offshore in situ testing and interpretation of deepwater soft clays." *Canadian Geotechnical Journal*, 48(4),543-556.

Merifield, R.S., White, D.J., and Randolph, M.F. (2008). "The ultimate undrained resistance of partially embedded pipelines." *Geotechnique*, 58(6), 461-470.

Murff, J.D., Wagner, D.A., and Randolph, M.F. (1989). "Pipe penetration in cohesive soil." *Geotechnique*, 39(2), 213–229.

Najjar, S.N., Gilbert, R.B., Liedtke, E.A., and McCarron, W. (2003). "Tilt table test for interface shear resistance between flowlines and soils." *OMAE*.

Oliphant, J., and Maconochie, A. (2006). "Axial pipeline-soil interaction." *Proc., Sixteenth International Offshore and Polar Engineering Conference*, San Francisco, California.

Pedersen, R.C. Olson, R.E., and Rauch, A.F. (2003) "Shear and interface strength of clay at very low effective stress." *Geotechnical Testing Journal*, 26(1).

White, D.J., Gaudin, G., Boylan, N., and Zhou, H. (2010). "Interpretation of t-bar penetrometer tests at shallow embedment and in very soft soils." *Canadian Geotechnical Journal*, 47, 218-229.

White, D.J., Bolton, M.D., Ganesan, S.A., Bruton, D., Ballard, J-C, and Langford, T. (2011). "SAFEBUCK JIP: Observations from model testing of axial pipe-soil interaction on soft natural clays." *Proc. Offshore Tech. Conf.*, Houston, Texas, OTC 21249.

White, D.J., and Cathie, D.N. (2011). "Geotechnics for subsea pipelines." *Frontiers in Offshore Geotechnics II*, London, ISBN 978-0-415-58480-7, 87-123.

White, D.J., and Cathie, D.N. (2010). "Geotechnics for subsea pipelines." *Proc. of the Second International Symposium on Frontiers in Offshore Geotechnics*, ISFOG, Perth, 87–124.

White, D.J., and Gaudin, C. (2008). “Simulation of seabed pipe-soil interaction using geotechnical centrifuge modeling.” *Proc. 1st Asia-Pacific Deep Offshore Technology Conference*, Perth, Dec 2008.

White, D.J., and Randolph, M.F. (2007). “Seabed characterization and models for pipeline-soil interaction.” *International Journal of Offshore Polar Engineering*, 17(3), 193-204.

Yan, Y., White, D.J., and Randolph, M.F. (2010). “Penetration resistance and stiffness factors in uniform clay for hemispherical and toroidal penetrometers.” *ASCE International Journal of Geomechanics*, Accepted for publication.

Yan, Y., White, D.J., and Randolph, M.F. (2011). “Investigations into novel shallow penetrometers for fine-grained soils.” *Frontiers in Offshore Geotechnics II*, London, ISBN 978-0-415-58480-7, 321-326.

Table 4.1. Summary of testing.

Test Set	Initial Embedment	Vertical Stress (kPa)	Vertical Displacement	Delta Time† (min)	Rate of Rotation (mm/s)
Vertical Displacement after Initial Penetration	measured	4, 6	measured	n/a	n/a
Vertical Stress	measured	4, 6, 8	measured	1	1
Embedment Depth	0.2D, 0.4D, 0.5D	4, 6	measured	1	1
Rate of Rotation	measured	6	measured	SR*	1, 5, 10
Episodic Shearing and Consolidation	measured	4, 6, 8	measured	15, 30, 60, 120, 180, 240, 360 or 1, 1440	1 (applied after variable time intervals)

Notes: †Delta time = time between initial penetration and start of rotation. *SR = until steady resistance measured.

Figure 4.1. Box core testing computer controlled load frame and model.

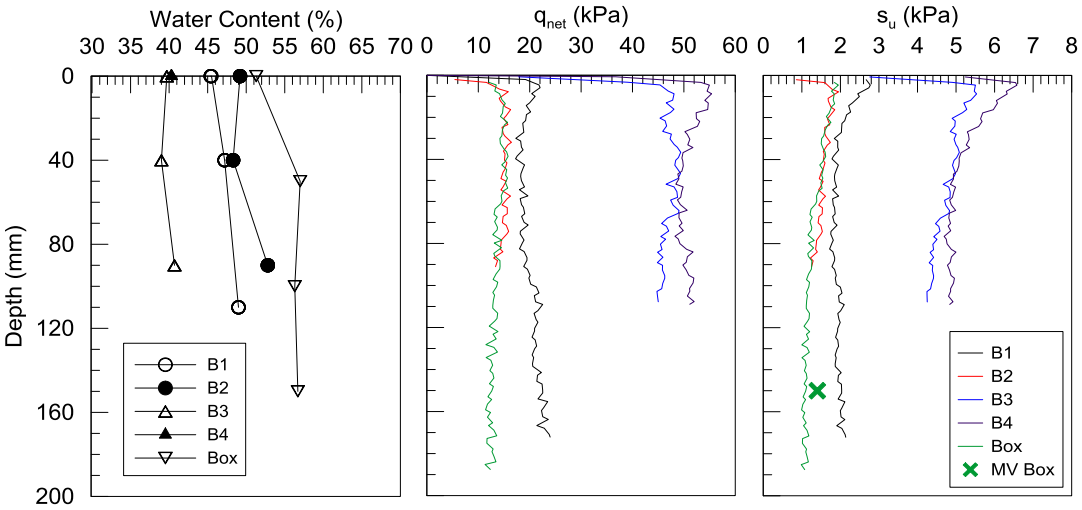

Figure 4.2. Water content and t-bar q_{net} and s_u (N_{tbar} = 11.5) profiles for the bucket and box samples.

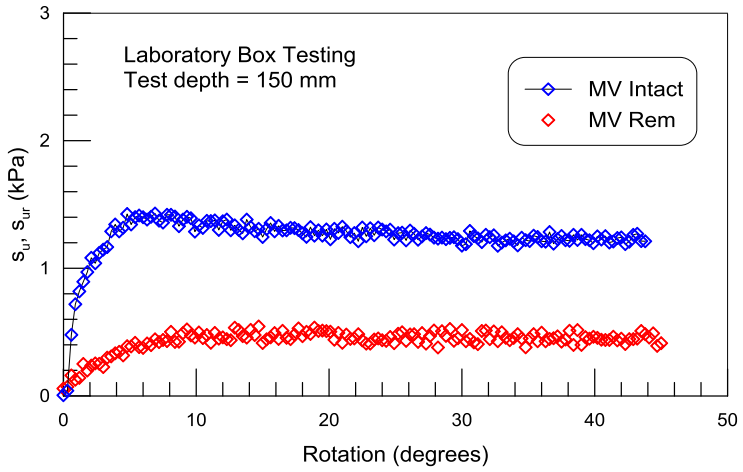

Figure 4.3. Intact and remolded shear strength testing with MV in the laboratory box at 150 mm depth.

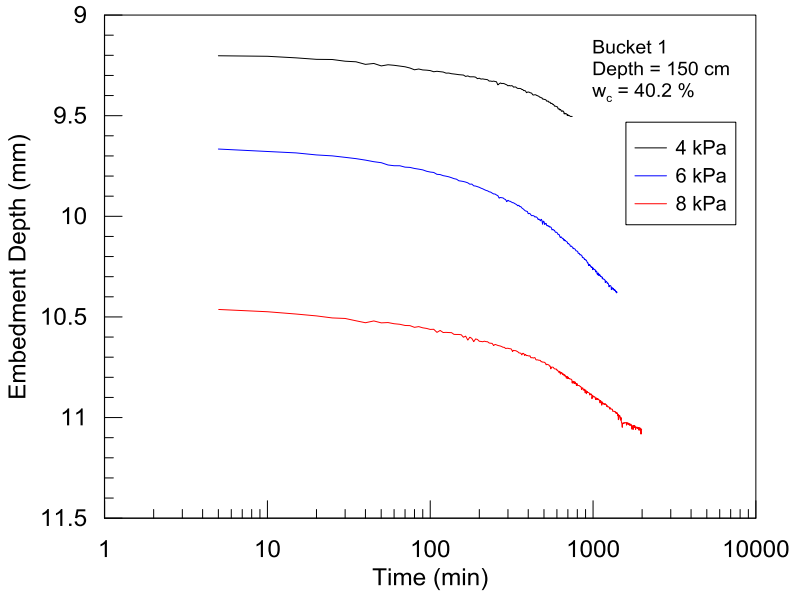

Figure 4.4. Embedment versus time for constant vertical stress increments applied to the toroid.

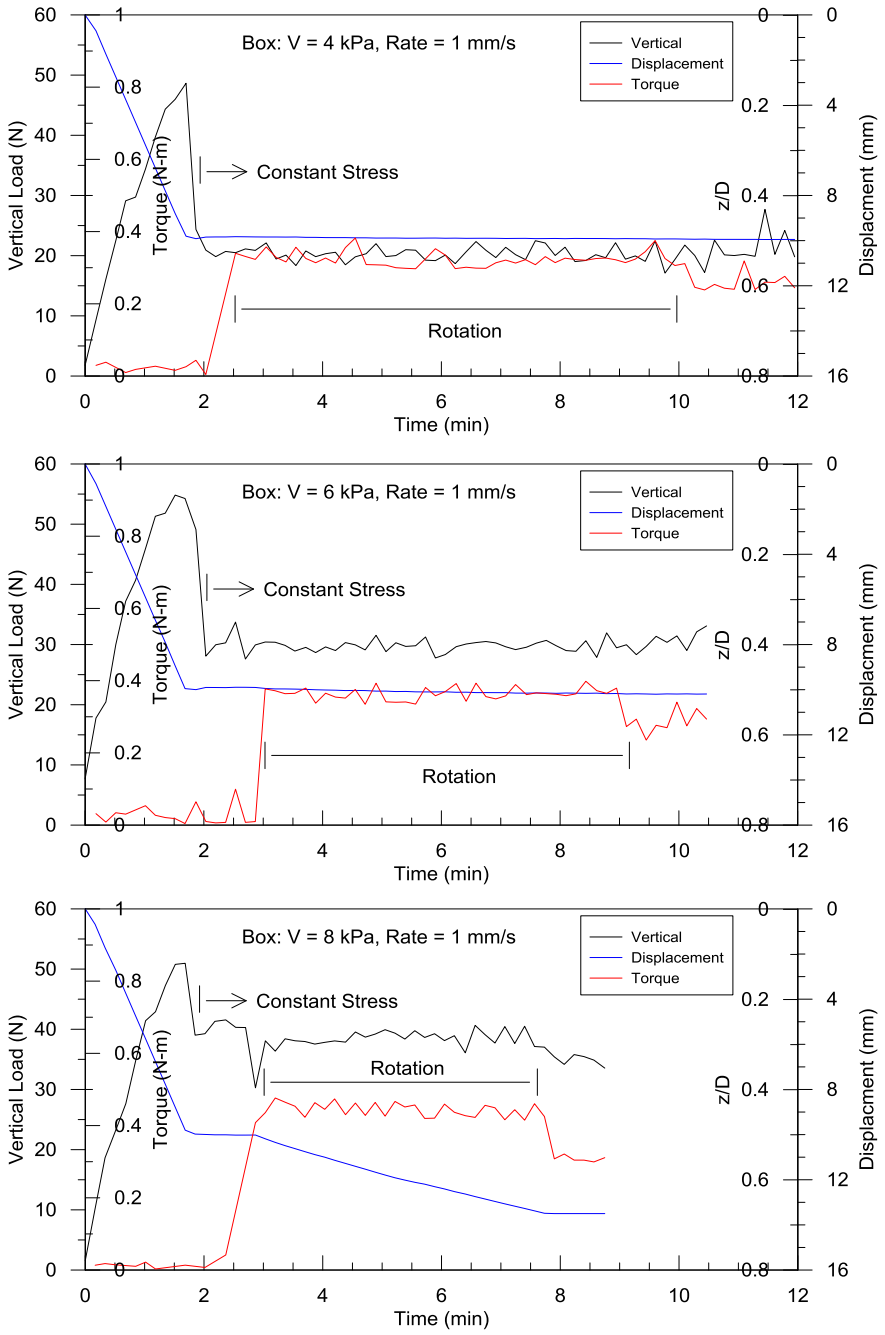

Figure 4.5. Load, displacement, and torque verses time for 4, 6 and 8 kPa vertical stress tests performed in the box.

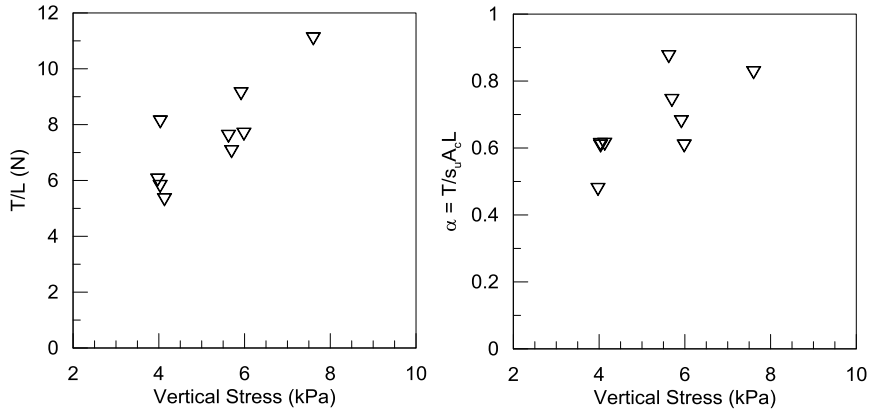

Figure 4.6. T/L and alphas versus vertical stress for tests performed in the box.

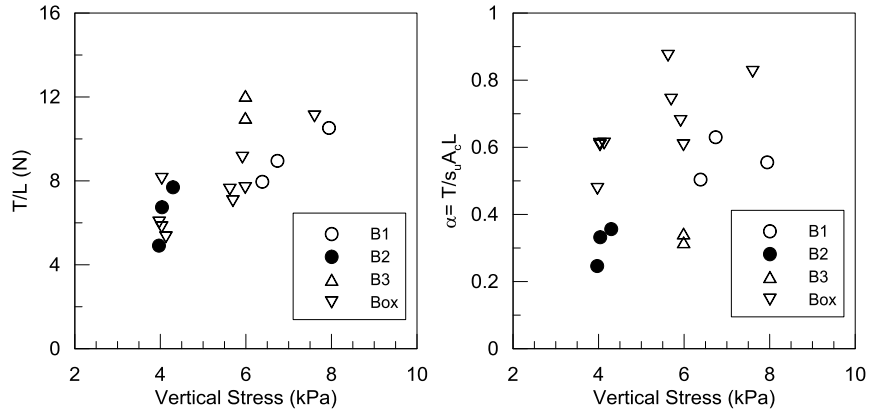

Figure 4.7. T/L and alpha versus vertical stress for tests performed in the box and the buckets.

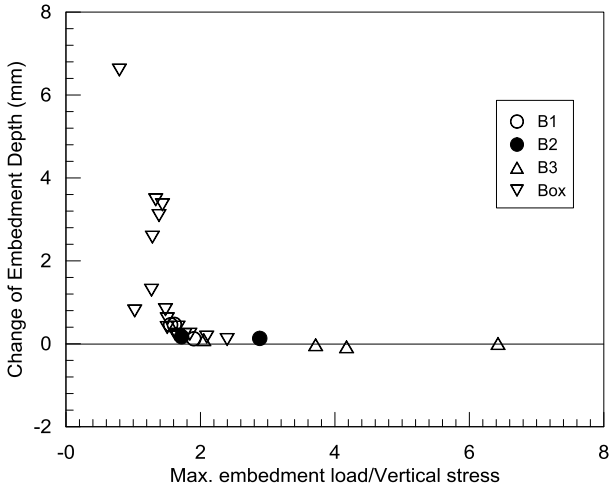

Figure 4.8. Change of embedment depth versus normalized maximum embedment stress.

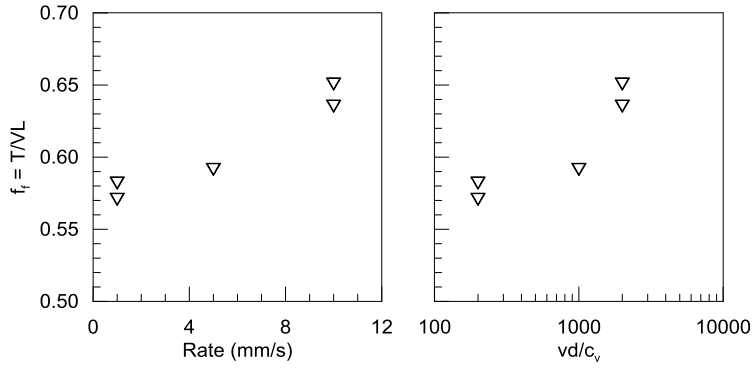

Figure 4.9. Friction factor versus rate of rotation and normalized velocity for tests performed in B4.

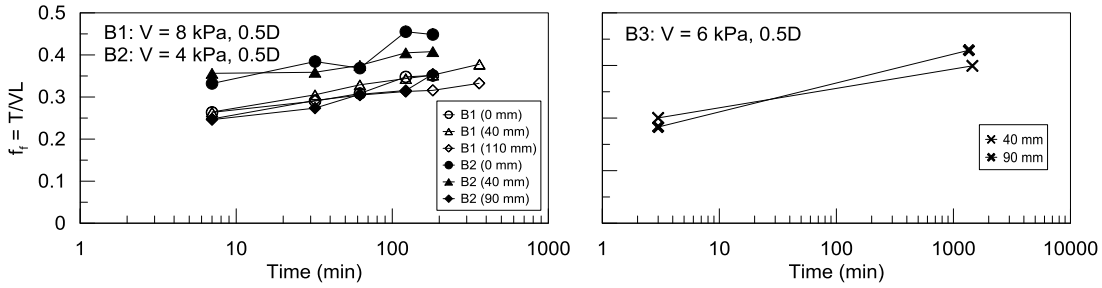

Figure 4.10. Friction factor f_f versus time for the episodic shearing tests.

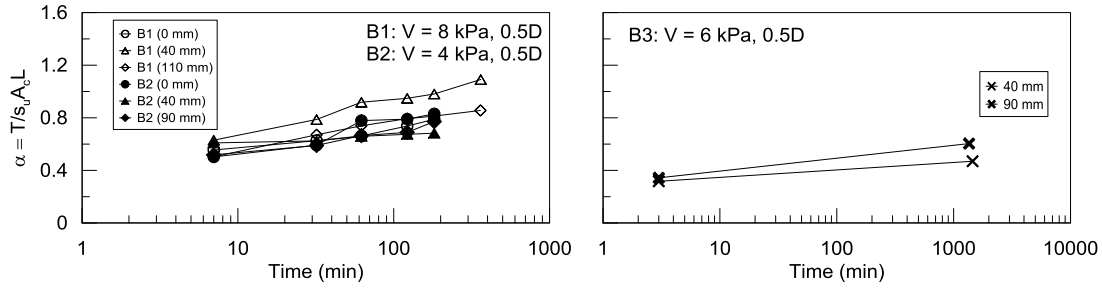

Figure 4.11. Alpha, α, versus time for the episodic shearing tests.

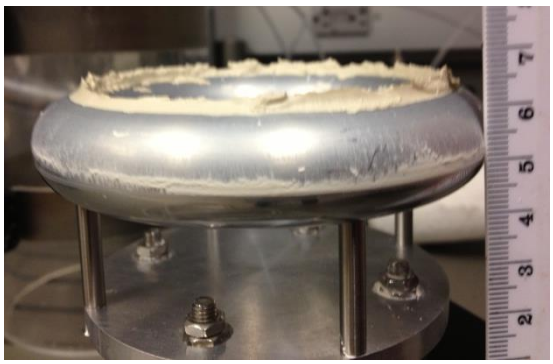

Figure 4.12. Wedging of soil on apex of toroid.

CHAPTER 5

SUMMARY AND CONCLUSIONS

The main objectives of this dissertation were to develop and assess testing equipment for characterization of offshore soft sediments collected in the box corer. Recommended testing protocol was developed for full flow penetrometers and the toroid based on testing observations. This section gives a general overview of findings presented in Chapters 2-4.

Chapter 2 presents results from measurement of the remolded undrained shear strength (s_{ur}) using miniature full flow penetrometers and push cone on remolded soft sediments in the laboratory. Testing showed measurement of s_{ur} to be simple and repeatable. Rough and smooth ball and t-bar penetrometers were compared and found to measure similar s_{ur}, but resistance measured by the smooth penetrometers stabilized in fewer cycles than the rough. The push cone is a quick and simple test which produces a unique s_{ur} assuming soil behavior is similar to that around a shallowly embedded conical footing (Houlsby & Martin 2003).

Chapter 3 presents results for miniature full flow penetrometer and laboratory motorized vane (MV) testing in very soft fine grained sediments collected by box corer. Full flow penetrometers and MV were used to profile undrained shear strength (s_u) and s_{ur} throughout the depth of the sample. High resolution data was easily collected with the t-bar and ball because of their large surface areas. The full flow failure mechanism engaged around the t-bar at shallower depths than the ball. Motorized vane testing is recommended to be performed in conjunction with full flow penetrometer testing to evaluate the bearing capacity factor N to convert penetrometer resistance to s_u or s_{ur} for given soil conditions. $N_{t\text{-}bar}$ tended to be greater

than N_{ball} with the relative standard deviation of $N_{t\text{-}bar}$ less than N_{ball}. From these testing observations, recommended testing protocol for full flow penetrometers and MV are presented.

Chapter 4 presents a study of the toroid as a form of model pipeline testing of box core samples. A series of tests were performed to evaluate the toroid for modeling axial pipeline movement along the seabed including: (1) vertical displacement after initial penetration (e.g., consolidation), (2) embedment depth, (3) vertical stress, (4) rate of rotation, and (5) rest period after shearing. Friction factor, f_f, and total stress, α, were evaluated from the last three test series (3-5) which are parameters typically used in pipeline design. The measured data fell within the range of those measured in previous pipeline studies including the SMARTPIPE (Bruton et al. 2009) and toroid testing in the centrifuge (Yan et al. 2011). Based on results and observations from this study, recommended testing protocol for the toroid in box core samples is given.

REFERENCES

ASTM Standards (2002). *Annual Book of Standards*, vol 4.80, Soil and Rock (I): D420-D5779. West Conshohocken, PA, USA.

Aubeny, C.P., Shi, H., and Murff, J.D. (2005). "Collapse loads for a cylinder embedded in trench in cohesive soil." *International Journal of Geomechanics*, 5(4), 320-325.

Barbosa-Cruz, E.R., and Randolph, M.F. (2005). "Bearing capacity and large scale penetration of a cylindrical object at shallow embedment." *Proc., 1st International Symposium on Frontiers in Offshore Geotechnics*, ISFOG 2005, Perth, WA, 615-621.

Boscardin, A.G. (2007). "Evaluation of miniature full flow penetrometers and push cone for laboratory measurement of remolded undrained shear strength of soft clays." *Masters of Science Thesis*, Univ. of Massachusetts Amherst, Amherst, MA.

Boscardin A.G., DeGroot D.J., and Lunne T. (2013). "Measurement of remolded undrained shear strength of soft clays using cyclic miniature penetrometers and push cone." *Geotechnical Testing Journal* (in review).

Boyland, G.S., and Row, G.T. (1991). "Deep-sea benthic sampling with the GEOMEX box corer." *American Society of Limnology and Oceanography*, 36(5), 1015-1020.

British Standards Institute (BSI) (1990). *Soils for civil engineering purposes – Part 7: Shear strength tests (total stress)*, Standard BS1377-7, London, BSI.

Bruton, D.A.S., White, D.J., Carr, M.C., and Cheuk, C.Y. (2008). "Pipe-soil interaction during lateral buckling and pipeline walking: The SAFEBUCK JIP." *Proc., Offshore Technology Conference*, Houston, Texas, OTC19589.

Bruton, D.A.S., White, D.J., Langford, T., and Hill, A.J. (2009). "Techniques for the assessment of pipe-soil interaction forces for future deepwater developments." *Proc., Offshore Technology Conference*, Houston, Texas, OTC20096.

DeGroot, D.J., Lunne, T., Andersen, K.H., and Boscardin, A.G. (2012). "Laboratory measurement of the remoulded shear strength of clays with application to design of offshore infrastructure." *Proc., 7th Int. Conf. Offshore on Site Investigation and Geotechnics*, London.

DeJong, J.T., Yafrate, N.J. and DeGroot, D.J. (2011). "Evaluation of undrained shear strength using full-flow penetrometers." *Journal of Geotechnical and Geoenvironmental Engineering*, 137(1), 14-26.

Denis, R., and de Brier, C. (2010), “Deep water tool for in-situ pipe-soil interaction measurement: recent developments and system improvement.” *Proc., Offshore Technology Conference*, Houston, Texas, OTC 20630.

Det Norske Veritas (2007). “On-bottom stability of submarine pipelines.” *Recommended Practices DNV RP-F109*.

Dingle, H.R.C., White, D.J., and Gaudin, C. (2008). “Mechanisms of pipe embedment and lateral breakout on soft clay.” *Canadian Geotechnical Journal*, 45(5), 636-652.

Einav, I., and Randolph, M. F. (2005). "Combining upper bound and stain path methods for evaluating penetration resistance." *International Journal for Numerical Methods in Engineering*, 63, 1991-2016.

Gaudin C., Clukey E.C., Garnier J., and Phillips R. (2011). “New frontiers for centrifuge modeling in offshore geotechnics.” *Proc. 2nd Int. Symposium on Frontiers in Offshore Geotechnics*, Perth, 155–188.

Guo, B., Song, S., Chacko, J., and Ghalambor, A. (2005). *Offshore Pipelines*, Amsterdam.

Hill, A.J., and Jacob, H. (2008). “In-situ measurement of pipe-soil interaction in deepwater.” *Proc., Offshore Technology Conference*, Huston, Texas, OTC19528.

Hill, A.J., White, D.J., Bruton, D.A.S., Langford, T., Meyer, V., Jewell, R., and Ballard, J-C. (2012). “A new framework for axial pipe-soil resistance, illustrated by a range of marine clay datasets.” *Proc., 7th Int. Conf. Offshore on Site Investigation and Geotechnics*, London, 367-377.

Houlsby, G.T. and Martin, C.M. (2003). “Undrained bearing capacity factors for conical footings on clay,” *Géotechnique*, 53(5), 513-520.

Kelleher, P., Low, H.E., Jones, C., Lunne, T., Strandvik, S., and Tjelta, T.I. (2011). “Strength measurement in very soft upper seabed sediments.” *Proc. 2nd International Symposium on Frontiers in Offshore Geotechnics*, Perth. 283–288.

Krost, K., Gourvenec, S.M., and White, D.J. (2011). “Consolidation around partially embedded seabed pipelines.” *Geotechnique*, 61, 167-173.

Ladd, C.C., and DeGroot, D.J. (2003). “Recommended practice for soft ground site characterization.” Proc., 12th *Panamerican Conference on Soil Mechanics and Geotechnical Engineering*, Boston, Massachusetts, 1, 3-57.

Landon, M.M., DeGroot, D.J., and Sheahan, T.C. (2007). "Non-Destructive sample quality assessment using shear wave velocity." *Journal of Geotechnical and Geoenvironmental Engineering*. 133(4), 424-432.

Langford, T.E., Dyvik, R. and Cleave, R. (2007). “Offshore pipeline and riser geotechnical model testing: practice and interpretation.” *Proc. Conf. on Offshore Mech. and Arctic Eng*., San Diego.

Low, H.E., and Randolph, M.F (2008). “Characterization of near seabed surface sediments.” *Proc., Offshore Technology Conference*, Huston, Texas, OTC19149.

Low, H.E., and Randolph, M.F. (2010). “Strength measurement for near-seabed surface soft soil using manually operated miniature full-flow penetrometer.” *Journal of Geotechnical and Geoenvironmental Engineering*, 136(11), 1565-1573.

Lu, Q., Hu, Y., and Randolph, M. F. (2001). “Deep penetration in soft clays with strength increasing with depth.” *Proceedings of the Eleventh (2001) International Offshore and Polar Engineering Conference*, 453-458.

Lunne, T., Andersen, K.H., Low, H.E., Randolph, M.F., and Sjursen, M. (2011). “Guidelines for offshore in situ testing and interpretation of deepwater soft clays.” *Canadian Geotechnical Journal*, 48(4), 543-556.

Lunne, T., Long, M., and Forsberg, C.F. (2003). "Characterisation and engineering properties of Onsøy clay." *Characterisation and Engineering Properties of Natural Clay*, 1, 395-427.

Lunne, T., Randolph, M. F., Chung, S. F., Andersen, K. H., and Sjursen, M. (2005) “Comparison of cone and T-bar factors in two onshore and one offshore clay sediments.” *Frontiers in Offshore Geotechnics*, 981-989.

Merifield, R.S., White, D.J., and Randolph, M.F. (2008). “The ultimate undrained resistance of partially embedded pipelines.” *Geotechnique*, 58(6), 461-470.

Murff, J.D., Wagner, D.A., and Randolph, M.F. (1989). “Pipe penetration in cohesive soil.” *Geotechnique*, 39(2), 213–229.

Najjar, S.N., Gilbert, R.B., Liedtke, E.A., and McCarron, W. (2003). “Tilt table test for interface shear resistance between flowlines and soils.” *OMAE*.

Oliphant, J., and Maconochie, A. (2006). “Axial pipeline-soil interaction.” *Proc., Sixteenth International Offshore and Polar Engineering Conference*, San Francisco, California.

Pedersen, R.C. Olson, R.E., and Rauch, A.F. (2003) “Shear and interface strength of clay at very low effective stress.” *Geotechnical Testing Journal*, 26(1).

Puech, A., Orozco-Calderon, M., and Foray, P. (2011). “Mini t-bar testing at shallow penetration.” *Proc., Frontiers in Offshore Geotechnics II*, London, UK.

Randolph, M. F. (2004). "Characterization of soft sediments for offshore applications." *Proceedings ISC-2 on Geotechnical and Geophysical Site Characterization*, 1, Porto, Portugal, 209-231.

Randolph, M.F., and Andersen, K.H. (2006). "Numerical analysis of t-bar penetration in soft clay." *International Journal of Geomechanics*, 6(6), 411-420.

Randolph, M.F., and Houlsby, G.T. (1984). "The limiting pressure on a circular pile loaded laterally in cohesive soil." *Geotechnique*, 34(4), 613-623.

Randolph, M. F., Martin, C. M., and Hu, Y. (2000). "Limiting resistance of a spherical penetrometer in cohesive material." *Geotechnique*, 50(5), 573-582.

Randolph, M.F., Low, H.E., and Zhou, H. (2007). "In situ testing for design for pipeline and anchoring systems." *Proc. of 6th Int. Conf. on Offshore Site Investigation and Geotechnics: Confronting New Challenges and Sharing Knowledge*, SUT, London, UK, 251.

Stewart, D.P., and Randolph, M.F. (1991). "A new site investigation tool for the centrifuge." *Proc. Int. Conf. Centrifuge 91*, Boulder, CO, 531-538.

Stewart, D.P., and Randolph, M.F. (1994). "T-bar penetration testing in soft clay." *Journal of Geotechnical Engineering*, 120(12), 2230-2235.

Tho, K.K., Leung, C.F., Chow, Y.K., and Palmer, A.C. (2012). "Deep cavity flow mechanism of pipe penetration in clay." *Canadian Geotechnical Journal*, 49, 59-69.

White, D.J., Bolton, M.D., Ganesan, S.A., Bruton, D., Ballard, J-C, and Langford, T. (2011). "SAFEBUCK JIP: Observations from model testing of axial pipe-soil interaction on soft natural clays." *Proc. Offshore Tech. Conf.*, Houston, Texas, OTC 21249.

White, D.J., and Cathie, D.N. (2010). "Geotechnics for subsea pipelines." *Proc. of the Second International Symposium on Frontiers in Offshore Geotechnics*, ISFOG, Perth, 87–124.

White, D.J., and Cathie, D.N. (2011). "Geotechnics for subsea pipelines." *Frontiers in Offshore Geotechnics II*, London, ISBN 978-0-415-58480-7, 87-123.

White, D.J., and Gaudin, C. (2008). "Simulation of seabed pipe-soil interaction using geotechnical centrifuge modeling." *Proc. 1st Asia-Pacific Deep Offshore Technology Conference*, Perth, Dec 2008.

White, D.J., Gaudin, G., Boylan, N., and Zhou, H. (2010). "Interpretation of t-bar penetrometer tests at shallow embedment and in very soft soils." *Canadian Geotechnical Journal*, 47, 218-229.

White, D.J., and Randolph, M.F. (2007). “Seabed characterization and models for pipeline-soil interaction.” *International Journal of Offshore Polar Engineering*, 17(3), 193-204.

Yafrate, N.J., and DeJong, J.T. (2005). “Considerations in evaluating the remoulded undrained shear strength from full flow penetrometer cycling.” *ISFOG-05: International Symposium on Offshore Geotechnics*, Perth Western Australia, 991-997.

Yafrate, N.J., and DeJong, J.T. (2006). “Interpretation of sensitivity and remolded undrained shear strength with full flow penetrometer.” *ISOPE*-06: *International Society for Offshore and Polar Engineering*, San Franciso, CA.

Yan, Y., White, D.J., and Randolph, M.F. (2010). “Penetration resistance and stiffness factors in uniform clay for hemispherical and toroidal penetrometers.” *ASCE International Journal of Geomechanics*, Accepted for publication.

Yan, Y., White, D.J., and Randolph, M.F. (2011). “Investigations into novel shallow penetrometers for fine-grained soils.” *Frontiers in Offshore Geotechnics II*, London, ISBN 978-0-415-58480-7, 321-326.

Zhou, H., and Randolph, M.F. (2009). “Numerical investigation into cycling of full-flow penetrometers in soft clay.*” Proc., 3rd Australian-New Zealand Younge Geotechnical Professionals Conf.*, 151-156.